THE UNIVERSITY OF CHICAGO

IMMUNOGLOBULIN A CONTROLS INTESTINAL VIRUS COLONIZATION TO PRESERVE IMMUNE HOMEOSTASIS

A DISSERTATION SUBMITTED TO THE FACULTY OF THE DIVISION OF THE BIOLOGICAL SCIENCES AND THE PRITZKER SCHOOL OF MEDICINE IN CANDIDACY FOR THE DEGREE OF DOCTOR OF PHILOSOPHY

COMMITTEE ON IMMUNOLOGY

BY

WIOLETTA LISICKA

CHICAGO, ILLINOIS

AUGUST 2024

TABLE OF CONTENTS

LIST OF FIGURES	
LIST OF TABLES	VII
ACKNOWLEDGMENTS	VIII
ABSTRACT	X
1. INTRODUCTION	1
1.1. Intestinal mucosal barrier components 1.1.1. Epithelial cells 1.1.2. Intraepithelial lymphocytes 1.1.3. Lamina propria lymphocytes	1 4
1.2. Ontogeny of intestinal IgA secreting plasma cells	8
1.3. T-dependent and T-independent IgA responses	11
1.4. Functions of sIgA	16
1.4.1. Impact bacterial IgA coating	
2. MATERIALS AND METHODS	23
2.1. Mice	23
2.2. Isolation of intraepithelial and lamina propria lymphocytes	24
2.3. Single cell tissue suspensions	25
2.4. Ex-vivo cell stimulation	25

2.5. Flow cytometry	. 25
2.6. Bacterial flow cytometry	. 26
2.7. In-vivo cell depletion	. 27
2.8. Antibiotic and antiviral treatments.	. 27
2.9. Viral infections	. 27
2.10. Microbial transfers	. 28
2.11. DSS-induced colitis	. 29
2.12. ELISA	. 30
2.13. Histology	. 30
2.14. DNA isolation	. 31
2.15. Microbial 16S rRNA Gene Sequencing.	. 32
2.16. Microbial DNA Shotgun Sequencing	. 32
2.17. IgA-MuAstV pulldown	. 33
2.18. RNA isolation	. 34
2.19. qPCR	. 34
2.20. RNA-seq library preparation.	. 34
2.21. Recovery of viral reads from the bulk RNA-seq	. 35
2.22. Mouse bulk RNA-seq data analysis	. 35
2.23. Single cell RNA-seq	. 37
2.24. Single cell RNA-seq data analysis	. 37
3. RESULTS	. 45
3.1. IgA-mediated regulation of the microbiota prevents antigen-driven expansion of $CD8\alpha\beta^+$ intraepithelial lymphocytes	
3.2. IgA prevents murine astrovirus expansion in the small intestine.	. 52

3.3. Germinal center-derived IgA plasma cells control the colonization of MuAstV in the small intestine	
3.4. IgA restricts norovirus colonization to protect the host against immunopathology 6	4
4. DISCUSSION	0
4.1. MuAstV-driven expansion of CD8αβ + IELs in IgA deficient hosts	0
4.2. Role of T-dependent IgA in controlling chronic enteric virus infection	4
4.3. Pathological implications of chronic viral infection in IgA deficient hosts	7
4.4. Conclusion and model	1
REFERENCES	3

LIST OF FIGURES

Figure 1: IgA+ plasma cell differentiation. 14
Figure 2: Functions of sIgA.
Figure 3: Novel model of IgA deficiency: IgA secretory deficient mouse
Figure 4: IgA controls microbiota to prevent expansion of classically restricted CD8 $\alpha\beta^+$ IELs. 49
Figure 5 supplemental to Figure 4: IgA controls microbiota to prevent expansion of classically
restricted CD8αβ+ IELs
Figure 6: IgA controls Murine Astrovirus to limit inflammation in the small intestine 56
Figure 7 supplemental to Figure 6: IgA controls Murine Astrovirus to limit inflammation in the
small intestine
Figure 8: GC-derived IgA plasma cells contribute to MuAstV control in the small intestine 62
Figure 9 supplemental to Figure 8: GC-derived IgA plasma cells contribute to MuAstV control in
the small intestine. 63
Figure 10: IgA maintains intestinal homeostasis to protect the host from immunopathology 67
Figure 11 supplemental to Figure 10: IgA maintains intestinal homeostasis to protect the host from
immunopathology69
Figure 12 Model of sIgA mediated regulation of intestinal immune homeostasis

LIST OF TABLES

Table 1: List of reagents.	39
----------------------------	----

ACKNOWLEDGMENTS

This thesis is a fruit of the hard work, efforts and creativity of many people. I am thankful to all those who made this journey possible. I am eternally grateful for a privilege of perusing this degree, and I am acutely aware that this would not have beem possible without the kindness, support and resources I received along the way.

I want to thank my mentor, Dr Bana Jabri, for her trust and encouragement throughout my time in her lab. I joined her lab back in 2017 as a Fulbright scholar, with little understanding of the field of immunology, and yet she welcomed me to the lab, with a lot of patience and grace. Under Bana's care, I have learned how to be a good scientist. Her support and mentorship were a crucial part of this journey and tremendously impacted my scientific and personal growth.

I would like to express my gratitude towards Dr Albert Bendelac for trusting me with this project. I am grateful for his advice, insight and time he devoted to this work. I have learned a lot as a scientist in the short time I spent working him.

I would like to thank my thesis committee, Dr Daria Esterhazy, Dr Maria-Luisa Alegre and Dr Yuxuan Miao. I am thankful for their support, career advice, and for pushing me to think critically and deeply about my work.

I am grateful for the communities I became a part of during my time at the University of Chicago: The Committee on Immunology and Jabri lab. Your insight at WIPs or lab meetings contributed to my growth as a scientist. Your kind words motivated me to keep going when I was struggling. There are many people in those communities that supported me, and to each of them, I owe thanks. A special thank you to Cezary Ciszewski, who had the questionable honor of teaching me flow cytometry, who would give me his honest advice when I needed it most.

I am forever indebted to my family: my parents and my siblings. Their support and kindness kept me going. The values instilled in me by my mom, Emilia, and my dad, Lech, were paramount in finalizing this process. Their support and encouragement allowed me to pursue many things in life I once deemed unattainable. I am grateful for my sister Natalia, who made me laugh, and listened when I needed it most. I am thankful to my in-laws, Cathy and Michael, and their sons, Aaron and Nicholas, who would take care of me and supported me when my family couldn't. I am grateful for Ula Cichon and her friendship. She is the most patient, kind and supportive friend one can imagine. I am lucky to have you all by my side.

Lastly, I would like to thank my husband, Zach, whom I met while in the lab. He taught me many experimental techniques while we were working together, but more importantly, he was a source of strength and perseverance. His passion and curiosity often inspired me to do better. I would not have been able to accomplish this without your help. I will dearly miss our time at the University of Chicago, the late experimental days, and the brunches by the lake. We created many wonderful memories in Chicago; I am excited and hopeful for the times to come, and the new chapter ahead.

ABSTRACT

The mucosal barrier of the gastrointestinal tract is essential for maintaining tolerance to the commensal microbiota and protecting the host from pathogenic infections. A vital component of this barrier is secretory IgA (sIgA), which coats up to 70% of the small intestinal microbiota and is the most abundant antibody isotype produced in mammalian gastrointestinal mucosa. sIgA is known to restrict or promote mucosal bacterial colonization, alter bacterial gene expression and metabolism, confer protection against mucosal infections, or neutralize toxins. This suggests that sIgA is crucial in establishing tolerance with the microbiota at the intestinal barrier. Confounding interpretations of IgA function is potential IgM compensation. IgM was reported to coat intestinal microbes in AID deficient mice and IgA deficient humans. These data point to a hypothesis that IgM may compensate for and control the microbiota in conditions of IgA deficiency. Analogous to IgA deficient patients, the original IgA deficient mouse model (Igha-/-) exhibits an increase of serum and mucosal IgM. We developed a novel model of IgA deficiency, IgA secretory deficient mouse (Ighasec-/-), which circumvents increased IgM production. This allowed us to address a long-standing question how IgA maintains immune homeostasis with the microbiota, and whether IgM compensates for IgA deficiency. Using SPF and GF Ighasec-/-, we observed a microbiotadependent expansion of CD8αβ+ intraepithelial lymphocytes (IELs) in the small intestine of IgA deficient mice. These IELs showed features of antigen drive and were licensed by BATF3 dependent dendritic cells. We identified that IgA neutralized murine astrovirus (MuAstV) to limit inflammatory T cell responses in the intestine. In the absence of IgA, MuAstV chronically infected intestinal epithelial cells and drove a CD8 $\alpha\beta$ + T cell expansion to limit host interferon responses and viral load. Notably, GC B cells and T cell-dependent IgA were necessary for the host to control MuAstV. In addition, we found that IgA was critical in controlling other enteric viruses, such as

murine norovirus strain CR6, and protecting the host from immunopathology. These data identify specific IgA-virome interactions essential for maintaining intestinal immune homeostasis.

1.INTRODUCTION

1.1.Intestinal mucosal barrier components

The mucosa lines organs and cavities in the body that are exposed to the external environment due to their physiological function. They cover up to ~400 m² of the human body and are involved in gas exchange (the lungs), food absorption (the gut), reproduction (the reproductive tract) or sensory input (the nose, eye, and tongue). One of the major challenges at mucosal surfaces is to protect against potential infections while ensuring efficient physiological function. At these selectively permeable mucosal sites, the interconnected physical, chemical, and immune barriers are present to establish the separation between the external environment and the body's internal milieu. Establishing this separation is extremely important in the gastrointestinal tract, colonized with diverse communities of commensal microbiota (≥10¹²/cm³ of luminal content)(Hooper et al., 2012).

1.1.1. Epithelial cells

The mucosa consists of one or more layer of epithelial cells, underlying loose connective tissue termed lamina propria, and the muscularis mucosae. Mucosal surfaces can be divided into two types: Type I mucosa (found in the intestine, lung, upper female reproductive tract) and type II mucosa (found in the eye, mouth, lower female reproductive tract) (Woodrow et al., 2012). Type I mucosal surfaces are characterized by a presence of a single layer of columnar epithelial cells connected by the intracellular tight junctions. In the intestine, the interconnected intestinal epithelial cells (IECs) form a physical barrier maintaining the separation of resident luminal microbiota from the host. This barrier is composed of several specialized cell types: (1) absorptive enterocytes (small intestine) or colonocytes (colon), (2) goblet cells, (3) Paneth cells, (4) Tuft cells, (5) enteroendocrine cells and (6) microfold cells. Absorptive enterocytes are the most numerous

population of IECs. Beyond their digestive and metabolic functions, absorptive enterocytes express various pattern recognition receptors (PRRs) allowing the sensing of conserved microbial patterns and maintenance of intestinal homeostasis(Price et al., 2018). Enterocytes also express polymeric Ig receptor (pIgR) which allows transport of polymeric immunoglobulins, such as immunoglobulin A (IgA), across the mucosa and into the intestinal lumen. Although less numerous, the lineage of secretory IECs, goblet and Paneth cells, are also crucial in supporting the intestinal mucosal barrier. Goblet cells are scattered between enterocytes and their abundance increases the distal small intestine and colon. These cells produce and secrete mucin glycoproteins, such as MUC2, the building blocks of mucus. Mucus is secreted constitutively but it also can be further induced in response to colonization with microbiota (Johansson et al., 2015) or pathogens (Bergstrom et al., 2010). Layers of viscous mucus physically separate commensals from the host tissue. Single, unattached layer of mucus coats the small intestine and increases in thickness distally, as does the density of commensal microbiota. In the colon, where the microbial abundance is the greatest, mucus contains two layers, with the inner layer remaining sterile and attached to the epithelium (Hansson & Johansson, 2010). Paneth cells are located in the crypts of the small intestine, where they produce and secrete antimicrobial enzymes, proteins, and peptides (AMPs). These include alpha and beta defensins, lysozyme, phospholipases, and C-type lectins (e.g. RegIIIγ) (Bevins & Salzman, 2011). Some AMPs (e.g. α-defensins) are expressed constitutively (Mukherjee & Hooper, 2015), while others (RegIIIy) are induced in response to microbial sensing (Brandl et al., 2007; Vaishnava et al., 2008) or interleukin 22 (IL-22) (Zheng et al., 2008). Dense scaffold of charged mucins retains secreted antimicrobials and together limit bacterial interactions with the host tissues. This is particularly important in the small intestine, where mucus is thinner and consist of a single layer. Mucus and antimicrobials are an important physical and chemical component of intestinal barrier, as deficiencies in either have detrimental effect on its function. Mice lacking core mucin MUC2 develop spontaneous colitis (Van der Sluis et al., 2006; Burgervan Paassen et al., 2011). Substantial bacterial contact with epithelial cells and increased inner mucus penetrability was observed in patients with active ulcerative colitis (Johansson et al., 2014). In RegIIIγ deficient mice, the separation between the commensals and the small intestinal epithelial cells is lost, resulting in increased activation of adaptive immune responses (Vaishnava et al., 2011). One of the Crohn's disease susceptibility alleles, ATG16L1, was linked to abnormal packaging and exocytosis of Paneth cell AMP-containing granules.

Tuft cells are a rare, specialized lineage of chemosensory cells important in regulating mucosal type 2 responses. These cells can produce interleukin 25 (IL-25) in response to succinate or helminths, which in turn activates gut resident group 2 innate lymphoid cells (ILC2) to produce interleukin 13 (IL-13) (Gerbe et al., 2016; Howitt et al., 2016; von Moltke et al., 2016; Nadjsombati et al., 2018). IL-13 promotes increased tuft cell and goblet cell differentiation, as well as smooth muscle hyperplasia (Schneider et al., 2018). Increased mucus production and smooth muscle contraction facilitate parasite expulsion, termed as 'weep and sweep'response.

Another chemosensory cell subset, enteroendocrine cells, represent only 1% of the IECs and secrete a variety of peptide hormones (e.g. 5-HT, somatostatin, PYY, CCK, GLP1/2) regulating appetite, pancreatic juice and bile secretion, intestinal motility in response to luminal nutrients(Gribble & Reimann, 2016).

Microfold cells (M cells) are found in the follicle associated epithelium (FAE) overlying the small intestinal Peyer's patches (PP) of the gut associated lymphoid tissue (GALT). These specialized cells perform transcytosis of luminal antigens across epithelium and into the subepithelial dome of the PPs. In the subepithelial dome, transcytosed antigens can be picked up

by the dendritic cells (DCs). Sampling of luminal antigens by M cells is an important step in initiating mucosal immune responses. Specifically, Peyer's patches are a major inductive site of immunoglobulin A (IgA) producing plasma cells (PCs). In mice lacking M cells the IgA responses are impaired(Rios et al., 2016). Deletion of M cell endocytic receptor glycoprotein 2 (GP2) attenuated the uptake of type-I piliated bacteria and antigen specific IgA responses (Hase et al., 2009). Induction of IgA responses in the PPs will be reviewed in grated detail in section 1.3.

1.1.2.Intraepithelial lymphocytes

Intraepithelial lymphocytes (IELs) are tissue resident immune cells localized above the basement membrane and in between intestinal epithelial cells. Intestinal IELs are predominantly T cells and can be divided into natural or peripherally induced based on their developmental pathways.

In mice, natural IELs include CD8 $\alpha\alpha$ + or double negative (DN) TCR $\gamma\delta$ or TCR $\alpha\beta$ expressing T cells. These cells develop independently of microbial or dietary antigens early in life. Natural TCR $\alpha\beta$ IELs acquire their fate in the thymus upon stimulation by agonist self-antigens(Leishman et al., 2002; McDonald et al., 2014). Natural TCR $\gamma\delta$ arise in and outside the thymus. These cells are selected to seed their niche by butyrophilin-like self-ligands expressed by intestinal epithelial cells (Di Marco Barros et al., 2016). Both TCR $\gamma\delta$ or TCR $\alpha\beta$ natural IELs acquire gut homing receptors CCR9 and integrin $\alpha_4\beta_7$ directly after development. CCR9 guides the cells towards CCL25 produced by IECs, while $\alpha_4\beta_7$ binds to mucosal addressin cell adhesion molecule 1 (MAdCAM1) of gastrointestinal vascular endothelial cells.

Peripherally induced IELs include CD8 $\alpha\beta$ + TCR $\alpha\beta$ and CD4+ TCR $\alpha\beta$ expressing T cells. These cells follow developmental pathways of conventional CD8+ or CD4+ T cells in the thymus. They acquire gut imprinting CCR9 and $\alpha_4\beta_7$ expression after interaction with cognate antigens

presented by retinoic acid (RA) producing DCs in the GALT(Mora et al., 2003; Iwata et al., 2004). Accumulation of peripherally induced IELs in the intestinal epithelial compartment depends on microbial or dietary antigens, as their numbers decrease in germ-free (GF) and antigen-free diet fed mice (Kawaguchi et al., 1993; Suzuki et al., 2002; Di Marco Barros et al., 2016; Lockhart et al., 2023). Their number increase in presence of specific microbial species or during infections. For example, Bacteroidetes derived β-hexosamidase induces differentiation of CD4+CD8αα+ IELs (Bousbaine et al., 2022). Colonization of GF mice with *Segmented filamentous bacteria* lead to accumulation of CD8αβ+ IELs. CD8αβ+ IELs responding to K^d-restricted listeriolysin O epitope (LLO₉₁₋₉₉) are recruited to intestinal epithelium after oral infection with pathogenic *Listeria monocytogenes* (Sheridan et al., 2014). Both CD8αβ+ and CD4+ IELs can be also recruited to the epithelial compartment upon enteric viral infection.

Once in the intestine, IELs receive and integrate myriad of environmental cues required for their retention and tissue adaptation. TGF- β signaling leads to downregulation of $\alpha_4\beta_7$ and upregulates integrin $\alpha_E\beta_7$ expression in IELs (El-Asady et al., 2005; Konkel et al., 2011; Zhang & Bevan, 2013). $\alpha_E\beta_7$ binds to epithelial cadherin (E-cadherin) and facilitates IEL tissue retention (Cepek et al., 1994; Schön et al., 1999). Interleukin-15 (IL-15) produced by IECs is an important survival signal for natural IELs. All intestinal IELs express aryl hydrocarbon receptor (AhR), which ligands include exogenous xenobiotics, microbiota- or diet- derived compounds and endogenous tryptophan metabolites. AhR signaling is required for IEL survival and maintenance (Li et al., 2011; Cervantes-Barragan et al., 2017; Panda et al., 2023).

The residency of the IELs at the mucosal barrier enables constant surveillance and rapid response to insults. The rapid responses are ensured by expression of NK receptors, the presence of cytotoxic granules containing granzyme and perforin, along with effector cytokine production.

In mice, both IEL subsets contain cytotoxic granules. Natural IELs appear to be more likely to express NK receptors. Expression of NKG2D-activating receptor recognizing non-classical MHC-I molecules, such as stress-induced MICA/B (human) or Rae1 (mouse), allows IELs to respond to potential insults without TCR engagement (Hüe et al., 2004; Zhou et al., 2007). In addition to activating NK receptors, IELs express slew of inhibitory receptors, keeping the cells at "activated, yet resting" state (Vandereyken et al., 2020). Presence of cytotoxic granules allows the direct killing of affected target cells(Müller et al., 2000). Production of effector cytokines, such as IFNγ, was shown to protect the host from overt pathology during *C. rodentium* infection (Navabi et al., 2017; Malik et al., 2023) and can control viral replication (Parsa et al., 2022). This functional specialization and strategic localization within epithelial layer allow rapid responses and effective protection of the intestinal barrier. Although IELs are critical immunological components of the intestinal barrier maintaining its homeostasis, uncontrolled activation or pathogenic reprogramming of IELs can lead to tissue destruction and loss of barrier integrity observed in celiac disease or inflammatory bowel diseases (IBD) (Cheroutre et al., 2011).

1.1.3. Lamina propria lymphocytes

Beneath the intestinal epithelium, separated from by the thin layer of basement membrane, lies the lamina propria. This layer of connective tissue provides mechanical support to intestinal villi, is highly vascularized and rich in lymphatics supporting nutrient absorption. It also contains a diverse array of mesenchymal stromal cells and immune cells, maintaining tissue homeostasis, regulating immune responses, and defending against pathogens. Major immune cell types represented in lamina propria include, among innate immune cells, mast cells, innate lymphoid cells (ILCs), macrophages, DCs and eosinophils; and among adaptive immune cells T cells and plasma cells (PCs). Mast cells are tissue resident myeloid cells characterized by the presence of

cytoplasmatic granules containing various immune modulatory mediators, including vasoactive histamine, aiding in initiation of immune responses. Mast cells are also potent producers of serotonin metabolite 5-HIAA. In the PPs, mast cell derived 5-HIAA controls DC positioning in the subepithelial dome and supported intestinal IgA responses (De Giovanni et al., 2024). Among ILCs, GATA-3+ ILC2s and RORyt+ ILC3s are the most abundant in the small intestinal lamina propria. Both subsets are important in reinforcing the intestinal barrier. ILC2s partake in antihelminth responses through production of IL-13 and IL-5 regulating goblet cell mucus production and smooth muscle hyperplasia. ILC3s produce IL-22, which provides protection against bacterial pathogens by inducing expression of antimicrobial peptide RegIIIy in the epithelium. Early in development, related RORyt+ Lymphoid Tissue inducer (LTi) cells play a key role in development of lymphoid tissues, including mesenteric lymph nodes (mLNs) and PPs(Eberl et al., 2004). Intestinal macrophages phagocytose and degrade cellular debris and invading pathogens; they also can express and respond to IL-10 to maintain tissue homeostasis (Hadis et al., 2011; Shouval et al., 2014). DCs initiate mucosal adaptive immune responses. Two main migratory DCs subsets can be localized in the intestinal LP: IRF8-/BATF3-dependent XCR1+CD103+CD11b- cDC1s and IRF4-/Notch2-dependent SIRP1\alpha+CD103+CD11b+ cDC2s. These cells can sample local antigens and migrate through lymphatics to the secondary lymphoid organs, where sampled antigens are presented to naïve T cells. In absence of inflammation, intestinal DCs induce gut-tropic IL-10 producing Foxp3+ peripheral regulatory T cells (pTregs), promoting tolerance to dietary and innocuous commensal microbiota-derived antigens(Lathrop et al., 2011; Kim et al., 2016). Another T cell subset often found in the LP are Roryt+ IL-17 and IL-22 producing Th17 cells, induced in response to specific commensals (SFB) or bacterial pathogens (Zheng et al., 2008; Ivanov et al., 2009).

At homeostasis, the intestinal lamina propria contains large numbers of antibody secreting PCs. Most of these PCs produce dimeric IgA. IgA+ PCs are distributed throughout the intestinal lamina propria, with the greatest abundance observed in the small intestine(Bunker et al., 2015; Earley, 2021). IgA-secreting PC numbers are low in the intestines of human infants (Perkkiö & Savilahti, 1980; El Kaissouni et al., 1998) and GF mice (Moreau et al., 1978; Earley, 2021), and can increase with age and upon microbial colonization, respectively. IgA responses are generated in the intestinal GALT: mLNs, PP, isolated lymphoid follicles, and cecal patch. Once induced, gut resident PCs produce enormous amounts of IgA, 40-60 mg/kg/day which can be secreted by IECs into the gut lumen (Fagarasan et al., 2010).

1.2.Ontogeny of intestinal IgA secreting plasma cells

The IgA producing PCs can differentiate from naïve B cell precursors in T cell dependent (TD) or T cell independent (TI) manner. In mice, naïve B cells can be divided into two subsets: B-1 and B-2 cells. B-1 cells can be further divided into B-1a and B-1b subsets based on CD5 surface expression. B-2 cell subset includes follicular (FO) B cells and marginal zone (MZ) B cells.

B-land MZ are classified as "innate-like" B cell subsets. In mice, bone marrow derived MZ B cells reside primarily in the MZ of the spleen. Their main function is capture and delivery of blood-borne antigens to splenic follicles, as well as rapid generation of low affinity IgM antibodies in response to blood-borne pathogens (Cinamon et al., 2008; Cerutti et al., 2013). B-l cells reside primarily in the peritoneal and pleural cavities. CD5+ B-la cells are a fetal hematopoietic stem cell-derived, self-renewing population of B cells with partially restricted repertoire (Bunker et al., 2015). B-la cells are major producers of "natural" IgM antibodies (i.e. germline encoded, produced without prior antigen encounter) recognizing polysaccharides or

phospholipids. Best described example is the protective anti-phosphorylcholine T15Id+ antibody recognizing moieties on bacterial cell wall of *S. pneumoniae*. CD5- B-1b cells can develop from both fetal and adult hemopoietic stem cells (HSC) (Barber et al., 2011) and opposed to B-1a cells, contain broad repertoire (Bunker et al., 2015). T-independent IgM responses generated by B-1b cells can protect the host from systemic *B. hermsii* and *S. typhimurium* infections. Unlike B-1a and MZ B cells, lipopolysaccharide-stimulated B-1b cells can readily switch to IgA in presence of RA and transforming growth factor β (TGF β). Furthermore, transfer of B-1b cells to *Rag1*-/- hosts (lacking T and B cells) results in generation of IgA+ PCs in the intestinal LP and coating of the luminal microbiota by sIgA (Bunker et al., 2015). These data suggest that intestinal IgA-producing PCs can originate from T-independent "innate-like" B-1b cell response in mice.

However, IgA+ PC primarily differentiate from bone marrow derived, conventional FO B cells of the B-2 lineage. These cells reside in the follicles of the secondary lymphoid organs, including PP and mLNs of the GALT. Following activation, their class-switch recombination towards IgA isotype can involve both TD and TI mechanisms, which can occur in mLNs and PPs (TD and TI) or isolated lymphoid follicles (TI). TD antigens are usually proteins (e.g. cholera toxin) while TI antigens include polyclonal activators such as LPS, or highly repetitive structures such as capsular polysaccharides.

1.3. T-dependent and T-independent IgA responses

Luminal antigens sampled by M cells within the follicle associated epithelium (FAE) are released into the DC-rich subepithelial dome (SED), and subsequently into the B cell follicles, where it can be deposited on follicular dendritic cells (FDCs) (Lycke & Bemark, 2017). Encounter with the cognate antigen and B cell activation leads to upregulation of CCR6 on the cell surface. CCR6 is a G-protein-coupled receptor mediating migration of recently activated B cells towards

CCL20, produced by FAE (Reboldi et al., 2016). This allows entry of recently activated B cells into the SED, where IgA CSR is initiated. CSR is mediated by activation-induced cytidine deaminase (AID) and takes place between two switch (S) regions. It requires expression of the germline transcripts initiated upstream the target S region (S α). The expression of germline transcripts required for the CSR is informed by the local cytokine milieu. The class switching to IgA isotype is instructed by TGF β (van Ginkel et al., 1999; Cazac & Roes, 2000; Gros et al., 2008), which in extracellular space is stored in a latent form, and can be activated by α v β 8 integrin present on SED resident DCs.

After CSR initiation, activated B cells can migrate back to the center of the PP and enter a local germinal center (GC). The GCs of the GALT in conventionally raised mice are chronically present due to continuous exposure to microbiota derived antigens (Fagarasan et al., 2010). The GCs are aggregates of FDCs, CXCR5+PD-1+ TFH cells and B cells, that can be divided into light and dark zone (Victora & Nussenzweig, 2022). In the dark zone, GCs B cells divide and undergo affinity maturation by initiation of somatic hypermutation (SHM). The SHM of the B cell receptor (BCR) is also mediated by the AID (Fagarasan et al., 2002). The cytidine deamination leads to introduction of point mutations in the variable regions of the immunoglobulin gene. Mutated BCRs are then selected based on their ability to efficiently uptake FDC deposited antigens and present them to TFH cells in the light zone. Upon recognition of peptide-MHCII complexes, TFH cells provide pro-survival selection signal through upregulation of the TNF superfamily molecule CD40L, which engages CD40 present on GC B cells (Cerutti, 2008). Recurring cycles of light zone antigen presentation and T cell help, followed by division and SHM in the dark zone, facilitates generation of high-affinity antibodies. Accordingly, CD40 deficient mice do not generate IgA responses following oral immunization with cholera toxin, a TD antigen (Bergqvist et al., 2006). Of note, sIgA is only slightly diminished the lumen of CD40 deficient mice, underlining the importance of TI pathway of IgA generation.

A significant proportion of the microbiota-binding sIgA can be derived from TI pathway. Analogous to the role of CD40L in TD responses, TI responses are also facilitated by the members of the TNF superfamily: A proliferation-inducing ligand (APRIL) and B cell-activating factor of the TNF family (BAFF) (Litinskiy et al., 2002; Castigli et al., 2005). These molecules can be produced by DCs, plasmacytoid DCs, eosinophils, stromal cells and IECs. Three B cell receptors can interact with BAFF/APRIL: B cell maturation antigen (BCMA), BAFF receptor (BAFFR) and transmembrane activator and calcium-modulator and cyclophilin ligand interactor (TACI). While TACI deficiency does not affect IgA responses to the TD antigen cholera toxin, it leads to 2-fold decrease in bacterial IgA-coating and luminal IgA titers (Grasset et al., 2020). sIgA generated in TI manner is characterized by low affinity.

1.3.1. Homing and tissue maintenance of IgA-secreting cells

IgA-switched B cells generated in PP migrate through lymphatics to mLNs, from where they enter the bloodstream though the thoracic duct and home to the intestinal LP (Bunker & Bendelac, 2018). Migration to the small intestinal LP is supported by integrin α4β7 and CCR9; α4β7 binds MAdCAM-1 on intestinal high endothelial venules, while CCR9 guides the cells towards CCL25 produced by IECs. Expression of gut-homing α4β7 and CCR9 is imprinted on IgA-switched cells by retinoic acid produced by RALDH2+ DCs of the GALT. IgA+ B cells can also express CCR10. CCR10 ligand, CCL28, can be produced by enterocytes, colonocytes, in the salivary gland, and the mammary gland during lactation, thus can support migration of IgA producing cells to other niches (Pan et al., 2000; Wilson & Butcher 2004). In-vivo neutralization of CCL28 results in decreased homing of CT-specific IgA PCs to the colon, and decreased

migration of IgA+ PCs to the mammary gland (Hieshima et al., 2004; Wilson & Butcher 2004). The latter abolishes IgA from the milk, which confers passive immunity in the infant's gut. IgA+ PCs can also migrate to the bone marrow, where they give rise to long lived plasma cells (Lemke et al., 2016).

Once in their respective niches, maintenance of differentiated IgA+ PCs can be supported by several factors, including APRIL, BAFF and IL-6(Lycke & Bemark, 2017). In the intestinal LP these cytokines can originate from several cellular sources. LP resident eosinophils can produce IL-6, APRIL, and BAFF in MyD88/TRIF-dependent manner (Chu et al., 2014). In mice lacking this subset, number of LP IgA PCs and fecal IgA titers are reduced. Eosinophils similarly contribute, along with stromal derived signals, to maintenance of long-lived plasma cells (LLPCs) in the bone marrow (Chu et al., 2011). In the gut, the IECs can be another source of APRIL and can further stimulate its production by LP DCs through thymic stromal lymphopoietin (TSLP) (He et al., 2007). It is yet to be determined whether additional stroma-derived factors or signals are involved in this process.

Initial studies investigating the relative lifespan and turnover of murine intestinal IgA+ PCs estimated their half-life to be 5 days, with maximal persistence of 7-8 weeks (Mattioli & Tomasi, 1973). More recently, it was demonstrated that IgA PC can persist in the LP for extended periods of time. Reversible colonization of GF mice with an auxotrophic *E.coli* K-12 strain induced robust specific IgA response, which persisted for 16 weeks. Importantly, the studied mice returned to germ-free state 48h after last oral inoculation, meaning that the induced response was maintained for over 100 days from the last antigenic exposure (Hapfelmeier et al., 2010). Similarly, the clonal composition of IgA repertoire in mice was stable over time, even when microbial composition was skewed by antibiotic treatment (Lindner et al., 2015). Lastly, IgA+ PCs generated in response to

toxins and pathogens appear to be long-lived. Oral immunization with CT-OVA generated IgA+ PCs that persisted in the LP for 9 months (Lemke et al., 2016). Rotavirus neutralizing IgA was detected in the stool 14 months after the first exposure, and protected the against subsequent infection (McNeal & Ward, 1995). This research suggests that at least some IgA+ PCs generated in response to commensals or pathogens can be maintained in the intestinal LP long-term.

1.3.2.IgA secretion

In the mucosa, IgA is secreted as a dimer, with C-terminal tailpiece of the antibody heavy chain linked to the joining (J) chain by disulfide bonds. The J chain can also bind to pIgR, present on the basolateral side of IECs. Binding of polymeric immunoglobulin to pIgR triggers internalization and transcytosis of the complex across the epithelium. At the apical side, the extracellular domain of pIgR is cleaved and the polymeric antibody is secreted into the lumen. The cleaved extracellular domain of pIgR, termed secretory component (SC), remains covalently bound to the IgA; secreted dimeric IgA linked to SC is termed secretory IgA (sIgA). Once in the lumen, some of the sIgA remains in the mucus layer, anchored to it by SC (Phalipon et al., 2002; Rogier et al., 2014). The vast majority of sIgA however is found in association with the luminal microbiota (Palm et al., 2014; Bunker et al., 2015). Thus, alongside the mucus and antimicrobial peptides, sIgA a key component of the intestinal mucosal barrier positioned at its forefront.

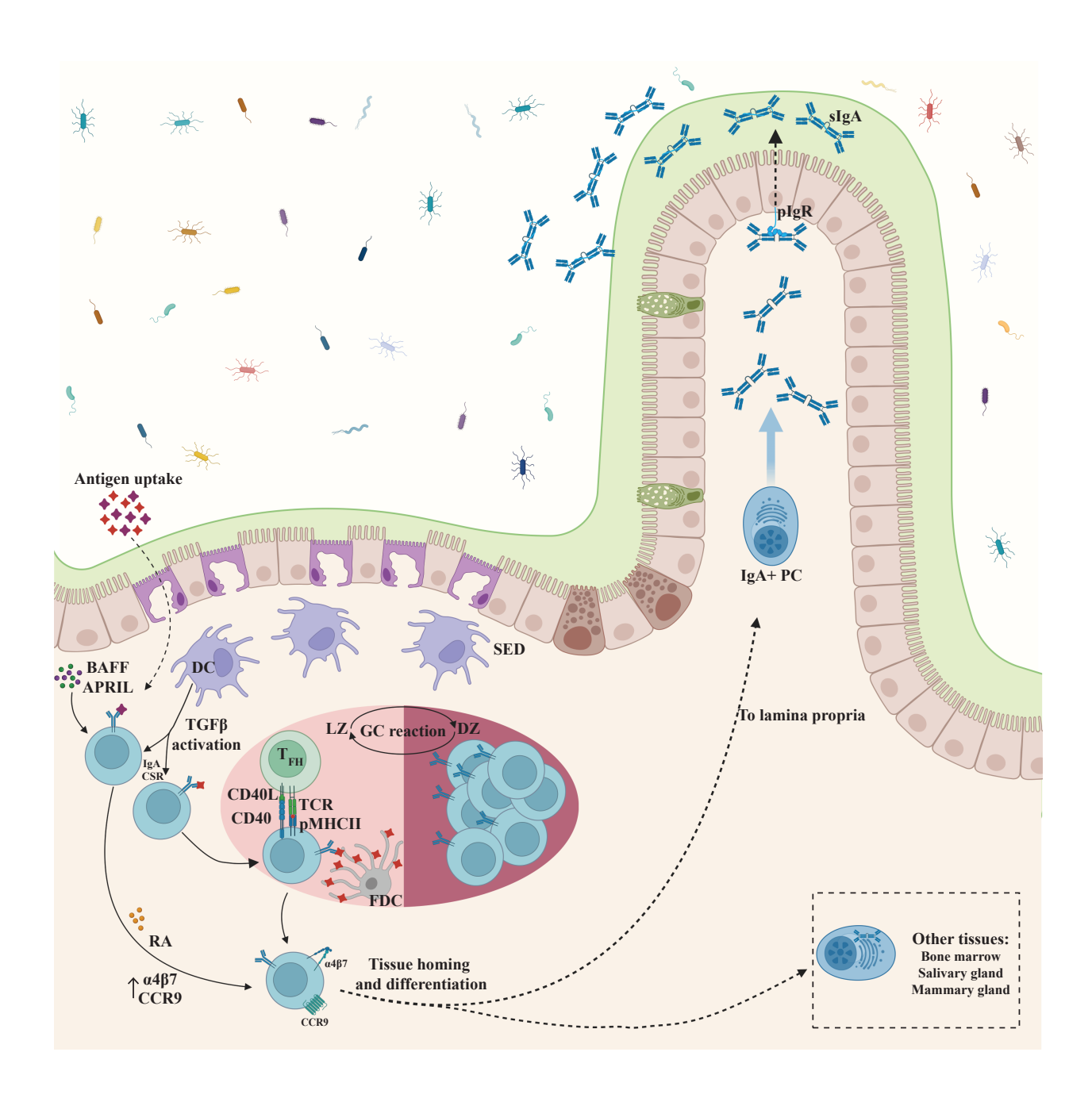


Figure 1: IgA+ plasma cell differentiation.

Naïve B cells are activated by their cognate antigen and migrate to SED, where the resident DCs activate latent TGFβ. This initiates IgA CSR. TI antigens (purple) can induce IgA response, further supported by local APRIL/BAFF produced by stromal and immune cells. TD antigen (red) activated B cells migrate to the local germinal center to undergo affinity maturation. In the dark zone B cells divide and hypermutate the variable regions of the immunoglobulin gene. This is followed by migration and selection in the light zone, where highest affinity BCR will allow efficient uptake of the cognate antigen deposited on FDCs. T_{FH} cells, after recognition of antigen processed and presented by the B cells, provide pro-survival selection signal through upregulation of the CD40L, which engages CD40 present on GC B cells.

Figure 1: IgA+ plasma cell differentiation continued.

Affinity matured cells exit the germinal center. Local signals, such as RA, promotes the upregulation of gut homing receptors. IgA+ B cells recirculate to enter mucosal sites, undergo differentiation into plasma cells, and secrete IgA. Secreted IgA can bind to pIgR via J chain and undergo transcytosis into the intestinal lumen. Luminal sIgA consists of IgA dimer bound by J chain and secretory component. SED, subepithelial dome. GC, germinal center. LZ, light zone. DZ, dark zone. T_{FH}, T follicular helper cell. APRIL, A proliferation-inducing ligand. BAFF, B cell-activating factor of the TNF family. CSR, class switch recombination.

1.4. Functions of sIgA

1.4.1.Impact bacterial IgA coating

sIgA performs various protective and homeostatic functions in the intestinal mucosa. Protective functions of sIgA include neutralization of ingested toxins and virulence determinants, facilitating immune exclusion of the pathogens, altering their motility, or agglutinating pathogens to promote their clearance. In homeostasis, sIgA can modulate composition or resident microbiota, regulate microbial colonization, and promote antigen uptake by M cells.

Compared to other antibody isotypes (e.g. IgG), IgA is a poor opsonin and a weak activator of the complement. At the mucosal surfaces sIgA often acts as a neutralizing antibody. It was previously reported that IgA protects from re-infection with rotaviruses (Blutt et al., 2012) and reoviruses (Silvey et al., 2001) in mice. The protective IgA antibody was neutralizing the T1L reovirus σ1 outer capsid protein, thereby preventing its adhesion to M cells and viral entry (Hutchings et al., 2004). sIgA can also neutralize bacterial toxins, such as cholera toxin of *V.cholerae*, and prevent its binding to IECs (Apter et al., 1993). sIgA facilitates immune exclusion of pathogens through agglutination and enchained growth. Monoclonal antibody specific to *S.* ser. Typhimurium[‡] O-antigen was shown to prevent systemic dissemination after oral infection. It was later demonstrated in vitro that IgA binding to *S.* ser. Typhimurium can agglutinate the bacteria at high densities and arrests its swimming mobility at low densities. Similarly, *V. cholerae* O-antigen specific IgA provided protection after the oral challenge, mediated agglutination of the bacteria and inhibited their motility in vitro (Levinson et al., 2015). It is unclear whether the observations made in the IgA-treated bacterial cultures are relevant or occur in vivo, where pathogen density is

[‡]S. enterica subspecies enterica serovar Typhimurium

vastly different. Enchained growth was proposed as an alternative mechanism of IgA-mediated protection, that seem to be more likely to take place in vivo. sIgA generated after oral immunization with inactivated *S.* ser. Typhimurium was shown to enchain progeny of dividing pathogen, generate clonal clumps of bacteria and accelerate its clearance (Moor et al., 2017). Lastly, highly IgA-coated bacteria isolated from stools of IBD patients can exacerbate DSS colitis outcomes once transferred to GF mice (Palm et al., 2014). In disease states, proficient IgA coating might point towards pathobionts.

Certain commensal bacteria can benefit from being bound by sIgA. Bacteroides fragilis was robustly colonizing specific mucosal niches in the colon when coated with IgA (Donaldson et al., 2018). Upon colonization, B. fragilis upregulated production of capsular polysaccharides to induce specific sIgA, which subsequently coated the bacteria and promoted the colonization. sIgA binding to capsular polysaccharides was also shown to alter bacterial gene expression. To maintain symbiotic relationship with the host, Bacteroides thetaiotaomicron downregulated expression of a specific capsular polysaccharide (CPS4) once it was bound by monoclonal IgA antibody in vivo (Peterson et al., 2007). This was later confirmed in immunocompetent mice; the modulation of capsular polysaccharide expression by B. thetaiotaomicron can provide a competitive advantage under immune pressure (Porter et al., 2017). Binding of sIgA to bacterial cell was also shown to modulate its metabolism, protect from bile or phages, or alter its motility (Rollenske et al., 2021). Lastly, sIgA can also exclude specific bacteria from privileged intestinal niches. For example, sIgA restricts colonization of epithelium-attaching SFB to the terminal ileum. SFB is IgA-coated, and its coating is T cell-dependent (Bunker et al., 2015). In IgA deficient hosts, the density of the SFB in the ileum increases, and the bacteria can attach to the jejunal epithelium (K. Suzuki et al., 2004; Earley et al., 2023).

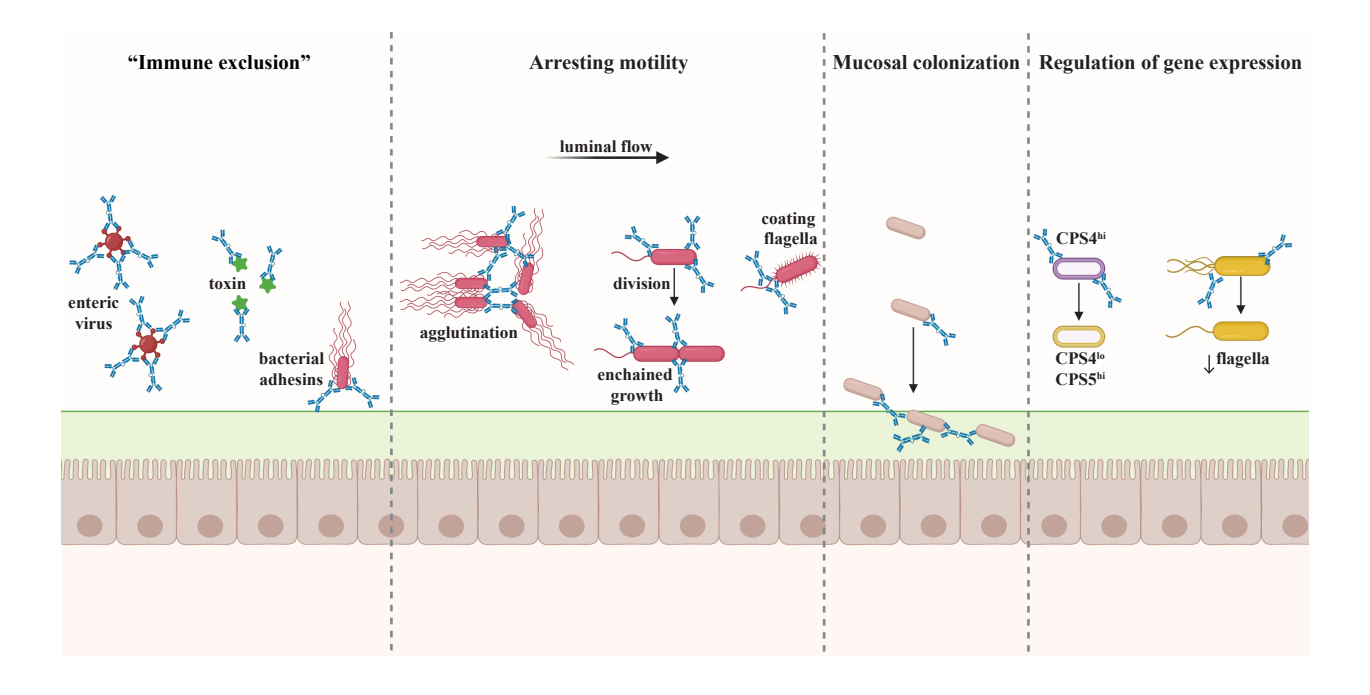


Figure 2: Functions of sIgA.

sIgA can facilitate immune exclusion by coating viral proteins or bacterial adhesins to prevent the cell entry. It can also neutralize bacterial toxins. sIgA can promote pathogen clearance by immobilizing its targets via agglutination, enchained growth, or direct binding to flagella followed by excretion with luminal flow. sIgA can promote mucosal colonization by specific commensals (*B. fragilis*). Binding of sIgA to bacteria can also modulate expression of capsular polysaccharides (CPS) or flagella.

1.4.2.Impact of IgA deficiency on disease

IgA deficiency is one of the most common primary immunodeficiencies, occurring at frequencies ranging from 1 in 300 to 1 in 18500, depending on the assessed population (Singh et al., 2014). Many IgA deficient individuals remain asymptomatic. However, some IgA-deficient patients are more susceptible to recurrent respiratory or gastrointestinal infections (Koskinen, 1996; Aghamohammadi et al., 2009). The incidence of allergies, and autoimmune diseases, such as rheumatoid arthritis or coeliac disease, is higher in IgA deficient patients (Collin et al., 1992; Ballow, 2002; Singh et al., 2014). The intestinal microbiome of IgA deficient patients was found to have altered composition when compared to control patients (Fadlallah et al., 2018; Catanzaro et al., 2019).

Very low serum and mucosal IgA levels in common variable immunodeficiency (CVID) patients had been associated with the prevalence of enteric viruses and gastrointestinal symptoms. Chronic norovirus infection in CVID patients was linked to development of inflammation and enteropathy (Strohmeier et al., 2023). While CVID can affect the production of other immunoglobulin isotypes besides IgA, the absence of mucosal IgA plasma cells specifically was correlated with increased inflammation and disrupted tissue homeostasis (Strohmeier et al., 2023). Furthermore, epidemiological studies have demonstrated that IgA deficiency sometimes progresses into CVID in humans, likely due to shared genetic predispositions (Hammarstrom et al., 2000; Singh et al., 2014).

Several genetic approaches were used to assess the role of IgA deficiency in mice. First mouse model of IgA deficiency was generated by deletion of IgA switch and constant region. IgA deficient mice presented no overt intestinal pathology in homeostasis, and only subtle changes in gut microbiota composition. Similar observations were made in mice lacking AID (Fagarasan et

al., 2002; Keiichiro Suzuki et al., 2004). Increase of IgM in mucosal secretions was prominent in both models. This was a consequence of the deletion of IgA switch region (IgA deficient mouse) and lack of CSR (AID deficient mice). IgM is a polymeric immunoglobulin associated with Jchain, can bind to pIgR and undergo transepithelial secretion, which made the role of IgA challenging to discern. Commensal microbiota in pIgR deficient mice was altered compared to controls (Reikvam et al., 2012). Surprisingly, pIgR deficient mice were more susceptible to dextran sodium sulfate (DSS) induced colitis (Murthy et al., 2006; Reikvam et al., 2012). This was in contrast to IgA deficient mice, which response to DSS treatment was comparable to that of control animals (Murthy et al., 2006). This further solidified a possibility of IgM secretion compensating for absence of sIgA. The caveat of pIgR deficient mouse model was the increased mucosal levels of IgG (Johansen et al., 1999). The discrepancies between models of IgA deficiency led us to design of a novel model of IgA deficiency, IgA secretory deficient mouse (Ighasec-/-), which bypasses the increased IgM production. This allowed us to address a long-standing question of how IgA maintains immune homeostasis with the microbiota, and whether IgM compensates for IgA deficiency.

1.5.Summary

The mucosal barrier of the gastrointestinal tract is essential for maintaining tolerance to the commensal microbiota and protecting the host from pathogenic infections. A vital component of this barrier is secretory IgA (sIgA), which coats up to 70% of the microbiota in the small intestine (Bunker et al., 2015) and represents the most abundant antibody isotype produced in the mammalian gastrointestinal mucosa (van der Heijden et al., 1987). IgA deficiency is one of the most common primary immunodeficiencies occurring at frequencies ranging from 1 in 300 to 1 in 18500 in various populations (Singh et al., 2014). While most IgA deficient individuals are

asymptomatic, some reports link IgA deficiency to increased susceptibility to infections (Koskinen, 1996; Aghamohammadi et al., 2009) and autoimmune diseases in humans (Collin et al., 1992; Ballow, 2002; Singh et al., 2014). Studies in mice suggest that sIgA may both restrict colonization by the adherent commensal segmented filamentous bacteria (SFB) (K. Suzuki et al., 2004; Earley et al., 2023) and promote mucosal bacterial colonization (Donaldson et al., 2018). Additional studies suggest that sIgA regulates bacterial gene expression and metabolism (Peterson et al., 2007; Peterson et al., 2015; Rollenske et al., 2021), confers protection against mucosal infections (Phalipon et al., 1995; Hutchings et al., 2004; Blutt et al., 2012; Moor et al., 2017), and neutralizes toxins (Lycke et al., 1999; Fernandez et al., 2003). Together these observations support a role for sIgA in regulating host-bacterial interactions at mucosal surfaces. While IgA deficiencies have been associated with increased viral infections in humans, no experimental evidence has demonstrated that IgA directly regulates viral colonization to ensure immune homeostasis.

Confounding interpretations of IgA function is potential IgM compensation. IgM is a pentameric immunoglobulin covalently associated with the joining chain (J-chain); thus, it can be transported to the intestinal lumen by polymeric Ig receptor (pIgR). IgM was reported to coat intestinal microbes in AID deficient mice (Bunker et al., 2015) and IgA deficient humans (Catanzaro et al., 2019). These data point to a hypothesis that IgM may compensate for and control the microbiota in conditions of IgA deficiency. Analogous to IgA deficient patients (Barros et al., 1985; Fadlallah et al., 2018), the original IgA deficient mouse model (*Igha-/-*) exhibits an increase of serum and mucosal IgM (Harriman et al., 1999). This emphasizes the need for a model of IgA deficiency devoid of increased IgM responses to assess the function of IgA.

To gain insights into how IgA deficiency may disrupt immune homeostasis we designed a novel mouse model of IgA deficiency devoid of compensatory IgM responses. The IgA secretory

deficient (Ighasec-/-) mouse was generated through deletion of the secretory tailpiece and its downstream polyadenylation (polyA) sites. Unlike in the original IgA deficient mouse (Igha-/-), which lack IgA switch and constant region, Ighasec-/- B cells retain the ability to class switch and express IgA on the cell surface. Using SPF and GF Ighasec-/-, we observed a microbiota-dependent expansion of CD8αβ+ intraepithelial lymphocyte (IELs) T cells in the small intestine of IgA deficient mice. These IELs showed features of antigen drive and were licensed by cDC1s. Using microbial transfers, metagenomic, and transcriptomic sequencing, we identified that IgA neutralized murine astrovirus (MuAstV) to limit inflammatory T cell responses in the intestine. In the absence of IgA, MuAstV chronically infected IECs and drove a CD8αβ+ T cell expansion to limit host interferon responses. Notably, GC B cells and T cell-dependent IgA were necessary for the host to control MuAstV. In addition, we found that IgA was critical in controlling other enteric viruses, such as murine norovirus strain CR6, and protecting the host from immunopathology. Our findings provide insight into specific IgA-virome interactions essential for maintaining intestinal immune homeostasis. Our study sheds light on the specific interactions between IgA and the gut virome, which are crucial for maintaining intestinal immune homeostasis and preventing immunopathology.

2.MATERIALS AND METHODS

This chapter includes experimental procedures from an article that was submitted for publication in Cell Host Microbe.

2.1.Mice

Batf3-/- (Strain #:013755) (Hildner et al., 2008), B2m-/- (Strain #:002087)(Koller et al., 2010) and K^bD^b -/- (Strain #:019995) (Vugmeyster et al., 1998), IL10-/- (Strain #:002251) (Kuhn et al., 1993) mice were purchased from The Jackson Laboratory and crossed to *Ighasec-/-* mice to generate double or triple knock-out lines. B cell deficient mice lacking IgH J locus, JH-/-, were using Cas9 GCTACTGGTACTTCGATGTC generated and protospacers and GCCATTCTTACCTGAGGAGA. Classical IgA deficient line, *Igha-/-*, lacking IgA switch region (Sa) and 5' fragment of the C1 α exon was generated using Cas9 and protospacers AAGCGGCCACAACGTGGAGG and TCAAGTGACCCAGTGATAAT. Secretory IgA deficient line, Ighasec-/-, lacking secretory tailpiece and downstream secretory polyadenylation signal (CSα + polyA) was generated using Cas9 and protospacers TGTCTGTGATCATGTCAGA and GGGGCCATCTCAAGAACTGC. JH-/-, IgA deficient mice and IL10-/- were rederived germ-free (GF) at Taconic Biosciences. GF mice were housed in gnotobiotic isolators at University of Chicago Gnotobiotic Research Animal Facility and routinely screened for sterility by culture or 16S rRNA gene qPCR. Some GF *Ighasec+/-* and *Ighasec-/-* mice were monocolonized with NYU1 MuAstV. Bcl6 fl/fl CD4^{Cre} and Bcl6 fl/fl CD21^{Cre} mice were obtained from Jason G. Cyster and were housed at UCSF animal facility. For experiments, littermates were used at 8-12 weeks of age unless specified otherwise. Mice were fed a standard chow diet. Animal husbandry and experimental procedures were performed in accordance with Public Health Service policy and approved by the University of Chicago Institutional Animal Care and Use Committee.

2.2. Isolation of intraepithelial and lamina propria lymphocytes

Intestines were excised and divided into segments as previously described(Earley et al., 2023). 12 cm of duodenum (measured from the pyloric sphincter), jejunum (measured from the middle), ileum (measured from the ileocecal valve) and entire colon (from the cecum to the rectum) were collected to isolate the immune cells for flow cytometry. In the small intestinal segments, any Peyer's patches were removed and discarded. Segments were opened longitudinally and washed in phosphate-buffered saline (PBS) to remove mucus and any fecal matter. Intestines were then cut into 1cm pieces. Tissue was transferred into 50 mL conical tubes containing 12 mL of IEL isolation media: RPMI 1640 (Corning) supplemented with 1% dialyzed FBS, 2mM EDTA (Invitrogen) and 1.5 mM MgCl₂ (Invitrogen). To isolate IEL fraction, conical tubes containing media and the tissue were placed horizontally in an orbital shaker and incubated at 37°C, 250 rpm for 20 minutes. The media was then strained through 100 µm cell strainer (Corning) and kept on ice, while the remaining tissue was transferred into 12 mL of fresh IEL isolation media incubated as described above. Second IEL fraction was than combined with the first IEL fraction. Remaining tissue was then transferred into 50 mL conical tubes containing 12 mL of LP isolation media: RPMI 1640 (Corning) supplemented with 20% FBS and 41.5 CDU/mL of collagenase from Clostridium histolyticum (type VIII) (Sigma-Aldrich, C2139). To isolate LP lymphocytes, conical tubes containing media and the tissue were placed horizontally in an orbital shaker and incubated at 37°C, 250 rpm for 20 minutes. Similarly to the IEL isolation, this step was repeated for the total of two incubations. Fresh media was used for both, and collected fractions were combined after the second incubation. To remove debris, cells isolated from IEL and LP fractions were resuspended in 10 mL of 40% Percoll (GE Healthcare) and centrifuged at 3000 rpm for 12 minutes at RT. After the centrifugation, the upper fraction containing debris was removed. The pelleted

lymphocytes were resuspended and washed with 10 mL of PBS supplemented with 2% FBS to dilute out remaining percoll. Pelleted cells were then resuspended in 1mL of PBS supplemented with 2% FBS and counted on a hemocytometer.

2.3. Single cell tissue suspensions

Peyer's patches (PP) and mesenteric lymph nodes (mLNs) were excised and incubated in RPMI supplemented with 10% fetal bovine serum (FBS) and collagenase VIII (Sigma-Aldrich, C2139) at 37 °C for 30 min. Digested tissues were pressed through 70 μm cell strainer (Corning) to obtain single cell suspensions and quantified.

2.4.Ex-vivo cell stimulation

Up to 2.5x10⁶ of isolated cells were used for ex-vivo stimulation to determine cytokine production. Cells were resuspended in RPMI supplemented with 10% FBS incubated for 2 h (37°C with 5% CO₂) in 48-well plates in presence of ionomycin (750 ng mL⁻¹, Sigma-Aldrich), phorbol 12-myristate 13-acetate (50 ng mL⁻¹, Sigma-Aldrich) and Golgi stop (BD). After incubation, the stimulation was quenched on ice with ice-cold FACS buffer (PBS with 2% FBS), cells were harvested and stained for flow cytometry.

2.5.Flow cytometry

Cells were incubated with Fc-block (CD16/32) for 10 min at 4°C to prevent any non-specific binding, followed by staining with dead dye (LIVE/DEAD Aqua, Thermo Fisher or Zombie NIR, Biolegend) for 15 min at 4°C to determine cell viability. Cells were then incubated with antibodies detecting cell surface antigens for 20 min at 4°C. BD Cytofix/Cytoperm kit was used for intracellular cytokine staining. Briefly, after cell surface staining, cells were fixed in the dark for 20 min at 4°C in fixation/permeabilization solution, washed, and incubated with antibodies

detecting intracellular cytokines in Perm/Wash buffer for 40 min at 4°C. eBioscience Foxp3 / Transcription Factor Staining Buffer Set was used for intracellular transcription factor staining according to manufacturer instructions. All antibodies used in the study are listed in Table 1. The cells were acquired on Cytek Aurora (Cytek Biosciences) or sorted on Symphony S6 (BD Biosciences), and recorded events were analyzed using FlowJo (BD Biosciences). In all experiments, the cells were pre-gated as follows: FSC, SSC, singlets, and live. CD8αβ+ IELs were gated CD45+, TCRβ+, CD4-, CD8α+, CD8β+. T_{FH} cells were gated CD45+, TCRβ+, CD4+, CD8α-, CD44hi, CXCR5+, PD-1+. GC B cells were gated CD45+, CD19+ TCRβ-, CD38-, CD95+/GL7+. IgA plasma cells were gated as described previously(Bunker et al., 2015), EpCAM-, CD45+/lo, lineage negative (Ter119-, F4/80-, CD3-, Ly6G-, NK1.1-, CD19-), IgA+, B220-. Intestinal epithelial cells (IECs) were gated CD45- EpCAM+. For downstream RNAseq analysis, 50000 IECs from the jejunum and ileum were sorted into RLT buffer (Qiagen) supplemented with 2-mercaptoethanol (Sigma-Aldrich).

2.6.Bacterial flow cytometry

Small and large intestinal luminal contents were taken from WT, *Igha-/-* and *Ighasec-/-* mice and resuspended at a concentration of 0.1mg/μl in 1X PBS supplemented with protease inhibitors (Cell signaling). Luminal contents were then homogenized on a vortex for 5 min. Fecal debris was pelleted at 400 g for 5 min. The supernatant was collected and centrifuged at 8000 g to pellet bacteria. The bacteria were then washed, pelleted, and stained with SYTO BC (ThermoFisher) followed by anti-IgA PE (Southern Biotech) and anti-IgM AF647 (Southern Biotech). Bacteria were gated FSC, SSC, SYTOBC+, and IgA+/IgM+.

2.7.In-vivo cell depletion

To deplete CD8αβ IELs, mice were injected intraperitoneally with 250 μg of anti-CD8β monoclonal antibody (Bio X Cell, 53-5.8, Rat IgG1) for three weeks every other day. To deplete CD4 T cells, mice were injected intraperitoneally with 250μg of anti-CD4 monoclonal antibody (Bio X Cell, GK1.5, Rat IgG2b) for four weeks every three days. Control animals were injected with corresponding isotype antibodies (Bio X Cell, HRPN, Rat IgG1 or LTF-2, Rat IgG2b) for the duration of the depletion studies. Efficacy of the depletion was confirmed by flow cytometry using anti-CD8β (BD Biosciences, H35-17.2) or anti-CD4 (Biolegend, RM4-4) antibodies.

2.8. Antibiotic and antiviral treatments

6-8-week-old *Ighasec+/-* and *Ighasec-/-* mice were provided ampicillin (1g L⁻¹), vancomycin (0.5g L⁻¹), neomycin (1g L⁻¹), and metronidazole (1g L⁻¹) in drinking water for four weeks as described previously(Hall et al., 2008). In some experiments, combination of metronidazole and vancomycin, or singular antibiotic was provided to the mice for the duration of the treatment. All antibiotics were purchased from Sigma.

Anti-retroviral and anti-viral drug cocktails were administered daily to 4-week-old *Ighasec+/-* and *Ighasec-/-* mice for 4 weeks by oral gavage as described previously(Liu et al., 2019; Lima-Junior et al., 2021). Anti-retroviral treatment consisted of 100 mg kg⁻¹ of tenofovir (Arcos Organics) and 60 mg kg⁻¹ emtricitabine (Fisher Scientific). Anti-viral treatment consisted of 30 mg kg⁻¹ acyclovir (Fisher Scientific), 10 mg kg⁻¹ lamivudine (Fisher Scientific) and 30 mg kg⁻¹ and ribavirin (Fisher Scientific).

2.9. Viral infections

Viruses were administered to 4–6-week-old GF *Ighasec+/-* and *Ighasec-/-* mice by oral gavage. EDIM was a gift from N. Altan-Bonnet (NIH). Dose administered was 10⁴ plaque forming units

(PFU) of EDIM as described previously (Ghosh et al., 2022). MNV-CW3 and MNV-CR6 were a gift from C. Wobus (University of Michigan Medical School). Mice were infected with 3x10⁶ PFUs of MNV-CW3 or MNV-CR6 as described previously (Dallari et al., 2021). T1L reovirus was obtained from T.S. Dermody (University of Pittsburgh). Mice were inoculated with 10⁸ PFU of T1L (Bouziat et al., 2017). MuAstV was purified from fecal pellets of broad-spectrum antibiotic treated Ighasec-/- mice. Briefly, 4-6 fecal pellets were collected into sterile bead-beating tube containing 1.0 mm zirconia/silica beads (Fisher Scientific). Homogenization was performed after adding 1 mL of sterile PBS using Bead Ruptor Elite mill homogenizer (Omni) at a speed of 5 m/s for 1 min. Homogenates were centrifuged at 17000g for 5 min at 4°C to pellet the beads and fecal matter. Supernatants were collected and centrifuged at 17000g for 5 min at 4°C. This step was repeated twice to remove any remaining debris. 400 µL of the supernatant was collected from the top and diluted tenfold. Solution was filtered through 0.22 µm syringe-driven filter unit (Millipore Sigma). Filtration step was repeated three times. Virus stock was aliquoted and stored at -80°C. Virus titer was quantified as genome copy per µL by qPCR. Pure stock of NYU1 MuAstV was obtained from K. Cadwell (NYU). Mice were inoculated with 109 genome copies/mouse of the MuAstVs used (Dallari et al., 2021).

2.10.Microbial transfers

To colonize GF *Ighasec+/-* and *Ighasec-/-* mice with microbiota, 3-4 fresh fecal pellets were collected from ASF donor mouse purchased from Taconic Biosciences, C57BL6/J purchased from Jackson Laboratories, *Ighasec-/-* housed in UofC Barrier I or Barrier II facilities or 13-species donor mouse provided by M. Mimee (University of Chicago). Feces were homogenized in 1mL of sterile PBS on a vortex for 3 min and centrifuged at 300 g for 5 min at 4°C to remove debris. 200 μL of the supernatant was administered to recipient mice by oral gavage. To colonize mice

with fecal filtrate, feces were collected from vancomycin/metronidazole treated *Ighasec-*/- mouse. Homogenate was prepared as described above. After debris removal, collected supernatant was centrifuged at 8000g for 10 min at 4°C to pellet any bacteria. Supernatant was then filtered three times through 0.22 μm syringe-driven filter unit (Millipore Sigma). An aliquot of the filtrate was treated with 50mJ/cm² of UV light using Spectrolink XL-1000 UV crosslinker (Spectroline) (Janowski et al., 2017). 200 μL of the filtrate was administered to recipient mice by oral gavage. To colonize mice with the *L. reuteri*, sequenced strain isolated from vancomycin/metronidazole treated mice was used. Single colony grown on MRS agar (Fisher Scientific) was picked to inoculate 10 mL of MRS broth (Fisher Scientific) and cultured anaerobically for 16-18h at 37°C. Bacteria were then pelleted, washed, and resuspended in 3 mL of sterile PBS. 200 μL of the suspension was administered to recipient mice by oral gavage. For all the microbial transfers, mice were colonized at 4-weeks of age and euthanized at 8 weeks of age.

2.11.DSS-induced colitis

2% or 2.5% DSS (MW ca 40000, Thermo Scientific) in water was administered to *Ighasec+/-* and *Ighasec-/-* mice housed in UofC Barrier I or UofC Barrier II previously infected with MNV-CR6 respectively. Mice were kept on DSS water for seven days, followed by regular water for two days and euthanized. Weight was recorded every day throughout the duration of the DSS protocol. Bacterial translocation to mLNs, colon length and histology was assessed. To determine the extent of bacterial translocation, mLNs were dissected aseptically, weighed, and homogenized in 500 μL of sterile PBS. 250 μL of homogenate was plated in duplicate on Brucella agar with 5% sheep blood, hemin and vitamin K. Plates were than cultured aerobically (overnight) or anaerobically (48h) at 37°C.

2.12.ELISA

Serum IgA or IgM levels were assessed using IgA mouse uncoated ELISA kit (Thermo Fisher) or IgM mouse uncoated ELISA kit (Thermo Fisher) according to manufacturer's protocol. Serum was serially diluted in 1x Assay Buffer A (Thermo Fisher). Dilution in the middle of standard curve was used to quantify IgA or IgM levels. Absorbance was read at 450 nm.

2.13. Histology

7 to 10 cm of duodenum, jejunum and ileum or whole colon were excised, cleaned of adipose tissue, and opened longitudinally. Intestinal content was removed. Starting from the most distal end and with the luminal side facing upwards, tissues were rolled into Swiss rolls. Tissue was then placed into histology cassettes and fixed with 10% formalin (Sigma-Aldrich) for H&E staining or with 4% PFA in PBS (Sigma-Aldrich) for immunofluorescence staining. Formalin fixed tissues were transferred into 70% ethanol, embedded in paraffin, and cut at 5 µm thickness. Paraffin embedding, tissue processing and H&E staining was performed by the Human Tissue Resource Center at the University of Chicago. Scoring of the H&E-stained colonic tissue was performed using parameters determined by Dr. Christopher Weber. Briefly, the entire length of the colon Swiss roll was measured using QuPath(Bankhead et al., 2017). Then sections of the mucosa were scored and measured based on appearance: 0- normal appearance, 1- mild edema, increased lamina propria lymphocytes and attenuation of epithelium without ulceration, 2- severe epithelial regeneration with signs of healed erosion, high immune cell infiltration and edema; 3- Severe edema, complete ulceration, and high inflammatory infiltration. Final score was calculated as a proportion of severely affected tissue versus the total length of the tissue.

PFA fixed tissues were rinsed with PBS and transferred into 30% sucrose solution (Sigma-Aldrich) and incubated overnight at 4°C. Cryopreserved tissues were then embedded in O.C.T. Compound (Sakura), frozen and stored at -80°C. Frozen tissues were cut at 5 μm thickness, dried and stored at -20°C until processing. Frozen tissue sections were permeabilized with 0.1% Triton X-100 (Sigma-Aldrich) in PBS, blocked in buffer containing normal rat and goat sera (Jackson Immuno Research) and stained overnight at 4°C. Antibodies used for immunofluorescence staining were anti-mouse B220 Alexa Fluor 750 (R&D), CD8β Alexa Fluor 647 (Biolegend), and IgA Alexa Fluor 488 (Southern Biotech). The slides were then washed three times with permeabilization buffer, briefly rinsed in water, and mounted with ProLong Diamond Antifade with DAPI (Thermo Fisher). The slides were imaged with the CRi Pannoramic SCAN 40x Whole Slide scanner or Olympus VS200 Slideview Research Slide Scanner at the University of Chicago Integrated Light Microscopy core.

2.14.DNA isolation

50-100 mg of the intestinal contents were collected from the middle 5cm of the jejunum, the last 5 cm of ileum, and the middle 5cm of the colon. Contents were transferred into 2mL screw-cap tube containing 0.1 mm BioSpec glass beads (Fisher Scientific), snap frozen on dry ice and stored at -80°C. Intestinal contents were homogenized in 1mL of InhibitEX buffer (Qiagen) using the Bead Ruptor Elite Bead mill homogenizer (Omni) on speed 6m/s for 3 min. DNA was purified from the lysates using QIAmp Fast DNA stool kit (Qiagen) according to manufacturer's protocol. DNA concentration was determined using the nanodrop UV spectrophotometer (ThermoFisher) or Qubit dsDNA Quantification Assay (ThermoFisher).

2.15.Microbial 16S rRNA Gene Sequencing

Extracted DNA was quantified, amplified, barcoded, sequenced, filtered, and analyzed as described previously (Barlow et al., 2020; Bogatyrev et al., 2020; Earley et al., 2023). Briefly, total absolute bacterial load was obtained with dPCR using the QX200 ddPCR system (Bio-Rad) with primers targeting the variable 4 (V4: 519F-806R) region of the 16S rRNA gene. For library preparation, 500 ng total DNA (determined by NanoDrop) was used to amplify the V4 region of 16S rRNA gene with barcoded primers. Obtained libraries were quantified with KAPA library quantification kit (Roche), normalized, multiplexed, and sequenced at average depth of 157,552 (2x300 bp) on an Illumina MiSeq v3 (Illumina). Sequences were processed with QIIME 2 (v2022.8.0) and SILVA (v138) for taxonomy assignment. Reads were rarefied to 55,000 reads based on the lowest read depth sample. For bacterial absolute abundance measurements, the relative abundance of each taxon was multiplied by the total microbial load in the sample. Filtering of low abundance taxon was performed by calculating the LOD based on 1. the number of 16S rDNA molecules input into the library preparation and 2. the number of sequencing reads. The minimum of the two LOD calculations was used and any ASV detected below the LOD was set to 0. Statistical comparisons were performed with the non-parametric Kruskal-Wallis rank sums tests with Benjamini-Hochberg multiple hypothesis testing correction using SciPy (v1.7.3) and statsmodels (v0.13.2).

2.16.Microbial DNA Shotgun Sequencing

200 ng of purified fecal DNA (determined by Qubit dsDNA High Sensitivity kit) was used to prepare libraries for metagenomic sequencing with Illumina DNA Prep kit (Illumina). Library was sequenced on an Illumina NovaSeq6000 S4 (2x150bp) with a read depth of 264 million reads. QC and host filtering was performed with KneadData (v0.12.0) using the mouse reference genome

(C57BL/6J). For marker-gene taxonomic analysis, host filtered sequences were analyzed with MetaPhlAn4 (v4.0.3). To determine all organisms present, k-mer analysis was performed on the host filtered sequences using Kraken2 (v2.1.3) with the entire NT database (last updated 11/29/2023) with a confidence threshold of 0.5. Reads assigned to species identified as less than 0.01% abundance were filtered out for the final read distribution. Reads assigned to the fungal kingdom and viral domain were retained to highlight the low abundance of non-bacterial microbial reads.

2.17.IgA-MuAstV pulldown

2-3 fresh fecal pellets were collected from GF or MuAstV monoassociated *Ighasec+*/- mice to pull-down IgA. Feces were homogenized in 500 μL 1X Tris-Buffered Saline, 0.1% Tween 20 (TBST) on a vortex for 5 min, and centrifuged for 5 min at 8000 g, 4°C. The supernatant was collected and centrifuged twice to remove any remaining debris. Pierce Protein L Magnetic Beads (Thermo Fisher) were added to the supernatants and incubated at room temperature with agitation for 1h. Beads were collected using EasySep magnetic stand (StemCell technologies) to pull down the IgA through kappa light chain. Supernatant was saved for downstream RNA isolation. Beads were washed three times with TBST, collected and incubated with RLT Plus buffer (Qiagen) supplemented with 2-mercaptoethanol. RNA from obtained lysates was purified using RNeasy Micro kit (Qiagen) according to manufacturer's specifications. 10 μL of obtained RNA was reverse transcribed to cDNA using SuperScript VILO cDNA kit. cDNA obtained from the supernatant and the bead-bound fraction was used to determine the number of MuAstV copies per reaction via qPCR.

2.18.RNA isolation

1 cm of tissue from the beginning of the duodenum, the middle of the jejunum, the end of the ileum, and the middle of the colon was excised and preserved in RNAprotect (Qiagen) overnight at 4°C. The preserved tissue was then stored at -80°C until processing. Tissue was thawed on ice and transferred to a screw-cap tube containing 450 μL of RLT Plus buffer supplemented with 2-mercaptoethanol and equal quantities of 1.0mm and 0.5 mm zirconium oxide beads (Next Advance). Tissue was homogenized three times for 30 sec at a speed of 6 m/s using Bead Ruptor Elite mill homogenizer (Omni), with 1 min incubation on ice between each cycle. RNA from the lysates was purified using RNeasy Plus Mini kit (Qiagen) with the optional on-column DNase I digest step according to manufacturer protocol.

2.19.qPCR

1 μg of RNA was reverse transcribed to cDNA using High-Capacity cDNA RT kit (Thermo Fisher) according to manufacturer's protocol. 10 ng of cDNA was used to measure the expression of the genes of interest via qPCR with TB Green Advantage qPCR Premix (Takara) on a Light Cycler 480 (Roche). The expression of the genes of interest was quantified and normalized to GAPDH using 1000*2^{- (Ct target- Ct housekeeping)} formula. To calculate the number of MuAstV copies per reaction, linearized plasmid standard curve was used. Primer pairs used in the study are listed in Table 1.

2.20.RNA-seq library preparation

RNA was purified as detailed above from jejunal and ileal tissue of anti-CD8β, or isotype treated *Ighasec+/-* and *Ighasec-/-* mice. 500 ng of RNA was used as input in the TruSeq Stranded mRNA Library Prep (Illumina) according to manufacturer's specifications.

50000 CD45- EpCAM+ IECs were sorted from the jejunum and the ileum of anti-CD8β, or isotype treated *Ighasec+/-* and *Ighasec-/-* mice. Two independent sorting experiments were performed. Cells were collected into RLT Plus buffer (Qiagen) supplemented with 2-mercaptoethanol. RNA was purified using RNeasy Micro kit (Qiagen) and quantified with Power SYBRTM Green RNA-to-C_T 1-Step kit. The SMART-Seq v4 Ultra Low input RNA kit (Takara) was used to generate cDNA from 10 ng of RNA. cDNA was amplified 9 cycles and purified according to manufacturer's protocol. 200 pg of purified cDNA was the used to generate RNA-seq libraries with Nextera XT DNA Library preparation kit (Illumina).

Obtained libraries were quantified with KAPA library quantification kit (Roche), normalized, multiplexed, and sequenced at a depth of 20 million reads per sample (100 bp) on a NovaSEQ-6000 (Illumina) at the University of Chicago Genomics Facility.

2.21.Recovery of viral reads from the bulk RNA-seq

Reads were assembled into contigs using Megahit (Li et al., 2015), and contigs were aligned to the nr protein database from NCBI using DIAMOND (Buchfink et al., 2015). Representative full genome sequences of Murine Astrovirus 1 were downloaded from NCBI Genbank, and a STAR (Dobin et al., 2013) alignment database was constructed out of those full genome sequences. Reads were then aligned to the full genomes using STAR. Recovered reads were normalized as follows: (#MuAstV reads/#reads total)10⁶.

2.22. Mouse bulk RNA-seq data analysis

Quality control filtering and normalization

All statistical analyses of the mouse RNA-seq data were performed using R (v.4.2.2). From the raw count matrices, genes expressed (i.e., having at least two counts) in fewer than two samples

were removed. The resulting matrices will be referred to as the count matrices. Counts were normalized by applying the variance stabilizing transformation (i.e. vst (), default parameters) from the DESeq2 R package (v.1.38.3)(Love et al., 2014). Batch effects were removed using the removeBatchEffect () function (batch = "sort_batch") from the limma R package (v.3.54.2)(Ritchie et al., 2015).

Differential expression and gene set enrichment

Comparisons of gene expression between sample groups were made using DESeq2 to fit a negative binomial generalized linear model with a group variable. Wald statistics were used to determine the significance of the group coefficient, i.e., the log2-fold change (LFC) in expression between groups. We used the Benjamini-Hochberg method for controlling the false discovery rate (FDR). The p values reported are FDR adjusted. Genes with an adjusted p-value of at most 0.05 were considered differentially expressed (DE) between groups. The LFCs and FDR-adjusted p values were given as input to the fgsea () function from the fgsea R package (v.1.24.0)(Korotkevich et al., 2021), which implements a pre-ranked gene set enrichment analysis. The rankings of the genes were based on the FDR-adjusted p values. The Gene Ontology Biological Processes (GO-BP) database (Ashburner et al., 2000; Gene Ontology, 2021) was the gene set used in the enrichment analyses. Enriched pathways (i.e., p < 0.05) were collapsed to independent pathways to avoid repetitive terms, using the fgsea collapsePathways () function.

Visualization

All plots illustrating gene expression levels use vst transformed expression. Heatmaps were plotted using the *Heatmap ()* function from the ComplexHeatmap R package (v.2.15.1) (Gu et al., 2016)

Heatmaps show the z-scored expression across samples; any values outside the range shown in the numerical legend were squished towards the maximum or minimum values shown.

2.23. Single cell RNA-seq

CD8αβ+ IELs from three *Ighasec*+/- and *Ighasec*-/- mice were isolated and stained as described above in "Flow cytometry" section. For cell hash-tagging, TotalSeq-ATM hashtag antibodies (Table 1) were added to each sample individually during the cell surface staining. The samples were then sorted together directly into FACS buffer, spun down and reconstituted in 1X PBS (calcium- and magnesium-free) containing 0.04% BSA. Samples were loaded on 10x Chromium Controller (10x Genomics) immediately after sorting. Libraries were constructed for gene expression data and TCR repertoire using Chromium Next GEM Single Cell 5' Library kit (v1.1). Capture, library preparation and sequencing were performed at the University of Chicago Genomics Facility.

2.24. Single cell RNA-seq data analysis

Quality control and normalization

The unique molecular identifier (UMI) count matrices obtained from the Cell Ranger output were imported into R (v.4.2.2) and processed with the R package Seurat (v. 4.3.0) (Hao et al., 2021). From this matrix, genes expressed (i.e., having at least one count) in fewer than three cell were removed. TCR related genes were also removed (i.e., genes having the following regex pattern "^T[cr][abdgr][vdjgd] ([^*]*)"). Low-quality cells were removed based on the following criteria: 1. Cells with >2.25% mitochondrial percentage were removed, 2. The thresholds for acceptable numbers of detected genes and UMIs per cell were determined by outliers in the joint distribution of unique UMIs and detected genes across cells. Cells with <950 or >3000 detected genes or <2000 or >7500 detected UMIs were discarded were discarded. Further, cells which did not have a

corresponding sequenced TCR read where also removed. Overall, 8240 cells passed the above criteria and were used for downstream analysis. To account for differences in sequencing depth across cells, UMI counts were normalized and scaled using regularized negative binomial regression via Seurat's sctransform () function(Hafemeister & Satija, 2019). The resulting normalized counts were used for visualization and clustering downstream analysis.

Clustering and identification of functional cluster markers

We performed principal component analysis (PCA) using the top 3000 highly variable genes. The top 20 principal components for each dataset were used to construct a shared nearest neighbor (SNN) graph and modularity-based clustering using the Louvain algorithm and a cluster resolution of 0.4 as part of the FindClusters () function from the R package Seurat(Hao et al., 2021). Uniform manifold approximation and projection (UMAP) visualization was calculated using 20 nearest neighbors for the local approximation of the manifold structure. To determine the functional profile of each cluster, FindAllMarkers () was run with the option "test.use= LR", which identifies marker genes by comparing expression of each gene in a cluster against its expression in the rest of the cells using a logistic regression test. Only genes significantly and strongly up regulated in the cluster were considered as potential functional markers.

Identifying expanded clones and enriched motifs

TCRs that did not have exactly one Cdr3a and one Cdr3b sequence were removed. Expanded clones were defined as unique TCRs that were expressed by at least 2 cells. Public clones are a subset of these, which are expressed in at least two samples (i.e., mice). Further, amongst these expanded clones, we found enriched motifs in the Cdr3b sequences of the expanded clones. We first identified lists of all possible k-mers for k=3-8 allowing gaps. We used a Fischer's exact test

to determine which k-mers were significantly enriched in Ighasec-/- mice (P < 0.05)— where the rows of the test table are condition (i.e., Ighasec+/- & Ighasec-/-) and the columns are whether the condition contains the motif. The entries than correspond to the number of expanded clones meeting the row and column descriptors.

Visualization

All plots illustrating gene expression levels use SCT transformed expression. Dot plots show the z-scored expression across conditions; any values outside the range shown in the numerical legend were squished towards the maximum or minimum values shown.

Table 1: List of reagents.

Reagent or Resource	Source	Identifier
Antibodies		
CD45 BV421 (30-F11)	Biolegend	Cat#103134
CD45 AF532 (30-F11)	Thermo Fisher	Cat#58-0451-82
CD3ε BUV737 (145-2C11)	BD	Cat#612771
TCRgd FITC (eBioGL3)	Thermo Fisher	Cat#11-5711-82
TCRβ BUV737 (H57-597)	BD	Cat#612821
CD4 BV785 (GK1.5)	Biolegend	Cat#100453
CD4 BUV615 (GK1.5)	BD	Cat#613006
CD4 BUV615 (RM4-4)	BD	Cat#751366
CD8β BV480 (H35-17.2)	BD	Cat#746835
CD8β BUV395 (H35-17.2)	BD	Cat#740278
CD8β AF647 (YTS156.7.7)	Biolegend	Cat#126612
CD8α APC/Fire 750 (53-6.7)	Biolegend	Cat#100766
CD8α APC-Cy7 (53-6.7)	Biolegend	Cat#100714
CD103 BV711 (M290)	BD	Cat#564320
CD69 APC (H1.2F3)	Biolegend	Cat#104514
CD69 BV650 (H1.2F3)	BD	Cat#740460
CD44 PE-Cy7 (IM7)	Biolegend	Cat#103030
PD-1 AF647 (29F.1A12)	Biolegend	Cat#135230
CXCR5 PE (L138D7)	Biolegend	Cat#145504
CD62L PE (MEL-14)	Biolegend	Cat#104408
IFNγ APC (XMG1.2)	BD	Cat#554413

Table 1: List of reagents continued.

IL10 PEcy7 (JES5-16E3)	Biolegend	Cat#505026
IL17a PE (ebio17B7)	Thermo Fisher	Cat#12-7177-81
TNF BB700 (MP6-XT22)	BD	Cat#566510
RORγt BV786 (Q31-37)	BD	Cat#564723
FOXP3 eflour450 (FJK-16s)	Thermo Fisher	Cat#48-5773-82
Tbet APC (4B10)	Biolegend	Cat#644814
GATA3 PerCP-eFluor710 (TWAJ)	Thermo Fisher	Cat#46-9966-42
EpCAM PerCp/Cy5.5 (G8.8)	Biolegend	Cat#118220
EpCAM BV605 (G8.8)	Biolegend	Cat#118227
CD19 BUV563 (1D3)	BD	Cat#749028
CD38 BB700 (90/CD38)	BD	Cat#742132
CD95 BV750 (Jo2)	BD	Cat#747413
GL7 PerCP/Cy5.5 (GL7)	Biolegend	Cat#144610
NK1.1 BV605 (PK136)	Biolegend	Cat#108753
NK1.1 BV570 (PK136)	Biolegend	Cat#108733
CD11C BV605 (N418)	Biolegend	Cat#117334
TER119 BV605 (TER-119)	Biolegend	Cat#116239
F4/80 BV605 (BM8)	Biolegend	Cat#123133
CD3ε BV605 (145-2C11)	Biolegend	Cat#100351
Ly6g BV605 (1A8)	Biolegend	Cat#127639
B220 APC/Fire 810 (RA3-6B2)	Biolegend	Cat#103278
B220 AF750 (RA3-6B2)	R&D	Cat#FAB1217S
IgA PE goat polyclonal	Southern Biotech	Cat#1040-09
IgA 488 goat polyclonal	Southern Biotech	Cat#1040-30
IgA BIOT goat polyclonal	Southern Biotech	Cat#1040-08
IgD BV421 (11-26c.2a)	Biolegend	Cat#405725
IgD BV605 (11-26c.2a)	Biolegend	Cat#405727
IgM BUV661 (II/41)	BD	Cat#750660
TotalSeq-C0301 anti-mouse Hashtag 1 (M1/42)	Biolegend	Cat#155961
TotalSeq-C0302 anti-mouse Hashtag 2 (M1/42)	Biolegend	Cat#155863
TotalSeq-C0303 anti-mouse Hashtag 3 (M1/42)	Biolegend	Cat#155865
TotalSeq-C0304 anti-mouse Hashtag 4 (M1/42)	Biolegend	Cat#155867
TotalSeq-C0305 anti-mouse Hashtag 5 (M1/42)	Biolegend	Cat#155869

Table 1: List of reagents continued.

TotalSag C0206 anti mavas Hashtar 6	Piologand	Cat#155871
TotalSeq-C0306 anti-mouse Hashtag 6 (M1/42)	Biolegend	Cat#1558/1
(1411/42)		
Biological Samples		
Fetal Bovine Serum	Biowest	Cat#S01520
Normal Goat Serum	JacksonImmunoResearch	Cat#005-000-121
Normal Rat Serum	JacksonImmunoResearch	Cat#012-000-120
Chemicals, Peptides, and		
Recombinant Proteins		
Corning TM RPMI 1640 with L-Glutamine	Fisher Scientific	Cat#MT-10043CV
EDTA, 0.5M, pH8.0	Thermo Fisher	Cat#AM9260G
1M MgCl2	Thermo Fisher	Cat#AM9530G
Collagenase from Clostridium	Sigma-Aldrich	Cat#C2139
histolyticum		
Cytiva Percoll TM Centrifugation Media	Fisher Scientific	Cat#45-001-747
Phorbol Myristate Acetate	Sigma-Aldrich	Cat#P1585
Ionomycin Calcium Salt from	Sigma-Aldrich	Cat#10634
Streptomyces conglobatus		
BD GolgiStop Protein Transport Inhibitor	BD	Cat#554724
Ampicillin sodium salt	Sigma-Aldrich	Cat#A9518
Vancomycin hydrochloride	Sigma-Aldrich	Cat#V2002
Neomycin trisulfate salt	Sigma-Aldrich	Cat#N1876
Metronidazole	Sigma-Aldrich	Cat#M1547
Emtricitabine	Fisher Scientific	Cat#AC462070050
Tenofovir	Fisher Scientific	Cat#AC461250250
Acyclovir	Fisher Scientific	Cat#A19151G
Lamivudine	Fisher Scientific	Cat#L02171G
Ribavirin	Fisher Scientific	Cat#R0077500MG
RNAprotect Tissue Reagent	Qiagen	Cat#76106
2-Mercaptoethanol	Sigma-Aldrich	Cat#M3148
Ethanol 200 Proof	Decon Labs Inc	Cat#DSP-MD 43
Inhibitex Buffer	Qiagen	Cat#19593
Cytiva HyClone TM Water	Fisher Scientific	Cat#SH3053801
10% Formalin Solution	Sigma-Aldrich	Cat#HT501128
Paraformaldehyde	Sigma-Aldrich	Cat#158127
Sucrose	Sigma-Aldrich	Cat#S9378
		•

Table 1: List of reagents continued.

Triton X-100	Sigma-Aldrich	Cat#X100
O.C.T. Compound	Sakura	Cat#4583
		1
Critical Commercial Assays		
SytoBC	Thermo Fisher	Cat#S34855
LIVE/DEAD® Fixable Aqua Dead	Thermo Fisher	Cat#L34966
Cell Stain Kit		
Zombie NIR™ Fixable Viability Kit	Biolegend	Cat#423106
BD Cytofix/Cytoperm Plus	BD	Cat#554714
Fixation/Permeabilization Solution Kit	771 F: 1	G 4400 5500 00
eBioscience TM Foxp3 / Transcription	Thermo Fisher	Cat#00-5523-00
Factor Staining Buffer Set QIAamp Fast DNA Stool Mini Kit	Qiagen	Cat#51604
QX200 ddPCR EvaGreen Supermix	Bio-Rad	Cat#1664034
Qubit dsDNA High Sensitivity	ThermoFisher	Cat#1004034
Illumina DNA Prep	Illumina	Cat#20018794
RNeasy Plus Mini Kit	Qiagen	Cat#74136
RNeasy Micro Kit	-	Cat#74130
High-Capacity cDNA RT kit	Qiagen Thermo Fisher	Cat#4368814
SuperScript TM VILO cDNA kit	Thermo Fisher Thermo Fisher	Cat#11754050
	Takara	
TB Green Advantage qPCR Premix		Cat#639676
Power SYBR TM Green RNA-to-C _T 1-Step kit	Fisher Scientific	Cat#50-591-795
Smart-Seq® v4 Ultra® low Input RNA	Takara	Cat#634889
kit	Tukuru	Cath 03 100)
Nextera XT DNA Library Preparation	Illumina	Cat#FC-131-1001
Kit		
TruSeq® Stranded mRNA Library	Illumina	Cat#20020595
Prep	T11	C-4#20010702
TruSeq® RNA CD Index Plate	Illumina	Cat#20019792
SuperScript TM II RT	Thermo Fisher	Cat#18064071
AMPure XT	Beckman Coulter	Cat#A63881
KAPA library quantification kit	Roche	Cat#07960140001
ProLong [™] Diamond Antifade Mountant with DAPI	Thermo Fisher	Cat#P36962
Pierce TM Protein L Magnetic Beads	Thermo Fisher	Cat#88850
IgA mouse Uncoated ELISA kit	Thermo Fisher	Cat#88-50450-86
	Thermo Fisher	Cat#88-50470-76
IgM mouse Uncoated ELISA kit	THEITHO FISHER	Cai#00-304/0-/0

Table 1: List of reagents continued.

Oligonucleotides		
GAPDH Forward 5'-	(Abadie et al., 2020)	N/A
AGGTCGGTGTGAACGGATTTG-3'		
GAPDH Reverse 5'-	(Abadie et al., 2020)	N/A
TGTAGACCATGTAGTTGAGGTC		
A-3'		
ORF1b Forward 5'-	(Yokoyama et al., 2012)	N/A
TACATCGAGCGGGTGGTCGC-3'		
ORF1b Reverse 5'-	(Yokoyama et al., 2012)	N/A
GTGTTACTAACGCGCACCTTTTC		
A-3'		
MNV Forward 5'-	(Bouziat et al., 2018)	N/A
ATGGTRGTCCCACGCCAC-3'	(D : 4 4 1 2010)	DI/A
MNV Reverse 5'-	(Bouziat et al., 2018)	N/A
TGCGCCATCACTCATCC-3' 18S rRNA Forward 5'-	(Blanchet et al., 2015)	N/A
GTTCCGACCATAAACGATGCC-3'	(Bianchet et al., 2013)	
directacearaactaridee-5		
18S rRNA Reverse 5'-	(Blanchet et al., 2015)	N/A
GTTCCGACCATAAACGATGCC-3'		
V4 16S rRNA 519 Forward 5'-	(Burggraf et al., 1997)	
CAGCMGCCGCGGTAA-3'		
V4 16S rRNA 806 Reverse 5'-	(Caporaso et al., 2011)	
GGACTACHVGGGTWTCTAAT-3'		
Universal Mouse Reference RNA	Thermo Fisher	Cat#QS0640
Other		
Bead Ruptor Elite bead mill	Omni International	Cat#19-040E
homogenizer		
Zirconium Oxide Beads 0.5 mm RNA	Next Advance	Cat#ZROB05-RNA
Free		
Zirconium Oxide Beads 1.0 mm RNA	Next Advance	Cat#ZROB10-RNA
Free		
BioSpec 0.1 mm Glass Beads	Fisher Scientific	Cat#NC0268065
BioSpec 1.0 mm Zirconia/Silica Beads	Fisher Scientific	Cat#NC9847287
LightCycler® 480 System	Roche	N/A
Cytek® Aurora	Cytek	N/A
CRi Pannoramic SCAN 40x Whole	3DHistech	N/A
Slide Scanner		
VS200 Slideview Research Slide	Olympus	N/A
Scanner		
EasyEights TM EasySep TM Magnet	Stemcell technologies	Cat#18103

Table 1: List of reagents continued.

QX200 ddPCR system	BioRad	Cat#1864001
Software and Algorithms		
QIIME2: 2022.8.0	(Bolyen et al., 2019)	
Silva (v138)	(Quast et al., 2013)	
SciPy (v1.7.3)	https://www.scipy.org/	
Statsmodels (v0.13.2)	https://www.statsmodels.o rg/stable/index.html	
Python 3.7.6	https://www.python.org/	
KneadData (v0.12.0)	https://github.com/biobak ery/kneaddata	
MetaPhlAn4 (v4.0.3)	https://github.com/biobak ery/MetaPhlAn	
R (v.4.2.2)	https://www.r-project.org	
GraphPad Prism 10	https://www.graphpad.co m	
FlowJo	https://www.flowjo.com	
QuPath	(Bankhead et al., 2017)	

3.RESULTS

This chapter includes results from an article that was submitted for publication in Cell Host Microbe.

3.1.IgA-mediated regulation of the microbiota prevents antigen-driven expansion of CD8 $\alpha\beta^+$ intraepithelial lymphocytes

To evaluate the contribution of IgA in preserving intestinal immune homeostasis without compensatory IgM production, we established a novel mouse model of IgA deficiency termed *Ighasec-/-*. This was achieved by deleting the secretory tailpiece along with its downstream polyadenylation (polyA) sites (Figure 3A). Unlike in the original IgA deficient mice (*Igha-/-*), which lack IgSα + IgCα1, *Ighasec-/-* B cells retain the ability to class switch and express IgA on the cell surface as observed in the Peyer's patches (Figure 3B). These IgA-switched B cells are incapable of maturing into IgA plasma cells within the intestinal lamina propria, resulting in an inability to secrete IgA (Figure 3C). This deficiency leads to decreased levels of both serum and bacterial-bound IgA (Figure 3D-E). Although we were unable to detect IgM-bacterial coating in both lines by FACS (Figure 3E), *Igha-/-* mice had a near 100-fold expansion of IgM plasma cells and a threefold increase in serum IgM, which was not found in the *Ighasec-/-* mice (Figure 3F-H). We therefore used the *Ighasec-/-* mice for all subsequent experiments to study IgA deficiency in the absence of potential IgM compensation, unless stated otherwise.

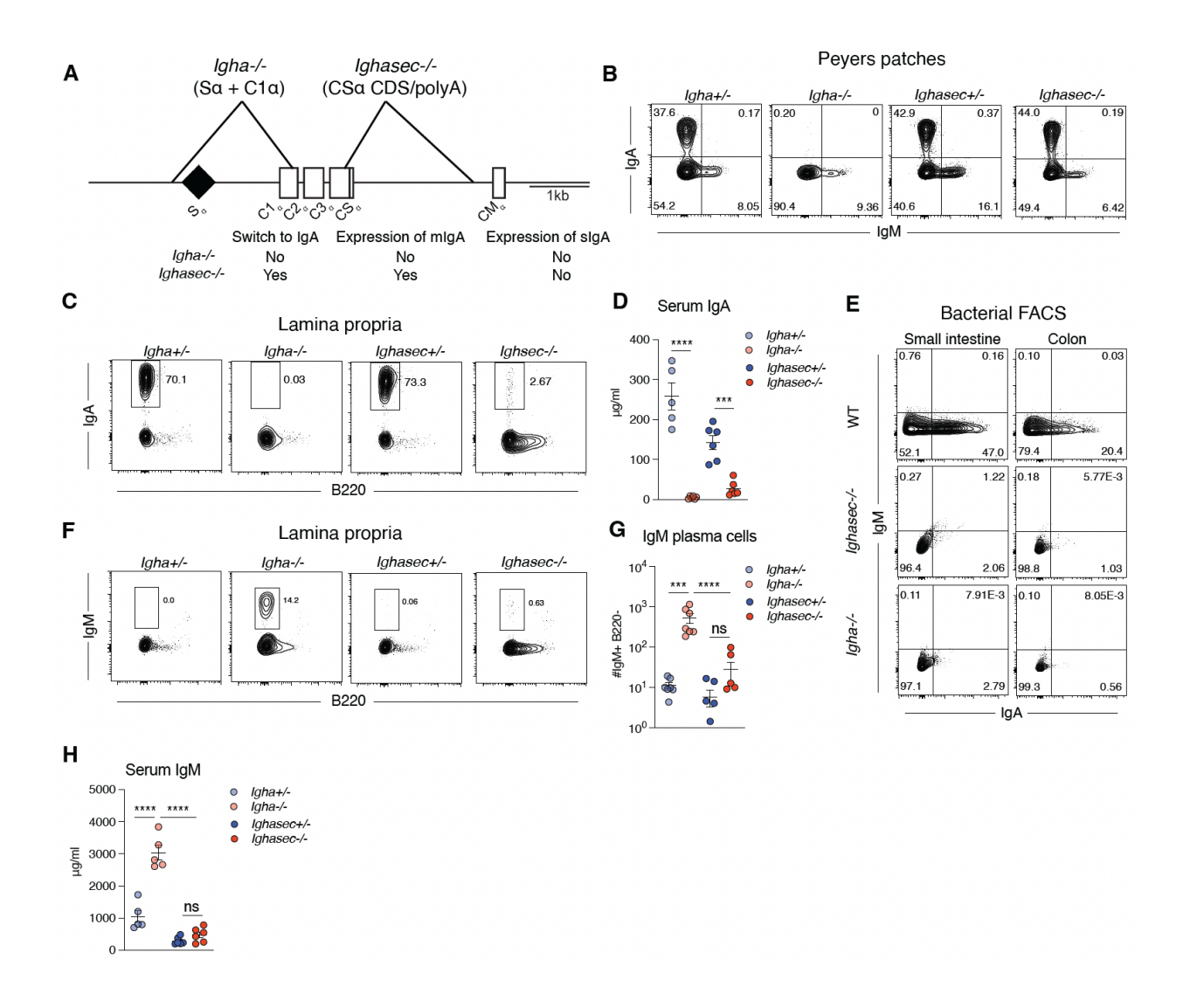


Figure 3: Novel model of IgA deficiency: IgA secretory deficient mouse.

(A) Schematic representation of Cα locus. Targeted deletion of Sα and C1α for classical IgA KO (*Igha-I-*) or CSα and polyA tail for Secretory IgA KO (*Ighasec-I-*) is depicted. (B) Representative plots of the frequencies of IgA+ and IgM+ switched cells among CD19⁺ B cells in the PP of SPF *Igha+I-* and *Igha-I-* or *Ighasec+I-* and *Ighasec-I-* mice. (C) Representative plots of the frequencies of IgA+ B220- PCs in the jejunal lamina propria (LP) of SPF *Igha+I-* and *Igha-I-* or *Ighasec+I-* and *Ighasec-I-* mice. (D) Amount of IgA, as determined by enzyme-linked immunoassay (ELISA), in the serum of SPF *Igha+I-* and *Igha-I-* or *Ighasec+I-* and *Ighasec-I-* mice. n = 5-6 mice/group. (E) Frequency of IgA-coated and IgM-coated bacteria in the small intestinal and colonic luminal contents of SPF wild-type (WT), *Igha-I-* or *Ighasec-I-* mice. (F and G) Representative plots of the frequencies (F) and number (G) of IgA+ B220- PCs in the jejunal LP of SPF *Igha+I-* and *Igha-I-* or *Ighasec-I-* mice. n = 6 mice/group. (H) Amount of IgM, as determined by ELISA, in the serum of SPF *Igha+I-* and *Igha-I-* or *Ighasec+I-* and *Ighasec-I-* mice. n = 5-6 mice/group. All data in this figure are pooled from at least two independent experiments and are represented as mean or mean ± SEM. **** P<0.0001, *** P<0.01, ** P<0.05 ns P≥0.05. Unpaired t-test (D), ANOVA with Tukey multiple comparison test (G, H).

Ighasec-/- mice showed a 50-fold increase in the number of intraepithelial CD8αβ⁺ T cells throughout the small intestine compared to littermate control Ighasec+/- mice (Figure 4A-B). In contrast, the number of unconventional T cell subsets, TCRαβ+ CD8αα+ or TCRγδ+ cells, or the conventional TCRαβ+ CD4+ intraepithelial lymphocytes (IELs) remained unchanged (Figure 5A). Expansion of the CD8αβ+ IELs occurred after weaning and was long-lived, persisting in up to 48-week-old Ighasec-/- hosts (Figure 4C). Furthermore, intracellular flow cytometry staining revealed increased IFNγ production by CD8αβ+ IELs in Ighasec-/- mice (Figure 4D). It is noteworthy that the expansion of CD8αβ+ T cells was also evident in mice lacking B cells (JH-/-), and in Igha-/- mice housed in the same facility as Ighasec-/- mice (Figure 4E-F), suggesting that IgM does not compensate to prevent the expansion of CD8αβ+ IELs in in multiple mouse models with IgA deficiency.

We next sought to better understand the mechanisms underlying the expansion of CD8 $\alpha\beta^+$ IELs. CD4 T cell depletion revealed that the expansion of CD8 $\alpha\beta^+$ IELs in *Ighasec-/-* was CD4 T cell-dependent (Figure 5B). Since the BATF3-dependent cDC1 dendritic cell lineage(Hildner et al., 2008) is important for cross-presenting viral, bacterial, and tumor antigens to activate CD8 $\alpha\beta$ T cells (Hildner et al., 2008; Naik et al., 2015), we generated *Ighasec-/- Batf3-/-* mice. The expansion of CD8 $\alpha\beta^+$ IELs was absent in these mice (Figure 4G), suggesting a role of cDC1s in priming this response.

Next, we aimed to determine the MHC molecule through which the expanded CD8 $\alpha\beta^+$ IELs in *Ighasec-/-* mice are restricted. β_2 -microglobulin (β_2 M) is an adaptor molecule capable of binding to classical MHCIa and numerous non-classical MHCIb molecules(Rodgers & Cook, 2005). *Ighasec-/- B2m-/-* mice had no detectable CD8 $\alpha\beta^+$ IELs (Figure 4H). To determine whether the CD8 $\alpha\beta^+$ IELs are classically MHCI restricted, we generated *Ighasec-/- K^bD^b-/-* triple deficient

mice lacking both MHCIa alleles. There was a significant reduction in CD8 $\alpha\beta$ + IELs in *Ighasec-/- KbDb-/-* compared to *Ighasec-/- KbDb+/-* littermate controls (Figure 4I), highlighting the significant contribution of classically restricted CD8 $\alpha\beta$ + T cells to the expansion of IELs in IgA-deficient mice. However, in the absence of classical MHCIa molecules, IgA deficiency was still associated with a higher number of IELs (Figure 5C). Therefore, we cannot exclude the possibility that β_2 M dependent, non-classical MHC molecules such as Qa-1 or Qa-2, may drive the expansion of IELs.

We then jointly analyzed the TCR repertoire and gene expression of CD8 $\alpha\beta^+$ IELs in *Ighasec-*/- mice using 10X 5' single-cell RNA-sequencing (scRNA-seq) with immune repertoire profiling and found evidence of antigen-driven expansion (Figure 4J). Further analysis of the scRNA-seq data showed that these expanded clones were predominantly present in a few clusters (clusters 0, 4, and 6) (Figure 4K-L), which exhibited relatively high expression of either T cell activation markers (*Cd69*, *Ifng*, *Nr4a1*) or cytotoxicity-associated genes (*Gzmb*, *Gzma*) (Figure 5D). Some of these expanded clones shared specific motifs in complementarity-determining region 3 (CDR3), that were observed across multiple IgA-deficient hosts but rarely in control mice (Figure 4M). These data further support the notion that CD8 $\alpha\beta$ + IELs expand in response to antigens presented by classical MHC class I molecules on BATF3+ DCs. Given that IgA coats the microbiota, we hypothesized that the expansion of CD8 $\alpha\beta$ + IELs was microbiota dependent. Consistent with this hypothesis, in germ-free (GF) *Ighasec-*/- mice, CD8 $\alpha\beta$ + IELs failed to expand or increase IFN γ production (Figure 4N-O).

Taken together, these results demonstrate that in the absence of IgA there is a microbiotadependent classical adaptive CD8 $\alpha\beta^+$ IEL immune response driven by cDC1s.

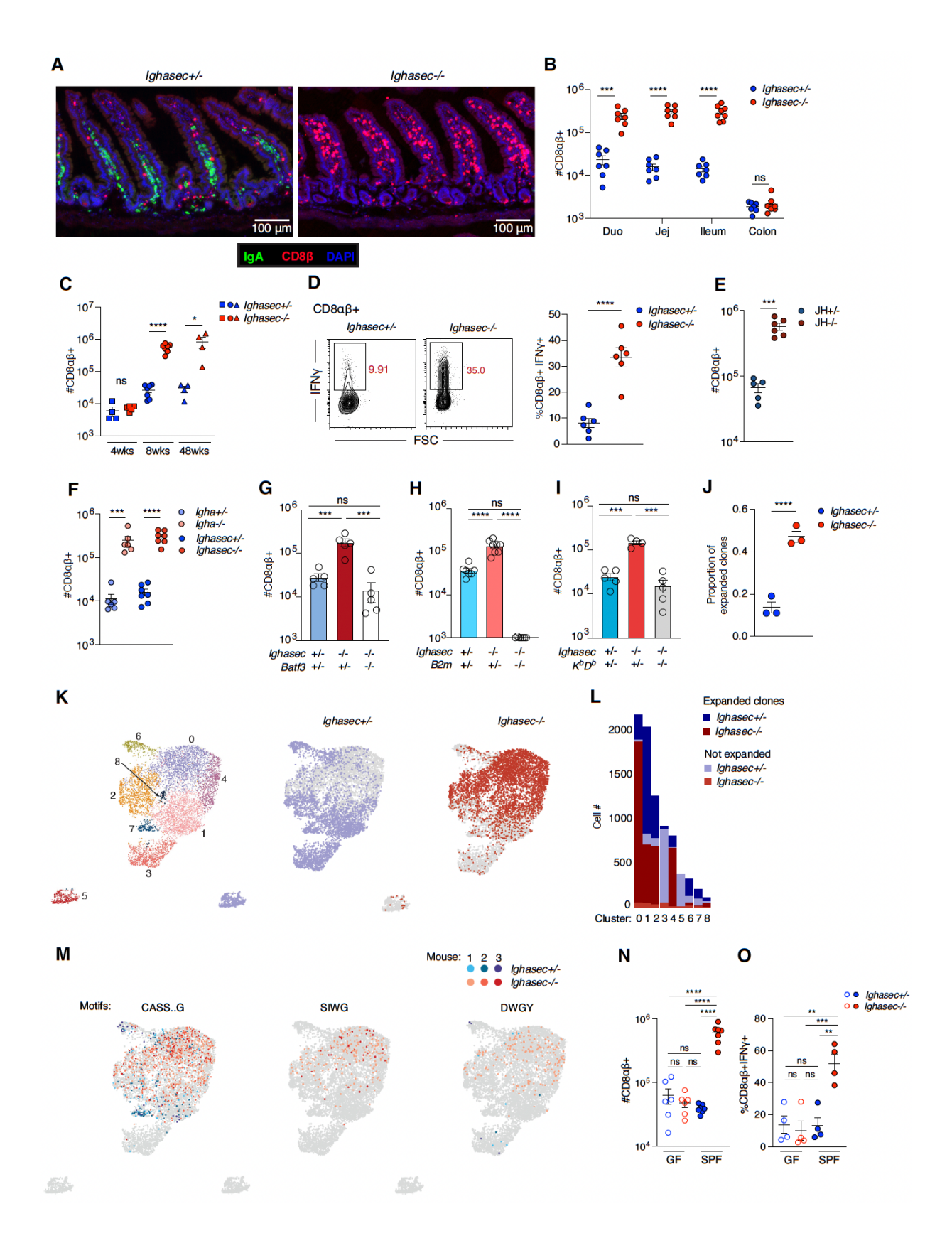


Figure 4: IgA controls microbiota to prevent expansion of classically restricted CD8αβ⁺ IELs.

Figure 4: IgA controls microbiota to prevent expansion of classically restricted CD8 $\alpha\beta^+$ IELs continued.

(A) Immunofluorescence staining of intestinal tissue using anti-IgA antibody (green), anti-CD8β antibody (red) and counterstained with DAPI (blue). Figure is a representative image from 4 independent Ighasec+/- and Ighasec-/- animals. (B) Number of CD8αβ⁺ IELs in each intestinal segment of Ighasec+/- and Ighasec-/- mice. n = 7 mice/group. (C) Number of CD8 $\alpha\beta^+$ IELs in the jejunum of 4-week, 8-week, and 48-week old *Ighasec+/-* and *Ighasec-/-* mice. n = 4-7 mice/group. (D) Representative (left) and summary (right) plots of the frequencies of IFN- γ^+ cells among CD8 $\alpha\beta^+$ IELs from the jejunum of Ighasec+/- and Ighasec-/- mice. n = 6 mice/group. (E and F) Number of CD8αβ⁺ IELs in the jejunum of JH+/- and JH-/- mice (E) or Igha+/- and Igha-/- or Ighasec+/- and Ighasec-/- mice (F). n = 5-6 mice/group. (G, H and I) Number of CD8 $\alpha\beta^+$ IELs in the jejunum of Ighasec+/-Batf3+/-, Ighasec-/-Batf3+/- and Ighasec-/- Batf3-/- mice (G) Ighasec+/-B2m+/-, Ighasec-/-B2m+/- and Ighasec-/-B2m-/- mice (H) $Ighasec+/-K^bD^b+/-$, Ighasec-/- K^bD^b +/- and Ighasec-/- K^bD^b -/- mice (I). n = 4-8 mice/group. (J) Proportion of expanded clones among CD8 $\alpha\beta^+$ IELs from the jejunum of *Ighasec+/-* and *Ighasec-/-* mice. Expanded clones were defined as unique TCRs that were expressed by at least 2 cells. n = 3 mice/group. (K) Uniform manifold approximation projection (UMAP) embedding of scRNA-seq profiles of CD8αβ+ IELs from the jejunum of *Ighasec*+/- and *Ighasec*-/- mice, colored by cluster (left) and by mouse genotype (right). (L) Bar chart representing the number of expanded or unique CD8αβ⁺ IEL clones in each transcriptional cluster (as in 1K). (M) UMAP (as in 1K), with cells in color (blues, Ighasec+/- mice; reds, Ighasec-/- mice) if they share the indicated public TRB CDR3 amino acid motif (top), and in gray otherwise. Periods in the motif CASS..G represent gaps. (N and O) Number of CD8 $\alpha\beta^+$ IELs (N) and the frequency of IFN- γ^+ cells among CD8 $\alpha\beta^+$ IELs (O) in the jejunum of GF and SPF *Ighasec+/-* and *Ighasec-/-* mice. n = 4-7 mice/group.

All data in this figure are pooled from at least two independent experiments and are represented as mean or mean \pm SEM. **** P<0.0001, *** P<0.001, ** P<0.01, * P<0.05 ns P<0.05. Unpaired t-test (B, C, D, E, F, N, O), ANOVA with Tukey multiple comparison test (G, H, I), LR mixed effect model (J).

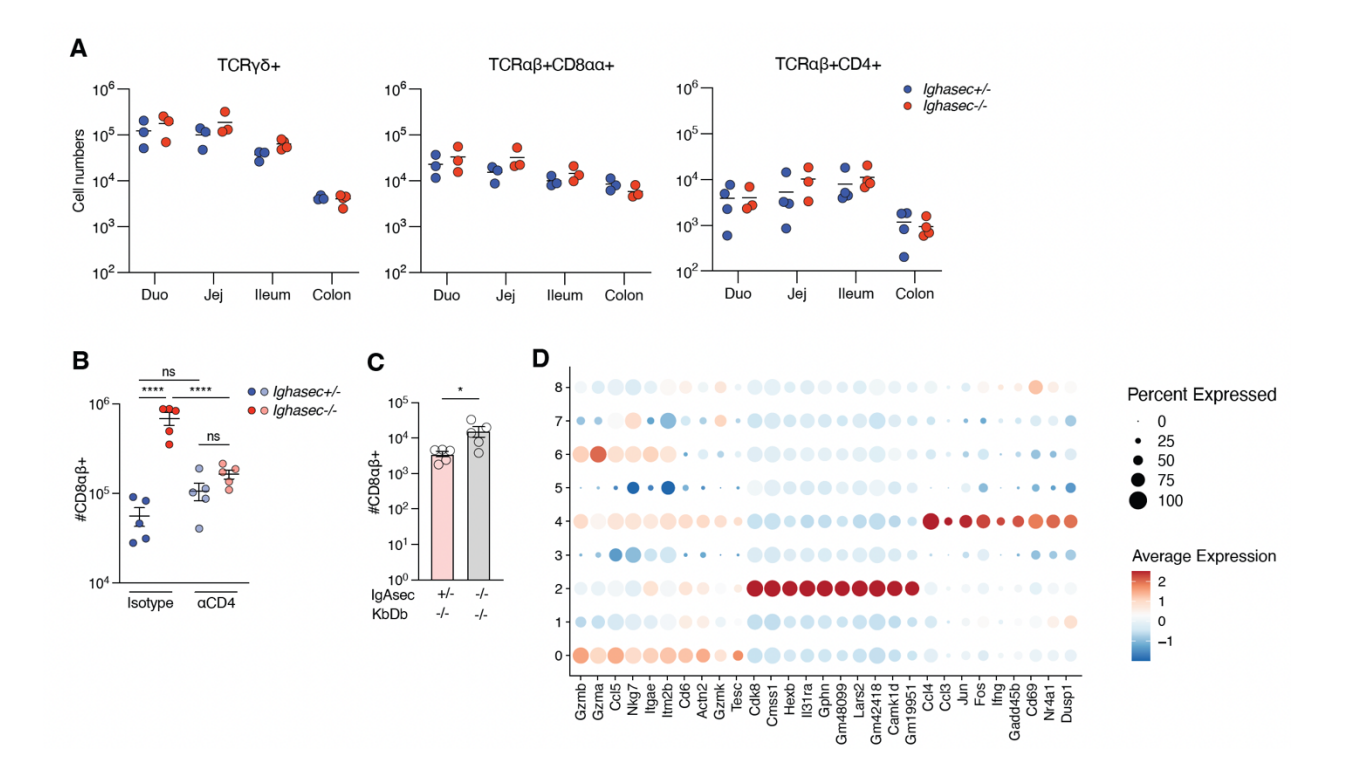


Figure 5 supplemental to Figure 4: IgA controls microbiota to prevent expansion of classically restricted CD8αβ+ IELs.

(A) Number of TCR $\gamma\delta$ +, TCR $\alpha\beta$ +CD8 $\alpha\alpha$ + and TCR $\alpha\beta$ +CD4+ IELs in each intestinal segment of Ighasec+/- and Ighasec-/- mice. n = 3 mice/group. (B) Number of CD8 $\alpha\beta$ + IELs in the jejunum of Ighasec+/- and Ighasec-/- mice after 4 weeks of isotype or anti-CD4 depleting antibody treatment. n = 5 mice/group. (C) Number of CD8 $\alpha\beta$ + IELs in the jejunum of Ighasec+/-KbDb-/- and Ighasec-/-KbDb-/- mice. n = 5 mice/group. (D) Dot plot representing expression (color) in clusters (rows) of top differentially expressed genes (columns) in CD8 $\alpha\beta$ + IELs from the jejunum of Ighasec+/- and Ighasec-/- mice. FDR-adjusted P <0.05; log2-fold change, log2FC > 0.25 using logistic regression test. Dot color: column z-scored, cluster average of log- and size-normalized gene counts (normalized expression). Dot size: percent of cells in cluster with positive expression of the gene.

All data in this figure are pooled from at least two independent experiments and are represented as mean or mean \pm SEM. **** P<0.0001, *** P<0.001, ** P<0.05 ns P≥0.05. Unpaired t-test (C), ANOVA with Tukey multiple comparison test (B).

3.2.IgA prevents murine astrovirus expansion in the small intestine.

To determine whether specific microbes induced the expansion of intraepithelial CD8 $\alpha\beta^+$ IELs in the small intestine of IgA deficient animals, we transplanted GF mice with limited consortia or complete microbiota from distinct animal facilities. Specifically, GF Ighasec+/- and Ighasec-/- mice were transplanted with fecal microbiota from five different sources: (1) University of Chicago SPF Barrier I room (Segmented filamentous bacteria (SFB)+, Helicobacter spp+, murine norovirus (MNV)+) (2) University of Chicago SPF Barrier II room (SFB-, Helicobacter spp-, MNV-), (3) C57BL/6J mice from Jackson laboratory (JAX), (4) altered Schaedler flora (ASF), and (5) a 13-species consortium. Limited consortia of microbes failed to induce expansion of CD8 $\alpha\beta^+$ IELs in *Ighasec-/-* recipients. In contrast, complex microbiota present in the mice at UofC Barrier I and II, and JAX microbiota led to the expansion (Figure 6A). These data, along with the observation that the CD8 $\alpha\beta$ + IELs were clonally expanded (Figure 4J-M), suggest that IgA regulates specific commensal microbes to restrain inflammatory CD8αβ⁺ T cell responses in the small intestine. While conducting our studies, we serendipitously identified a single litter of Ighasec-/- mice in UofC Barrier II that had low numbers of CD8αβ⁺ T cells (Figure 6B). We propagated the mice from the CD8 $\alpha\beta^+$ low litter and found that the progeny maintained the low CD8 $\alpha\beta^+$ phenotype, further supporting the hypothesis that expansion of intraepithelial CD8 $\alpha\beta^+$ T cells in IgA deficient mice was associated with distinct microbiota.

To identify microbes driving inflammatory T cell responses in IgA deficient hosts, we performed 16S rRNA gene sequencing of intestinal luminal contents. We utilized animals from UofC Barrier II (Hpp-, MNV-, SFB-) for the 16S rRNA gene sequencing since Ighasec-/- mice housed in this facility exhibited the CD8 $\alpha\beta$ ⁺ T cell expansion but lacked microbes, such as SFB, known to be regulated by IgA(K. Suzuki et al., 2004; Earley et al., 2023). We sequenced intestinal

luminal contents from each segment of co-housed Ighasec+/- and Ighasec-/- mice, as well as CD8αβ-low versus CD8αβ-high Ighasec-/- litters. The analysis of the bacterial communities in the small intestines of Ighasec+/- mice, compared with those of Ighasec-/- mice, revealed no significant differences in either relative or absolute genera abundances (Figure 7A). In addition, we did not find any bacterial taxa that segregated with the CD8αβ high phenotype (Figure 7B).

To further investigate which IgA-controlled microbe may be driving the expansion of CD8 $\alpha\beta^+$ IELs, we performed a limiting dilution fecal microbiota transfer. First, we aimed to reduce microbiota diversity via antibiotic treatment. 4-week treatment with vancomycin (V) and metronidazole (M) did not reduce the CD8 $\alpha\beta^+$ T cell expansion in *Ighasec-/-* hosts, suggesting the microbe was V/M resistant (Figure 7C). We confirmed that fecal microbiota transfer from V/M treated *Ighasec-/-* mice to GF mice was sufficient to induce CD8αβ⁺ T cell expansion (Figure 7D). Next, we performed serial dilutions of V/M Ighasec-/- feces and transferred to GF mice (Figure 7E). 4-weeks post transfer, we observed the expansion of intraepithelial CD8 $\alpha\beta^+$ IELs in Ighasec-/- recipients of 10⁴-fold diluted fecal material (Figure 7F). Metagenomic sequencing of the fecal content revealed that 99.8% of filtered bacterial reads (4,274,184 out of 4,284,095) were mapped to Limosilactobacillus reuteri (Figure 7G). Furthermore, microbial profiling with MetaPhlAn, which utilizes unique clade-specific marker genes, identified L. reuteri as the only microbial species present (Figure 7G). However, monocolonization with L. reuteri isolate obtained from the fecal material of this animal failed to induce expansion of CD8 $\alpha\beta^+$ IELs in the small intestine of IgA deficient recipients (Figure 7H). Intriguingly, the transfer of fecal material itself was sufficient to drive this response in *Ighasec-/-* hosts (Figure 7H). This suggested that other components of microbiota, not detected by DNA shotgun metagenomic sequencing, are present in the diluted fecal material and induce CD8 $\alpha\beta^+$ IEL expansion in IgA deficient hosts. These findings,

coupled with the observation that anti-viral gene programs were highly ranked in the gene set enrichment analysis of whole intestinal tissue RNA-seq data for differentially expressed genes between *Ighasec-/-* mice and littermate controls (Figure 7I), led us to investigate the hypothesis that viruses targeted by IgA might be driving the expansion of CD8αβ+ IELs.

To test the hypothesis that viruses were sufficient to drive the CD8 $\alpha\beta^+$ IEL expansion in IgA deficient mice, we colonized GF mice with fecal filtrate from *Ighasec-/-* recipient of the diluted fecal material (Figure 6C). Remarkably, the filtrate alone was sufficient to drive the expansion of intraepithelial CD8 $\alpha\beta^+$ T cells in IgA deficient recipients (Figure 6D). Furthermore, UV treatment of the filtrate prevented the expansion in *Ighasec-/-* mice, suggesting that CD8 $\alpha\beta^+$ IEL expansion may require an actively replicating virus (Figure 6D). We next administered an antiviral drug cocktail consisting of lamivudine, ribavirin, and acyclovir, which targets retroviruses, RNA viruses, and DNA viruses (Liu et al., 2019). Strikingly, *Ighasec-/-* mice that had received the anti-viral drug cocktail exhibited a reduction in CD8 $\alpha\beta^+$ IELs, whereas broadspectrum antibiotics (ampicillin, vancomycin, metronidazole, neomycin), had no effect (Figure 6E). The absence of an effect following treatment with the antiretroviral drugs emtricitabine and tenofovir(Lima-Junior et al., 2021) suggested that viruses other than retroviruses were likely responsible for the expansion of CD8 $\alpha\beta^+$ IELs.

Since neither eukaryotic DNA viruses detected by metagenomic sequencing (Figure 7G) nor anti-retroviral treatment altered CD8αβ⁺ IEL expansion (Figure 6E), we hypothesized that RNA virus may be driving the IEL response. Analysis of the intestinal tissue RNA-seq data of the diluted fecal material recipient mice and SPF mice from Barrier II facility (*Hpp*-, SFB-, MNV-) identified Murine Astrovirus (MuAstV) as a potential candidate (Figure 7J). MuAstV is a positive-sense, single-stranded RNA virus endemic to many mouse facilities(Ng et al., 2013), which can

cause chronic infections in RAG deficient hosts(Yokoyama et al., 2012). While MuAstV was present at very low levels in SPF Ighasec+/- mice, there was a 1000-fold increase in viral load across the small intestine of SPF Ighasec-/- hosts (Figure 6F). MuAstV was undetectable in GF Ighasec+/- or Ighasec-/- animals (Figure 6F). Furthermore, taking advantage of the CD8 $\alpha\beta^+$ low Ighasec-/- litters (Figure 6B), we found that presence of MuAstV correlated with the expansion of CD8 $\alpha\beta^+$ IELs (Figure 6G).

We next tested whether the presence of MuAstV was sufficient for the CD8 $\alpha\beta^+$ IEL expansion in *Ighasec-/-* mice from Barrier II facility (SFB-, *Hpp*- and MNV-). As shown in Figure 6H, colonization of *Ighasec-/-* GF mice with fecal microbiota from *Ighasec-/-* CD8 $\alpha\beta^+$ low donor, in which MuAstV was undetectable, failed to induce the expansion of CD8 $\alpha\beta^+$ IELs. However, supplementing this microbiota with MuAstV was sufficient to drive the CD8 $\alpha\beta^+$ IEL expansion in *Ighasec-/-* but not control mice. Furthermore, monoassociation with MuAstV was sufficient to drive CD8 $\alpha\beta^+$ IEL expansion in *Ighasec-/-*, but not control animals, and reached levels comparable to those found in SPF *Ighasec-/-* mice (Figure 6H). Together these data show that MuAstV, and not other members of UofC Barrier II microbiota, drive the expansion of CD8 $\alpha\beta^+$ IELs in IgA deficient animals.

MuAstV was shown to infect goblet cells and enterocytes in the small intestine(Ingle et al., 2021). Depletion of CD8αβ cells with an anti-CD8β depleting antibody revealed that CD8αβ⁺ IELs play an important role in regulating the MuAstV load in intestinal epithelial cells (IECs) of *Ighasec-/-* mice (Figure 6I). Furthermore, the absence of CD8αβ⁺ T cells (Figure 7K) led to further increased expression of genes involved in innate immune sensing (TLR3, MyD88), inhibition of viral replication (ZC3HAV1, Adar, Eif2ak, Slfn9), and interferon-inducible proteins (Ifi27l2, IFITM3, PML) in the small intestinal tissue of *Ighasec-/-* but not control mice (Figure 6J).

Collectively, these data demonstrate that, while unable to clear the virus, $CD8\alpha\beta^+$ IELs maintain homeostasis by regulating viral load and limiting host innate immune responses.

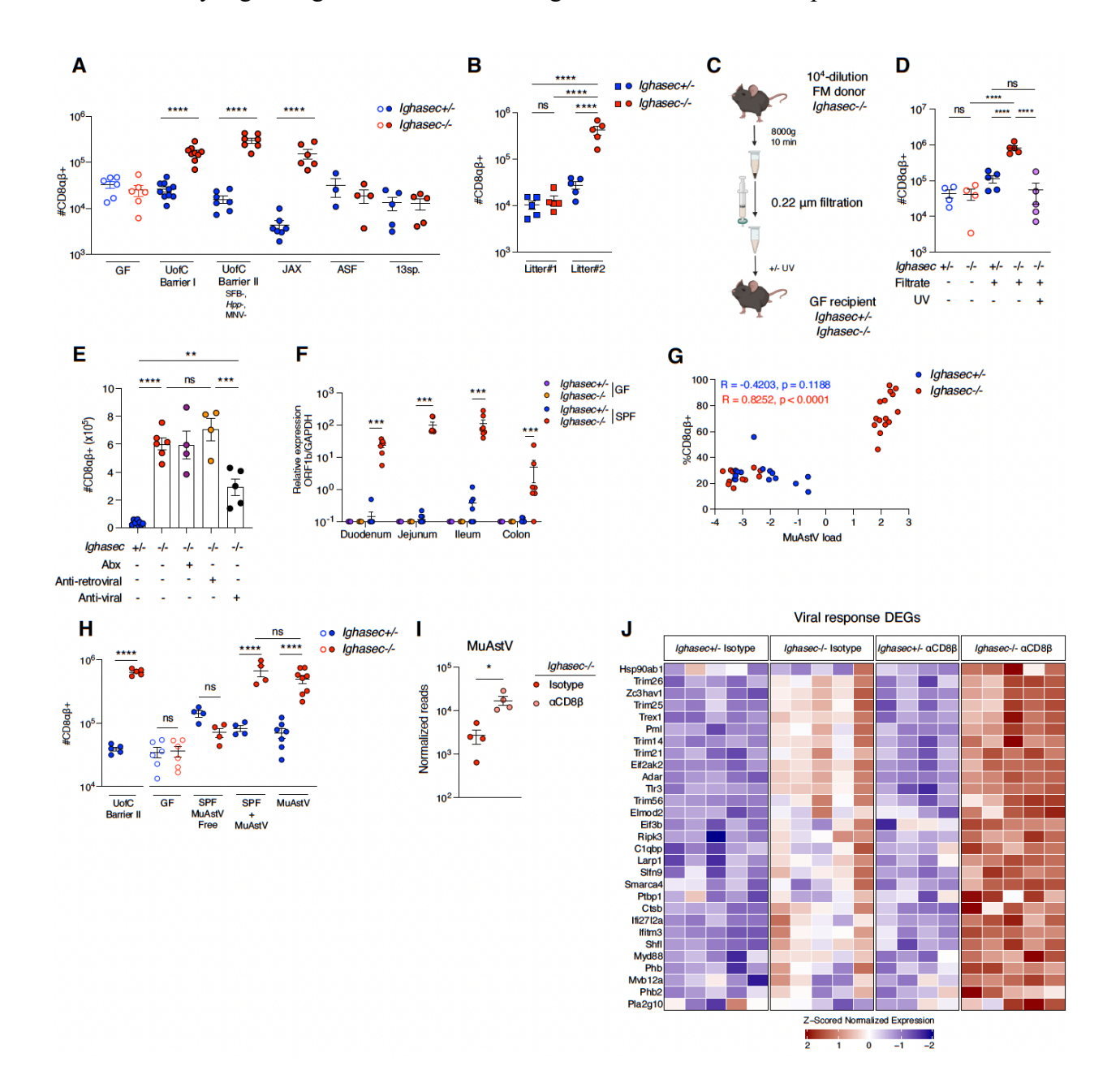


Figure 6: IgA controls Murine Astrovirus to limit inflammation in the small intestine.

- (A) Number of CD8 $\alpha\beta^+$ IELs in the jejunum of ex-GF *Ighasec+/-* and *Ighasec-/-* mice colonized with different microbiota (x axis). n = 4-9 mice/group. (B) Number of CD8 $\alpha\beta^+$ IELs in the jejunum of *Ighasec+/-* and *Ighasec-/-* mice from different litters (x axis). n = 5 mice/group.
- (C) Experimental scheme of fecal material filtration and UV inactivation experiment in *Ighasec+/-* and *Ighasec-/-* mice.

Figure 6: IgA controls Murine Astrovirus to limit inflammation in the small intestine continued.

(**D**) Number of CD8αβ⁺ IELs in the jejunum of GF control or filtrate (with or without UV inactivation) colonized *Ighasec+/-* and *Ighasec-/-* mice. n = 4-5 mice/group. (**E**) Number of CD8αβ⁺ IELs in the jejunum of SPF, broad-spectrum antibiotic, anti-retroviral, and anti-viral treated *Ighasec+/-* and *Ighasec-/-* mice. n = 4-6 mice/group. (**F**) Murine astrovirus (MuAstV) load, as measured by qPCR, relative to *Gapdh* in each intestinal segment of GF and SPF *Ighasec+/-* and *Ighasec-/-* mice. n = 7 mice/group. (**G**) Paired analysis of CD8αβ⁺ IEL frequency and MuAstV load in the jejunum of *Ighasec+/-* and *Ighasec-/-* mice. Annotated with Pearson correlation coefficient and p-value. (**H**) Number of CD8αβ⁺ IELs in the jejunum of SPF and GF *Ighasec+/-* and *Ighasec-/-*, or ex-GF *Ighasec+/-* and *Ighasec-/-* mice 4 weeks after colonization with MuAstV free microbiota (SPF MuAstV Free), MuAstV free microbiota supplemented with MuAstV (SPF + MuAstV) or MuAstV alone (MuAstV). n = 4-7 mice/group. (**I**) Normalized reads of MuAstV in sorted jejunal epithelial cells of isotype and anti-CD8β treated *Ighasec-/-* mice. n = 4 mice/group. (**J**) Heatmap of the z-scored expression of viral response genes (rows) in the ileal tissue of isotype and anti-CD8β treated *Ighasec-/-* mice. n = 5 mice/group.

All data in this figure are pooled from at least two independent experiments and are represented as mean or mean \pm SEM. **** P<0.0001, *** P<0.001, ** P<0.05 ns P<0.05. Unpaired t-test (A, I), ANOVA with Tukey multiple comparison test (B, D, E, G), Mann-Whitney test (F).

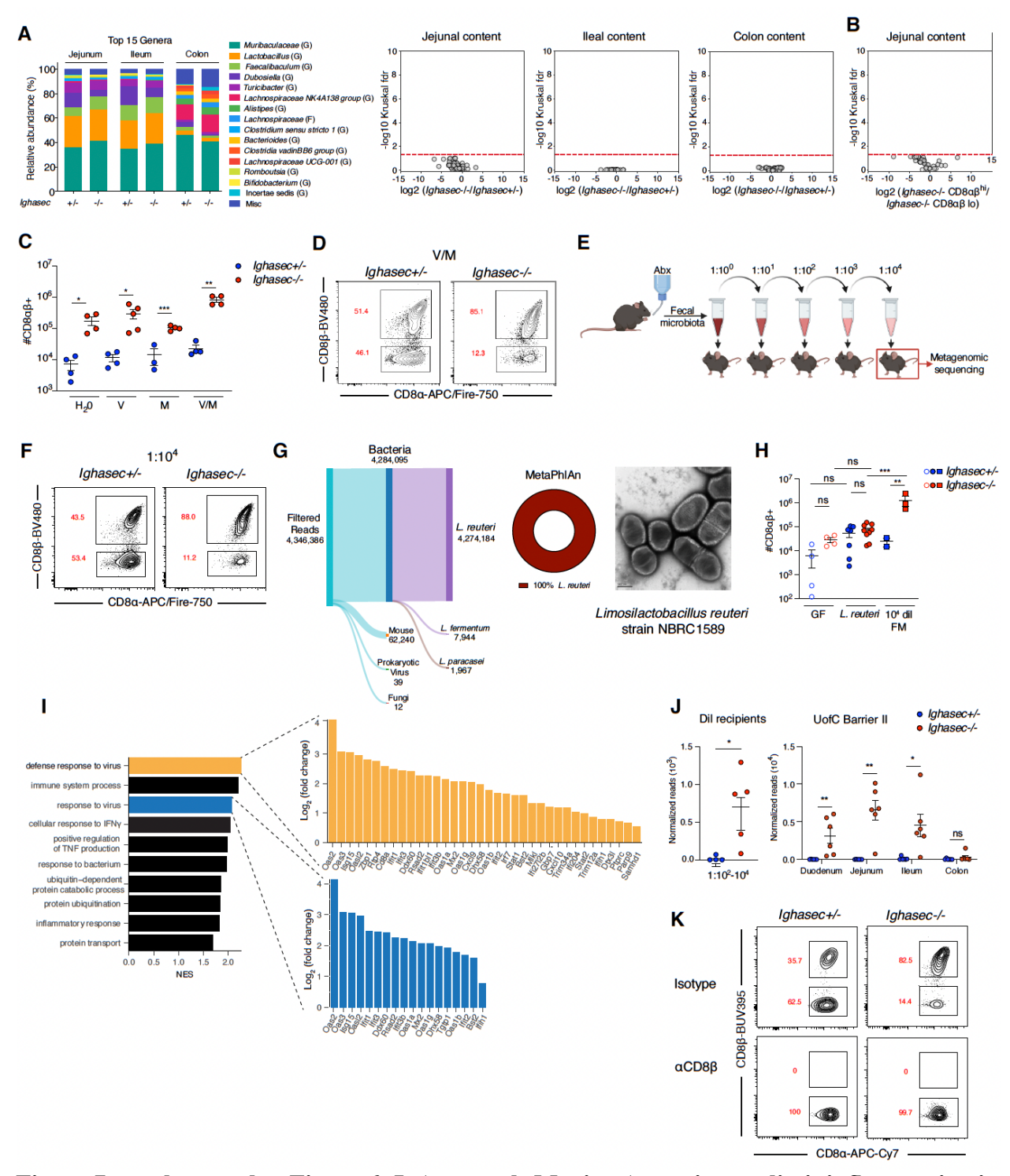


Figure 7 supplemental to Figure 6: IgA controls Murine Astrovirus to limit inflammation in the small intestine.

Figure 7 supplemental to Figure 6: IgA controls Murine Astrovirus to limit inflammation in the small intestine continued.

(A) Average relative abundance of the top 15 genera (left) and fold-change of absolute abundances (x axis, log₂ fold change) of different bacterial genera (right) and their statistical significance (y axis, -log₁₀ of the FDR adjusted P value) in Ighasec+/- versus Ighasec-/- mice housed at UofC Barrier II based on 16S rRNA gene sequencing. Red dashed line indicates a significant threshold of p<0.05. (B) Fold change of absolute abundances (x axis, log₂ fold change) of different bacteria genera and their statistical significance (y axis, $-\log_{10}$ of the FDR adjusted P value) in Ighasec-/- CD8αβ+ IEL high versus Ighasec-/- CD8αβ+ IEL low mice based on 16S rRNA gene sequencing of the jejunal luminal content. Red dashed line indicates a significant threshold of p<0.05. (C) Number of CD8αβ⁺ IELs in the jejunum of SPF *Ighasec*+/- and *Ighasec*-/- mice after 4 weeks of treatment with depicted antibiotic regimens (x axis). n = 4-5 mice/group. (D) Representative plots of the frequencies of CD8αβ⁺ IELs in the jejunum of *Ighasec*+/- and Ighasec-/- recipients 4 weeks post V/M microbiota transfer. (E) Experimental scheme of antibiotic treatment and limiting dilution experiment in Ighasec+/- and Ighasec-/- mice. Metagenomic sequencing was performed using jejunal content from 1:10⁴ dilution recipient 4 weeks after colonization. (F) Representative plots of the frequencies of CD8αβ⁺ IELs in the jejunum of Ighasec+/- and Ighasec-/- recipients 4 weeks post 10⁴ diluted V/M microbiota transfer. (G) Sankey diagram (left) depicting read distribution of detected phyla and any species greater than 0.01% relative abundance identified in the fecal content of 10⁴ diluted V/M microbiota recipient based on k-mer analysis with Kraken2. Donut chart (middle) representing MetaPhlAn4 marker-gene taxonomic analysis of the fecal content of 10⁴ diluted V/M microbiota recipient. Transmission electron microscopy (right) of L. reuteri strain NBRC1589 identified in the microbiota of Ighasec-/- recipient after antibiotic treatment and limiting dilution transfer. (H) Number of CD8 $\alpha\beta^+$ IELs in the jejunal tissue of GF control, L. reuteri monocolonized or 10^4 dil fecal material recipient *Ighasec+/-* and *Ighasec-/-* mice. n=2-9 mice/group. (I) Normalized enrichment scores (NES) of gene ontology (GO) assignments for top 10 GO terms enriched in the RNA-seq of the jejunal tissue of SPF Ighasec-/- mice versus Ighasec+/- mice. DEGs are shown for the specific pathways of interest. (J) Normalized reads ((#MuAstV reads/#reads total)106) of MuAstV recovered from RNAseq data of the jejunal tissue from Ighasec+/- and Ighasec-/- recipients after antibiotic treatment and limiting dilution transfer (left) or SPF Ighasec+/- and Ighasec-/- mice from UofC barrier II (right).

All data in this figure are pooled from at least two independent experiments and are represented as mean or mean \pm SEM. **** P<0.0001, *** P<0.001, ** P<0.05 ns P≥0.05. Unpaired t-test (C), ANOVA with Tukey multiple comparison test (H) Mann-Whitney test (J).

3.3.Germinal center-derived IgA plasma cells control the colonization of MuAstV in the small intestine

In control *Ighasec+/-* mice, monoassociation with MuAstV led to an increase in the number of IgA plasma cells (PCs) in the small intestine (Figure 8A). Furthermore, the frequency and number of IgA-switched germinal center (GC) B cells in the Peyer's patches (PPs) and mesenteric lymph nodes (mLNs) of these animals was increased (Figure 8B-C). Importantly, MuAstV was found to be coated by IgA in the lumen of *Ighasec+/-* animals (Figure 8D). Together, these data suggest that under physiological conditions, MuAstV induces IgA switched GC responses and the generation of lamina propria IgA plasma cells likely involved in controlling the MuAstV load in the small intestine. Furthermore, taking advantage of the retained IgA-switching in the *Ighasec-/-* model, we demonstrated that MuAstV induced expansion of GC B cells and T follicular helper (T_{FH}) cells (Figure 9A-B) and increased IgA class switching (Figure 9C) in the PPs. Finally, we confirmed under SPF conditions, that in presence of MuAstV, *Ighasec-/-* mice exhibited PP hyperplasia (Figure 9D), GC B and TFH cells expansion (Figure 9E-F) and increased IgA switching in the PP (Figure 9G). These findings suggest that MuAstV promotes a T cell-dependent IgA response.

IgA class switching occurs via both T cell-independent and -dependent mechanisms (Macpherson et al., 2000; Bunker et al., 2015). T-dependent responses take place in GCs of mLNs and PPs, where B cells can undergo somatic hypermutation and affinity maturation through interaction with TFH cells (Mesin et al., 2016). To formally test whether T-dependent IgA responses were required to control MuAstV, we analyzed Bcl6^{fl/fl} mice crossed with CD4-Cre or

CD21-Cre, lacking TFH or GC B cells, respectively. Noteworthy, these mice exhibited a comparable number of IgA PCs in the small intestinal lamina propria to control animals (Figure 9H-I). In accordance with our hypothesis, TFH or GC B cell deficient mice displayed an expansion of MuAstV in the intestinal tissues (Figure 7E-F). In GC B cell deficient hosts this was associated with an expansion of CD8 $\alpha\beta^+$ IELs in the small intestinal tissue (Figure 7G), similarly, to *Ighasec-/-* mice (Figure 4B and 6G).

Overall, these data demonstrate that GC-derived IgA PCs regulate MuAstV load in the small intestine, maintaining immune homeostasis and limiting CD8 $\alpha\beta^+$ T cell expansion.

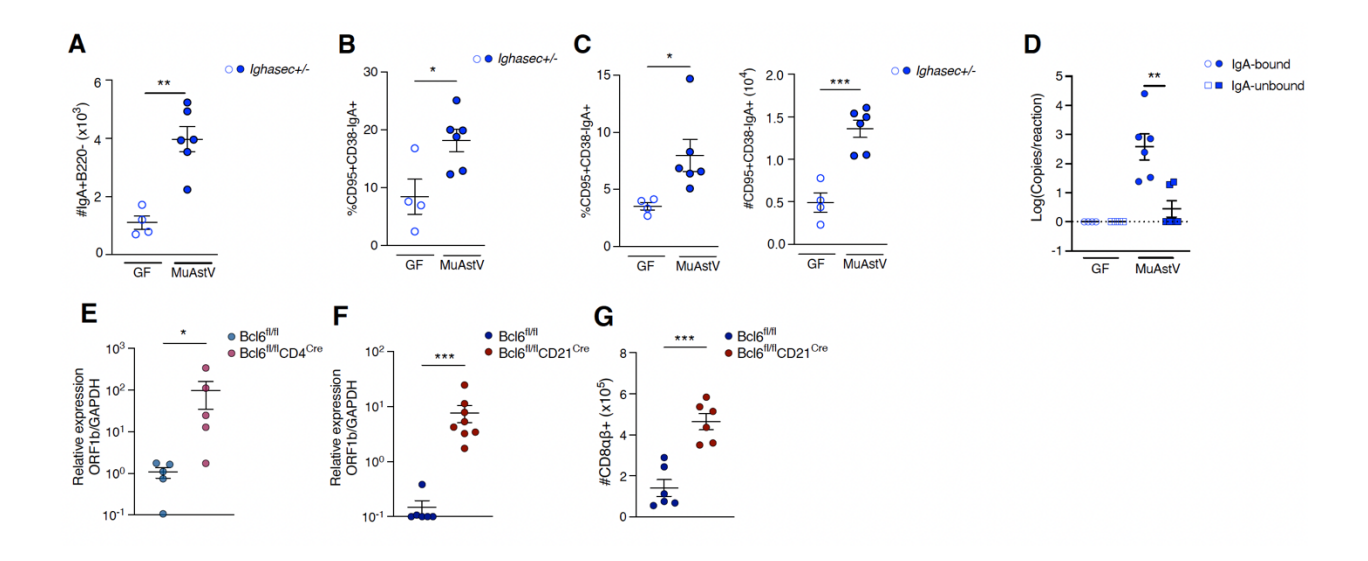


Figure 8: GC-derived IgA plasma cells contribute to MuAstV control in the small intestine.

(A) Number of IgA⁺ PCs in the jejunal LP of GF or MuAstV-monocolonized *Ighasec*+/- mice. n = 4-6 mice/group. (B) Frequency of IgA-switched cells among CD38⁻CD95⁺ GC B cells in the PPs of GF or MuAstV monocolonized *Ighasec*+/- mice. n = 4-6 mice/group. (C) Frequency (left) and number (right) of IgA-switched cells among CD38⁻CD95⁺ GC B cells in the mLNs of GF or MuAstV monocolonized *Ighasec*+/- mice. n = 4-6 mice/group. (D) Number of MuAstV copies per reaction in fecal extracts of *Ighasec*+/- in IgA-bound and IgA-unbound fractions. n = 4-6 mice/group. (E and F) MuAstV load, as measured by qPCR, relative to *Gapdh* in the jejunum of Bcl6^{fl/fl} and Bcl6^{fl/fl}CD4^{Cre} (E) or Bcl6^{fl/fl} and Bcl6^{fl/fl}CD21^{Cre} mice (F). n = 5-8 mice/group. (G) Number of CD8 α β⁺ IELs in jejunum of SPF Bcl6^{fl/fl} and Bcl6^{fl/fl}CD21^{Cre} mice. n = 6 mice/group.

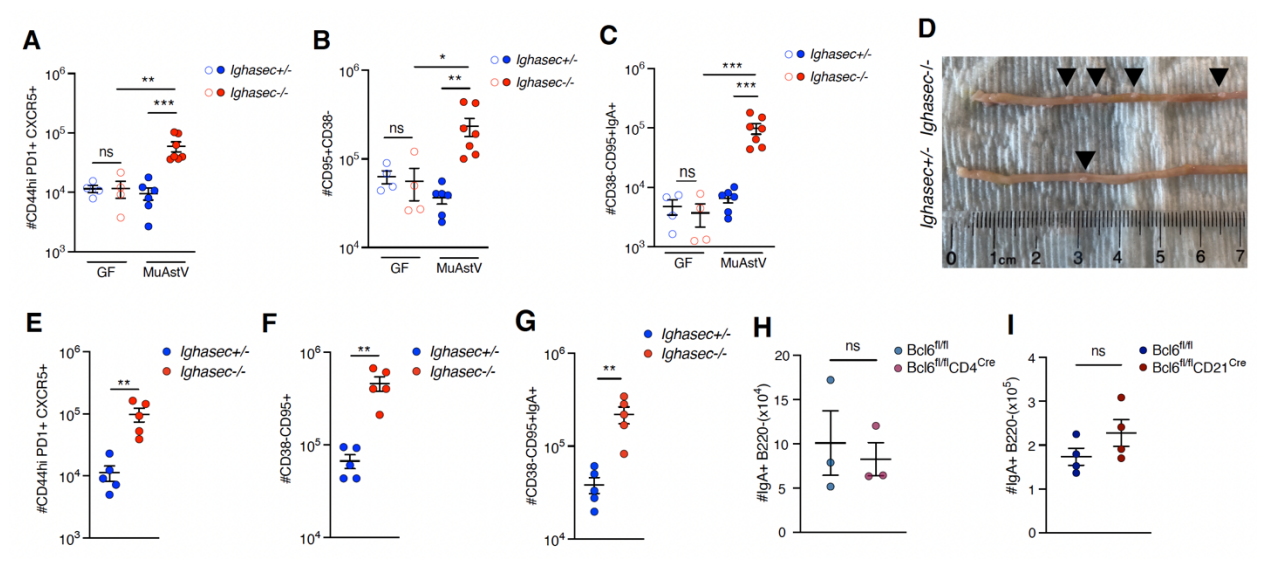


Figure 9 supplemental to Figure 8: GC-derived IgA plasma cells contribute to MuAstV control in the small intestine.

(A and B) Number of CD44^{hi}CXCR5⁺PD-1⁺ T_{FH} cells among CD4⁺ T cells (A) and CD38⁻CD95⁺ GC B cells among CD19⁺ B cells (B) in the PPs of GF or MuAstV monocolonized *Ighasec+/-* and *Ighasec-/-* mice. n = 4-7 mice/group. (C) Number of IgA switched cells among CD38⁻CD95⁺ GC B cells in the PPs of GF or MuAstV monocolonized *Ighasec+/-* and *Ighasec-/-* mice. n = 4-7 mice/group. (D) Representative image of the *Ighasec+/-* (bottom) and *Ighasec-/-* (top) intestines with black arrows depicting PPs. (E and F) Number of CD44^{hi}CXCR5⁺PD-1⁺ T_{FH} cells among CD4⁺ T cells (E) and CD38⁻CD95⁺ GC B cells among CD19⁺ B cells (F) in the PPs of SPF *Ighasec+/-* and *Ighasec-/-* mice. n = 5 mice/group. (G) Number of IgA switched cells among CD38⁻CD95⁺ GC B cells in the PPs of SPF *Ighasec+/-* and *Ighasec-/-* mice. n = 5 mice/group. (H and I) Number of IgA PCs in the jejunal LP of Bcl6^{fl/fl} and Bcl6^{fl/fl}CD4^{Cre} (H) or SPF Bcl6^{fl/fl} and Bcl6^{fl/fl}CD21^{Cre} (I). n = 3-4 mice/group.

All data in this figure are pooled from at least two independent experiments and are represented as mean or mean \pm SEM. **** P<0.001, *** P<0.001, ** P<0.01, * P<0.05 ns P<0.05. ANOVA with Tukey multiple comparison test (A, B, C), Unpaired t-test (E, F, G, H, I).

3.4.IgA restricts norovirus colonization to protect the host against immunopathology

We next aimed to determine whether we could extend the role of IgA in limiting viral colonization and CD8 $\alpha\beta^+$ IEL expansion to other RNA viruses. To address this, we infected GF *Ighasec-/-* and control animals with enteric viruses belonging to the *Caliciviridae* and *Reoviridae* families and assessed the CD8 $\alpha\beta^+$ IEL numbers in the small intestine. Among the enteric viruses used, only the chronic murine norovirus CR6 (MNV-CR6)(Nice et al., 2013) induced CD8 $\alpha\beta^+$ IEL expansion in the small intestine of IgA-deficient hosts (Figure 11A), and this was observed throughout the entire small intestine (Figure 11B). The increase in CD8 $\alpha\beta^+$ IELs in *Ighasec-/-* mice was associated with a significant increase in MNV-CR6 in the small intestine 4 weeks post-colonization (Figure 10A). Intriguingly, CD8 $\alpha\beta^+$ IEL expansion was not observed after infection with reovirus (T1L strain), murine rotavirus (EDIM) or MNV-CW3 (Figure 11A), suggesting that IgA was not required for the clearance of these viruses.

These observations suggest IgA restrict other enteric viruses beyond MuAstV, such as MNV-CR6, to limit CD8 $\alpha\beta^+$ IEL expansion. However, while sIgA plays a role in preventing reinfection with reovirus(Hutchings et al., 2004) and rotavirus(Blutt et al., 2012), it does not play a role in preventing chronic colonization of the gut by these enteric viruses, suggesting a selective role of IgA in the regulation of the gut virome.

Lastly, we wanted to assess whether the expansion of enteric viruses in IgA-deficient mice can influence the host's response to tissue injury. We exposed IgA-deficient mice and controls from the UofC Barrier I (*Hpp*+, SFB+, MNV+) to 2% dextran sulfate sodium (DSS) for seven days to induce intestinal tissue damage. At baseline, we did not observe any difference in intestinal permeability in the IgA-deficient mice raised in this barrier facility (Figure 11C). However, after

DSS administration, we observed significant colonic shortening (Figure 11D) and bacterial translocation to the mLNs (Figure 11E).

We next sought to determine whether the presence of MuAstV or MNV-CR6 in the microbiome impacts colitis outcomes in IgA-deficient animals. We used mice propagated from MuAstV free litters (Figure 6B) raised in UofC Barrier II, lacking endogenous MNVs for these experiments. We did not observe any difference in weight loss or colon shortening in MuAstV colonized IgA-deficient animals compared to littermate controls or MuAstV-negative controls (Figure 10B-C). Murine noroviruses (MNVs) were previously identified to exacerbate colitis in genetically susceptible hosts(Lencioni et al., 2008; Cadwell et al., 2010; Basic et al., 2014). We infected MuAstV free Ighasec+/- and Ighasec-/- mice from Barrier II (Hpp-, SFB-, MNV-) with MNV-CR6 and 3-4 weeks post-infection subjected them to 2.5% DSS for seven days. We observed that MNV-CR6 infected IgA-deficient hosts lost significantly more body weight than uninfected IgA-deficient or MNV-CR6 infected control IgA-sufficient mice (Figure 10B). Furthermore, colonic shortening and colon pathology were more prominent in MNV-CR6-infected IgAdeficient hosts than in infected control mice or uninfected IgA-deficient mice (Figure 10C-D). These results suggest that secretory IgA plays an important role in limiting DSS colitis in mice colonized with MNV.

We next wanted to extend these findings to another model of colitis. Previous reports identified elevated luminal IgA levels in IL-10 deficient hosts (Gomes-Santos et al., 2012). To determine the role of IgA in the development of colitis in IL-10 deficient mice, we transferred conventional microbiota from UofC Barrier I (SFB+, Hpp+, MNV+) to GF *Ighasec-/-* IL-10-/- or *Ighasec+/-* IL-10-/- hosts. IL-10 deficient hosts lacking IgA lost more body weight than controls (Figure 11F). We observed more colonic pathology at the experimental endpoint in

Ighasec-/- IL-10-/- mice (Figure 11G). To determine the impact of MNV-CR6 on the colitis development in IL-10 deficient mice lacking IgA, we transferred MuAstV-free UofC Barrier II microbiota (SFB-, Hpp-, MNV-) with or without MNV-CR6 to Ighasec+/- IL-10-/- or Ighasec-/- IL-10-/- mice. All ofthe Ighasec-/- IL-10-/- mice colonized with UofC Barrier II microbiota and MNV-CR6 developed rectal prolapses by the experimental endpoint (Figure 10E) and had increased colonic pathology (Figure 10F). In sharp contrast, none of the MNV-CR6 infected Ighasec+/- IL-10-/- hosts and only one Ighasec-/- IL-10-/- mouse receiving MNV-free UofC Barrier II microbiota developed a rectal prolapse by the experimental endpoint (Figure 10E). Taken together these observations indicate that the combination of IgA-deficiency and presence of MNV leads to exacerbated colitis outcomes.

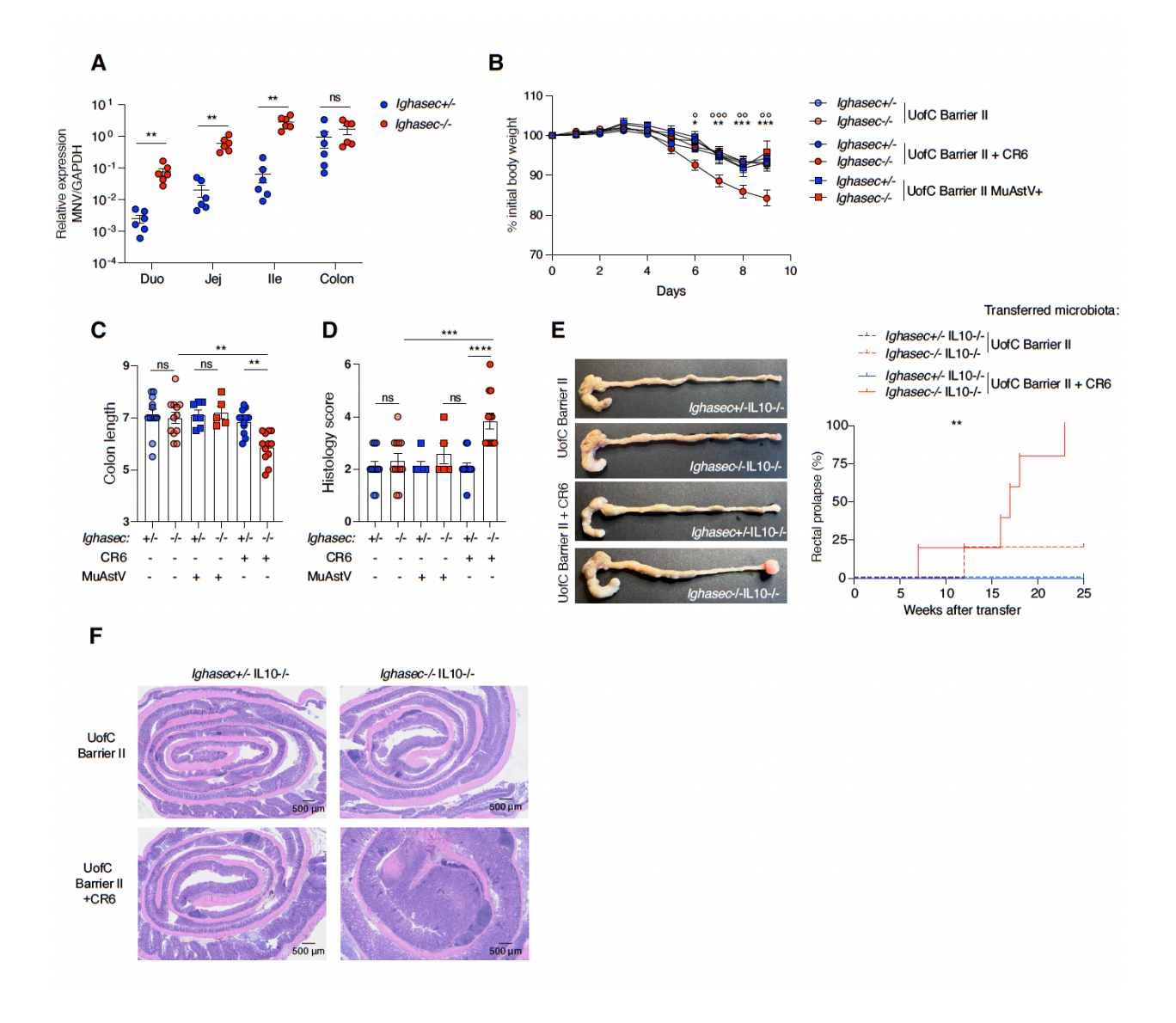


Figure 10: IgA maintains intestinal homeostasis to protect the host from immunopathology.

(A) MNV-CR6 load, as measured by qPCR, relative to *Gapdh* in the duodenum, jejunum, ileum, and colon of *Ighasec+/-* and *Ighasec-/-* mice. n = 6 mice/group. (**B and C**) Percent of initial body weight change (B) and colonic shortening (C) of the *Ighasec+/-* or *Ighasec-/-* virus-free mice or MNV-CR6 infected, and MuAstV⁺ mice after exposure to 2.5% DSS in water. n = 5-12 mice/group. In (B), ° indicates the effect due to the infection status (i.e. *Ighasec-/-* UofC Barrier II versus *Ighasec-/-* UofC Barrier II + CR6), while * indicates the effect due to genotype (i.e. *Ighasec+/-* UofC Barrier II + CR6 versus *Ighasec-/-* UofC Barrier II + CR6) at given timepoints. (**D**) Colon tissue Swiss roll histology scores of the *Ighasec+/-* or *Ighasec-/-* virus-free mice or MNV-CR6 infected, and MuAstV⁺ mice after exposure to 2.5% DSS in water. n = 5-12 mice/group.

Figure 10: IgA maintains intestinal homeostasis to protect the host from immunopathology continued.

(E) Representative image (left) and rectal prolapse incidences (right) in *Ighasec+/-* IL-10-/- and *Ighasec-/-* IL-10-/- mice colonized with UofC Barrier II microbiota or UofC Barrier II microbiota with MNV-CR6. n = 3-5 mice/group. **(F)** Representative H&E staining of the colon from (E) at the onset of the prolapse.

All data in this figure are pooled from at least two independent experiments and are represented as mean or mean \pm SEM. **** P<0.001, *** P<0.01, ** P<0.01, ** P<0.05 ns P \ge 0.05. °° P<0.001, °° P<0.01, ° P<0.05. Mann-Whitney test (A), Unpaired t-test (B, C, D), Mantel-Cox test (E).

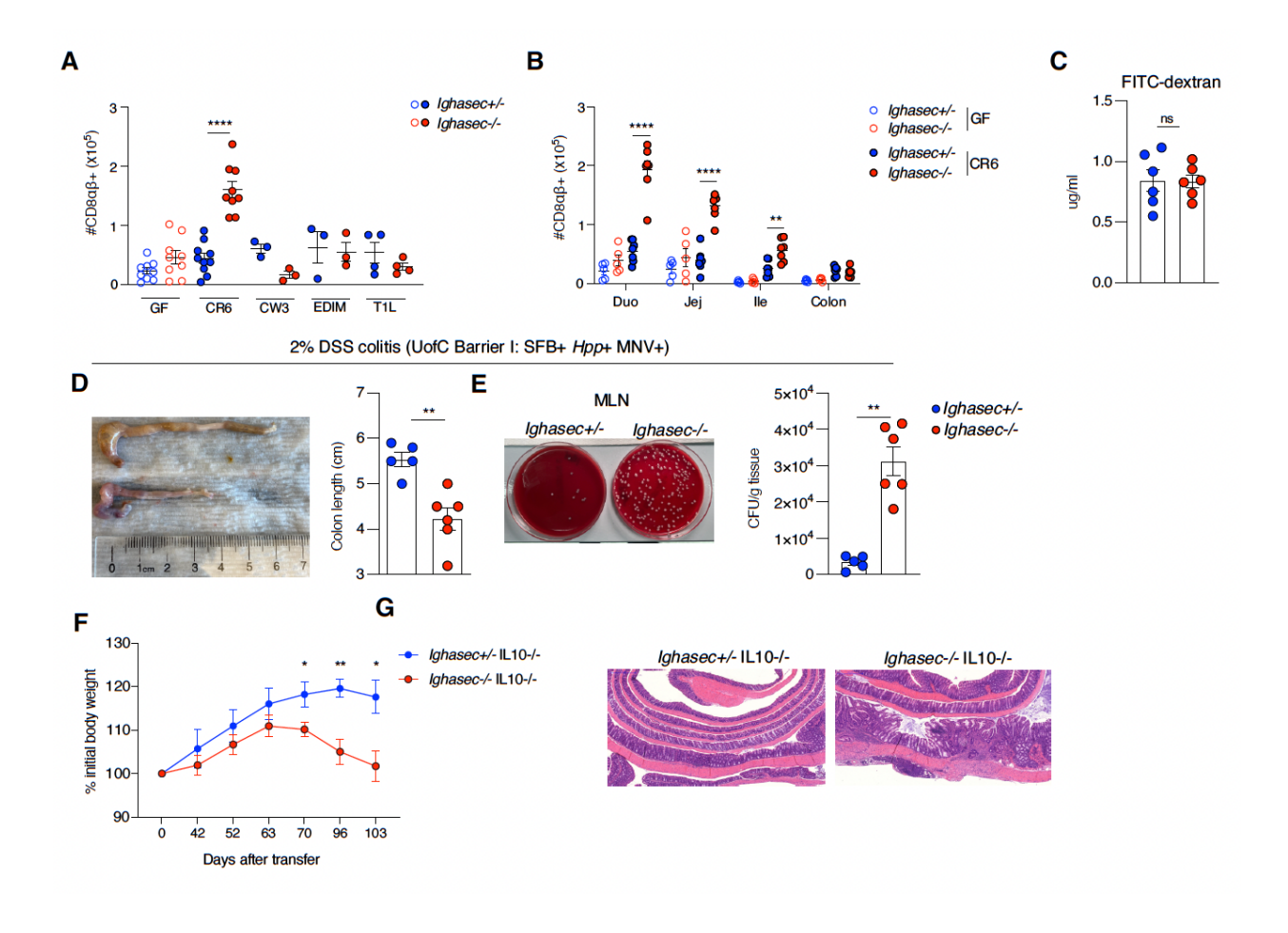


Figure 11 supplemental to Figure 10: IgA maintains intestinal homeostasis to protect the host from immunopathology.

(A) Number of CD8αβ⁺ IELs in the jejunum of ex-GF *Ighasec+/-* and *Ighasec-/-* mice colonized with different viruses (x axis). n = 3-9 mice/group. (B) Number of CD8αβ⁺ IELs in each intestinal segment of ex-GF *Ighasec+/-* and *Ighasec-/-* mice colonized with MNV-CR6. n = 5-7 mice/group. (C) Intestinal permeability measurement by serum FITC-dextran concentration in *Ighasec+/-* and *Ighasec-/-* mice housed in UofC Barrier I. n = 6 mice/group. (D) Representative image (left) and measure of colonic shortening (right) in *Ighasec+/-* and *Ighasec-/-* mice after exposure to 2% DSS in water. n = 6 mice/group. (E) Representative image (left) and quantification of bacterial translocation to the MLNs (right) of *Ighasec+/-* and *Ighasec-/-* mice after exposure to 2% DSS in water. n = 6 mice/group. (F) Percent of initial body weight change of the ex-GF *Ighasec+/-* IL-10-/- and *Ighasec-/-* IL-10-/- mice at indicated timepoints post colonization with UofC Barrier I microbiota. (G) Representative H&E staining of the colon of ex-GF *Ighasec+/-* IL-10-/- and *Ighasec-/-* IL-10-/- at the experimental endpoint.

All data in this figure are pooled from at least two independent experiments and are represented as mean or mean \pm SEM. **** P<0.0001, *** P<0.001, ** P<0.01, * P<0.05 ns P≥0.05. Unpaired t-test (A, C, D, E, F, G), ANOVA with Tukey multiple comparison test (B).

4.DISCUSSION

Numerous epidemiological studies suggest a potential role for germinal center IgA responses in maintaining homeostasis, preventing infections, and mitigating the development of immune-mediated disorders (French et al., 1995; Mazanec et al., 1995; Koskinen, 1996; Kumar et al., 2002; K. Suzuki et al., 2004; Blutt et al., 2012; Singh et al., 2014; Rawla et al., 2024). However, the rarity of overt disease in patients or mice with IgA deficiency raises questions about the precise role of IgA in pathophysiology and the potential compensatory role of IgM in preventing pathology. Thus far, few phenotypes were observed in IgA deficient animals, and mainly relate to changes in microbial composition, rather than host immune responses or intestinal pathology. Using a novel mouse model of IgA deficiency, we were able to address these long-standing questions.

4.1.MuAstV-driven expansion of CD8αβ + IELs in IgA deficient hosts

MuAstV is a non-enveloped, positive-sense, single-stranded RNA virus endemic to many mouse facilities (Ng et al., 2013), and it can cause acute and asymptomatic infection in wild-type animals and chronic infections in RAG deficient hosts (Yokoyama et al., 2012). In this study, we have found that sIgA binds MuAstV and protects the hosts from chronic infection. The chronic MuAstV infection leads to expansion of peripherally induced CD8αβ+ IELs, but not the peripherally induced CD4+ IELs or natural IEL subsets. The expansion of CD8αβ+ IELs was also present in *Igha-/-* hosts, in which we and others have observed increased IgM responses. This suggested that IgM cannot compensate for IgA to protect the host from persistent MuAstV infection. Similar observations were made in IgA deficient humans, where presence of IgM in the lumen and IgM coating of the resident microbiota was not sufficient to prevent the dysbiosis (Catanzaro et al., 2019; Jørgensen et al., 2019). Moreover, sIgA in healthy controls versus compensatory IgM in IgA

deficient patients seems to have different patterns of bacterial coating. Certain taxa can be equally well coated by both IgA and IgM, while others are preferentially coated by either IgA or IgM. For example, *Enterobacteriaceae*, overrepresented in the microbiome IgA deficient patients, was not targeted by IgM (Fadlallah et al., 2018; Catanzaro et al., 2019). Taken together, this data suggests that IgM may not be sufficient to compensate for certain IgA biological functions in the intestinal lumen.

The expanded CD8αβ+ IELs were primed by BATF3+ cDC1s in presence of CD4 help and were classically restricted. The number of CD8 $\alpha\beta$ + IELs in *Ighasec-/- KbDb-/-* mice was reduced to that of Ighasec+/- K^bD^b+/- littermate controls. However, it remains to be tested whether other, nonclassical MHClb molecules, are involved in this response. We did observe minor, although significant, increase of CD8 $\alpha\beta$ + T cells in *Ighasec-/-* K^bD^b -/- hosts in comparison to Ighasec+/- KbDb-/- controls. Some of non-classical MHCIb molecules can present peptides to CD8+ T cells. For example, S. epidermidis colonization of the skin leads to accumulation of CD8 $\alpha\beta$ + T cells restricted to the MHCIb molecule H2-M3, which can present N-formyl bacterial or mitochondrial peptides (Linehan et al., 2018). H2-M3 was also shown to present L. monocytogenes derived peptides to CD8+ T cells during infection (Pamer et al., 1992). Qa-1 can present MHCI leader peptides, but also bacteria- and virus- derived peptides to CD8+ T cells. These include peptides derived from cytomegalovirus (CMV) (Tomasec et al., 2000; Mazzarino et al., 2005; Anderson et al., 2019). CD8+ T cells restricted to Qa-2 family member H2-Q9, presenting a peptide derived from viral capsid, are induced during mouse polyoma virus infection (Swanson et al., 2008). Our tissue RNA-seq dataset revealed an upregulation of non-classical MHCIb molecule from Qa-2 family, H2-Q6 in SPF IgA deficient hosts. Therefore, it is plausible that some CD8αβ+ T cells can be restricted non-classical MHClb molecules and contribute to the

anti-viral response. To formally test this, we would need to assess the CD8 $\alpha\beta$ + IEL expansion in *Ighasec-*/- mice crossed to H2-M3, Qa-1 and Qa-2 deficient background.

The expanded CD8αβ+ IELs produced IFNγ and expressed high levels of cytotoxicity-associated genes (Gzmb, Gzma). Their repertoire profiling provided the evidence of antigen-driven clonal expansion. Some of the expanded clones shared specific motifs in the CDR3 region, that were observed across multiple IgA deficient hosts but rarely in control mice. This suggested that CD8 $\alpha\beta$ + IELs present in IgA deficient hosts can be induced in response to virus-derived antigens. Future experiments would need to be performed to elucidate the specificity of the TCRs containing shared CDR3 motifs. The set of enriched TCRs, unique TCRs and a control OT-I TCR would be cloned and expressed a NFAT-GFP+ hybridoma, reporting TCR signaling (Yang et al., 2014). To assess whether these TCRs can indeed respond to peptides derived from MuAstV, GFP upregulation can be measured of the co-cultured hybridomas with splenic DCs pulsed with viral lysates. The OT-I TCR expressing hybridoma or K^bD^b-/- DCs would be utilized in the assay as a negative control. We would expect to observe GFP upregulation in the hybridoma expressing TCRs containing specific CDR3, but not unique, or control OT-I TCR when co-cultured with MHC-I sufficient DCs. To identify epitopes recognized by these TCRs, a peptide library can be generated, containing peptide candidates with predicted binding to mouse MHCI. Virus-derived or SIINFEKL peptides would be tested for their ability to stimulate TCR signaling in the NFAT-GFP+ hybridoma cell lines. MuAstV genome consists of three open reading frames (ORF). ORF1a and ORF1b encodes serine protease, viral genome-linked protein, and RNA-dependent RNA polymerase, while ORF2 encodes capsid proteins (Cortez et al., 2017). The candidate peptides would be generated from these proteins.

In-vivo depletion of the CD8 β + cells suggested that the expanding CD8 $\alpha\beta$ + IELs limit hosts type I IFN responses and viral load in epithelial cells. However, the exact role of these cells in IgA deficient or B cell deficient hosts remains elusive. We did not observe intestinal pathology in Ighasec-/- mice chronically infected with the virus. That was also true after the CD8β+ cell depletion. It is possible that long-term depletion would be required to observe any pathology in response to chronic infection. This is however unlikely, as MuAstV-infected, 18- to 24-week-old SCID mice (B and T cell deficient) and NOG mice (B, T and NK cell deficient) presented no overt intestinal pathology either (Morita et al., 2021). MuAstV infection in mice does not lead to diarrhea, a classical sign of infection observed in humans, other mammals, and avian species (Cortez et al., 2017). Studies of human astroviruses suggested that specific serotypes (serotype 3) can be associated with higher fecal shedding and more severe gastroenteritis in children(Caballero et al., 2003). Infections with highly divergent astrovirus VA1 strains were also reported in children at the time of the celiac disease diagnosis (Smits et al., 2010). This strain was also associated with acute gastroenteritis outbreak among young children(Finkbeiner et al., 2009). VA1 and related strains have been also reported as a cause of viral encephalitis following bone marrow transplantation (Brown et al., 2015; Naccache et al., 2015; Lum et al., 2016) or in X-linked agammaglobulinemia (Quan et al., 2010; Frémond et al., 2015). Out of five cases reported, four were fatal. Lastly, astroviruses have been shown to cause encephalitis or encephalomyelitis in other mammals including minks and cattle (Blomström et al., 2010; Li et al., 2013). Therefore, it is possible that other MuAstV strains that could drive pathology in IgA deficient hosts exist.

Of note, we did observe an expansion of other IEL subset after 4-week CD8 β depletion study. Therefore, it is possible that some of the function of the CD8 $\alpha\beta$ + IELs in the IgA deficient hosts is compensated by other IEL subsets after the depletion. To address this, short-term depletion study

could be performed, where tissue histology, epithelial proliferation, intestinal permeability, and viral load can be determined prior the expansion of other IEL subsets.

Lastly, in immunocompromised hosts the MuAstV tropisms expands from goblet cells to absorptive enterocytes. In WT mice, in situ hybridization studies showed that MuAstV RNA is mainly detected in Muc2+ goblet cells. This is in stark contrast to Rag2-/-Il2rg-/- mice, where MuAstV RNA was abundantly detected in Ace2+ enterocytes throughout the duodenal villi, as well as in Muc2+ goblet cells (Ingle et al., 2021). We detected MuAstV RNA in the epithelial RNA-seq dataset, suggesting that MuAstV tropism in IgA deficient hosts might also include enterocytes of the small intestine. A major challenge for the immune system is establishing the balance between efficient pathogen elimination while avoiding damage to self as a consequence. Thus, it is possible that the efficient virus elimination by CD8 $\alpha\beta$ + T cells poses a greater fitness cost to the host compared to its tolerance.

4.2. Role of T-dependent IgA in controlling chronic enteric virus infection

Using TFH or GC B cell deficient mice, we have demonstrated that T-dependent IgA was important in controlling MuAstV infection. Both GC B cell and TFH deficient mice exhibited significant increase of the MuAstV in the intestinal tissue. Moreover, in the GC B cell deficient hosts, the MuAstV was associated with an expansion of CD8αβ⁺ IELs in the small intestine, similarly to IgA deficient hosts. These results suggested that GC-derived, TD IgA responses are important to control the MuAstV colonization. This can be further supported by the literature, where the IgA induced during the primary viral infection, specific to an outer capsid protein, protected the host from the reinfection (Silvey et al., 2001; Hutchings et al., 2004). However, it is possible that TI IgA participates in the response and control of the MuAstV. CD40-/- mice lack GCs and are unable to mount TD IgA responses (Kawabe et al., 1994). The luminal IgA titers and

number of IgA producing PC in the LP of these mice are not affected(Bergqvist et al., 2006). Similarly, the TI responses are intact. Therefore, infection of CD40-/- mice with MuAstV, assessment of the virus clearance and the intestinal immune responses should provide insight into the contribution of TI IgA responses to virus control.

Of note, we also analyzed the IEL compartment of TFH deficient mice and noted a severe decrease in number of the natural TCR $\alpha\beta$ + CD8 $\alpha\alpha$ + IEL subset. Among TCR β + cells in these mice, nearly all were expressing CD8 $\alpha\beta$ heterodimer. Since the CD4^{Cre} can delete the floxed Bcl6 gene at the double positive stage of the thymocyte development, we were cautious to relate the displacement of CD8 $\alpha\alpha$ + IELs with the increased viral load. Indeed, recent report had demonstrated that Bcl6 is required for the thymic development of the natural TCR $\alpha\beta$ + CD8 $\alpha\alpha$ + IELs in the thymus (Xing et al., 2024).

Our lab has developed a luminal IgA isolation protocol from feces of WT mice using protein L magnetic beads (Earley, 2021). Isolated IgA was used to prevent SFB from colonizing the jejunum in GATA4 deficient mice, in which IgA responses are diminished (Earley, 2021). This approach was successful in demonstrating the role of IgA in controlling bacterial colonization. It could also be utilized to determine whether luminal sIgA from MuAstV seronegative or seropositive mice can prevent its colonization in IgA deficient hosts. IgA can be isolated from lumens of WT mice with or without previous MuAstV infection and supplemented orally to IgA deficient hosts at the time of the first exposure. It was previously demonstrated that antibodies isolated from rabbits previously immunized with conserved MuAstV capsid peptides were successful in precenting chronic MuAstV infection in *Rag1-/-* mice (Ingle et al., 2019). Therefore, we speculate that IgA isolated from animals previously exposed to MuAstV would prevent the chronic colonization.

The IgA pulldown experiment of MuAstV from fecal matter suggests that IgA coats the capsid of MuAstV. The reovirus protective IgA responses were also generated towards specific capsid protein, σ 1, responsible for virus entry. The host receptor and the viral receptor binding sites responsible for MuAstV entry into the cell are not known. However, some insights can be made from structural studies of human astrovirus. It was demonstrated that neutralizing antibodies generated in immunized rabbits target conserved residues of VP25/VP27 spike protein of the virus capsid to prevent cell attachment (Espinosa et al., 2019; Ricemeyer et al., 2022). It is therefore likely that sIgA controlling the chronic MuAstV colonization of IgA deficient hosts also targets components of the capsid protein. We have not determined the repertoire or specificity of antibodies generated in response to MuAstV infection. The repertoire analysis of PCs generated in response to MuAstV infection in monocolonized WT mice would allow to assess the diversity of generated antibody repertoire, the extent of somatic hypermutation and their clonal relationship. To assess the specificity of the sIgA generated in response to MuAstV, monoclonal antibodies (mAbs) would be generated according to the protocol utilized previously in Bendelac lab (Ho et al., 2016; Bunker et al., 2017). This method was successful in evaluating the specificities of homeostatic sIgA. To generate the antibodies, the BCR sequences from the repertoire analysis can be used. Cloned antibodies could be tested for polyreactivity (i.e. ability to bind to structurally unrelated and diverse antigens), and their ability to bind the MuAstV, its capsid protein, spike, or nonstructural proteins by ELISA. The unbiased approach of mAb generation using single cells sorted cells from various anatomical locations (e.g. IgA switched B cells from the PPs, MLN, IgA+ PCs from LP, mammary or salivary glands, BM) can be also utilized to assess the reactivity of IgA from distinct tissues towards the MuAstV. Finally, highly reactive antibodies can be tested in-vivo for their ability to prevent infection in IgA deficient hosts.

One mechanism by which IgA prevents chronic MuAstV infection is through neutralization and immune exclusion. However, several reports suggest that IgA specific towards internal virus proteins can be involved in effective clearance. For example, IgA specific to matrix (M) protein of measles virus was shown to effectively inhibit virus replication intracellularly. M protein has been shown to be important in regulation of viral RNA synthesis, capsid assembly, and virion release from the cell. Monoclonal IgA specific to M protein did not neutralize the virus, compared to IgA targeting hemagglutinin involved in cell attachment and entry (Zhou et al., 2011). However, once added to the basal surface of polarized transwell cultures of previously infected pIgR+ cells, the antibody significantly decreased the viral titers compared to no antibody or pIgR- target cell controls (Zhou et al., 2011). In-vitro data suggests that similar intracellular IgA-dependent mechanism could be involved in blocking HIV replication (Huang et al., 2005; Wright et al., 2006). Lastly, non-neutralizing monoclonal IgA specific to VP6 protein of rotavirus conferred protection in vivo and facilitated virus clearance in chronically infected SCID mice (Burns et al., 1996). Therefore, it is plausible that some of the sIgA induced in response to MuAstV infection targets nonstructural proteins of the virus, and interact with its targets in the endosomal compartment during the transcytosis to confer protection.

4.3. Pathological implications of chronic viral infection in IgA deficient hosts

In addition to MuAstV, we found that persistent strain of murine norovirus CR6 (MNV-CR6) induced CD8 $\alpha\beta$ + IEL expansion in the small intestinal tissue, but not the colon. The viral load was increased throughout the small intestine of the infected IgA deficient animals compared to the IgA sufficient controls. The viral load was equally high in the colon of infected animals. Other enteric viruses tested, T1L reovirus, EDIM rotavirus, and acute MNV-CW3 failed to induce the expansion of CD8 $\alpha\beta$ + IELs in the IgA deficient hosts. It was demonstrated previously, that *Igha-/-* can

resolve rotavirus infection, though with a slower kinetics (Blutt et al., 2012). Similarly to the T1L reovirus, sIgA was involved in protection from subsequent rotavirus infection (Silvey et al., 2001; Blutt et al., 2012). Both viruses can be detected in the intestinal tissue after the second infection of *Igha-/-* mice, while the virus is undetectable in re-challenged IgA sufficient animals. It is important to note however, that during the T1L reinfection, the viral levels detected in the PPs were 3-fold lower compared to primary infection (Silvey et al., 2001). Similarly, fecal viral antigen shedding after rotavirus infection decreases significantly after the 2nd and 3rd exposure (Blutt et al., 2012). Since investigators detected no other rotavirus-specific antibody isotype present in the feces after the infection (Blutt et al., 2012), based on these observations, it is likely that the clearance of these viruses can depend on the innate or T cell adaptive immune responses (Johansson et al., 2007).

Having identified two viruses that can alter intestinal immune homeostasis in IgA deficient animals, we asked whether either could exacerbate pathology. We have found that MNV-CR6 infected IgA deficient hosts developed more severe response to DSS ingestion. In comparison to the control groups (uninfected *Ighasec-*/- or infected *Ighasec+*/- animals), MNV-CR6 infected *Ighasec-*/- hosts had lost more weight starting at day 6 of the treatment, suffered increased colonic shortening and more colonic pathology at the experimental endpoint. The MuAstV colonization had no impact on the DSS induced pathology in IgA deficient hosts. This was interesting, as both viruses induced the CD8 $\alpha\beta$ + IEL expansion. The involvement of CD8 $\alpha\beta$ + IELs in the induction of colonic pathology in DSS-treated, MNV-CR6 infected IgA deficient hosts is therefore unclear. To determine whether the expansion of these cells drives the phenotype observed, the CD8 β depletion can be performed. If these cells are indeed important, the depletion should alleviate the pathology observed in MNV-CR6 infected IgA deficient hosts. Alternatively, MNV-CR6 could

induce a distinct immune response in the colon, other than CD8 $\alpha\beta$ + IEL expansion, when sIgA is absent. The MNV-CR6 was detected at the highest levels in the ileum and colon, and while we detected some MuAstV in the colon, the highest levels were detected in the small intestine. Our RNA-seq of the intestinal compartments showed no significantly upregulated genes in the colon of MuAstV infected mice. We have not assessed the differentially regulated pathways in IgA deficient hosts in response to the MNV-CR6 infection alone or during DSS administration. It is possible that some distinct pathways can be induced in the colon of MNV-CR6 infected animals, that upon secondary trigger (DSS) could result in increased pathology. Indeed, it was demonstrated previously, that mutation in Crohn's disease susceptibility allele, ATG16L1 gene involved in the autophagy, can exacerbate DSS outcome in the presence of a specific virus. DSS administration in Atg16L1 hypomorphic animals previously infected with MNV-CR6 resulted in increased colonic pathology, as well as villus atrophy in the distal ileum(Cadwell et al., 2010). The pathological changes to the intestine were alleviated by blocking either TNF α or IFN γ . Finally, IgA was shown to be important in restricting colonization of IEC adherent SFB in GATA4 deficient mice. SFB-colonized GATA4 deficient mice exhibited increased mortality following C. rodentium infection. The expansion of SFB in these animals altered immune responses to the pathogen, characterized by increased production of TNF and IFNγ by CD8αβ+ IELs. TNF blockade decreased the observed mortality (Earley, 2021). It is therefore possible that other factors we have not detected are driving the pathology in MNV-CR6 infected IgA deficient hosts.

Finally, we were able to extend these findings to another colitis model, IL-10 deficiency. We have observed increased rectal prolapse incidence and colonic pathology in *Ighasec-/-* IL-10-/- mice colonized with specific microbiota and MNV-CR6 compared to control animals. It was previously reported that in IL-10 deficient hosts have elevated luminal IgA levels (Gomes-Santos et al., 2012).

Furthermore, MNV infection in IL-10 deficient hosts was shown to induce colonic hyperplasia, edema and immune infiltration of the LP and submucosa. Altogether, this data demonstrates that multifaceted interactions between genetic, immune, environmental factors can result in tissue destruction. Further experiments need to be performed to elucidate the nature of the factors at play in the sIgA deficient MNV-CR6 infected hosts contributing to pathology in response to DSS or in the context of IL-10 deficiency.

The prevalence of gastrointestinal viruses, prolonged viral shedding, and gastrointestinal symptoms are commonly observed in CVID patients, particularly those with very low serum and mucosal IgA levels (van de Ven et al., 2014). Increase in type-I/III IFN gene signatures, IFNy production, and the number of CD8αβ+ IELs in intestinal biopsies was observed in CVID enteropathy (Shulzhenko et al., 2018; Strohmeier et al., 2023). CVID enteropathy affects about 15% of CVID patients and is characterized by celiac disease-like villous blunting and malabsorption. Chronic norovirus infection in these patients have been associated with the enteropathy and dysregulated immune responses (Strohmeier et al., 2023). While CVID can affect the production of other immunoglobulin isotypes besides IgA, the absence of mucosal IgA plasma cells specifically was correlated with increased inflammation and disrupted tissue homeostasis (Strohmeier et al., 2023). These consequences were further exacerbated in the presence of norovirus infection. Taken together, these observations in humans and our findings in mice highlight an important link between IgA deficiency, failure to regulate chronic colonization by select viral pathobionts, dysregulated inflammatory immune responses, and disease. The place of viruses in IgA-mediated immunopathology relative to other types of microbes, such as commensal or pathogenic bacteria, remains an open question that warrants further exploration.

4.4.Conclusion and model

In this study, we found that sIgA responses protected the host from chronic MuAstV or MNV-CR6 colonization. sIgA regulating MuAstV colonization is T-dependent and at least in part, GC-derived. Moreover, we demonstrate that antigen driven CD8αβ+ IELs play a compensatory function in regulating MuAstV load, albeit without the capacity to eliminate the virus completely. Together these results suggest that IgA may play a critical role to prevent chronic colonization by viruses that depend on the adaptive, rather than the innate immune response, for their clearance.

Potential for IgM compensation was confounding the determination of IgA function in the past. Intriguingly, despite the elevated serum IgM and IgM PCs in the intestinal lamina propria, expansion of CD8αβ⁺ IELs and persistent MuAstV infection was also evident in *Igha-/-* hosts. These data suggest that IgM response may not qualitatively substitute for the IgA responses. This agrees with the recent findings emphasizing that the expression of IgA BCR supports efficient B cell participation in Peyer's patch GCs, memory B cell and PC generation (Raso et al., 2023).

While the absence of IgA has been linked to an increased risk of various immune-mediated disorders, these are only observed in around 20-30% of individuals with selective IgA deficiency (Singh et al., 2014; Rawla et al., 2024). Consistently, we did not observe any overt disease or alterations in intestinal morphology in our IgA-deficient mouse colonies, even when mice were chronically colonized by MuAstV, and CD8αβ+ IELs were expanded. Our findings shed light on the relatively rare association between IgA deficiency and immunopathology in the context of colitis. We demonstrated that IgA deficiency promotes colitis in the presence of (1) a specific virus and (2) a predisposing environmental or genetic factor. Specifically, we found that IgA-deficient mice develop colitis only when exposed to MNV-CR6 (but not MuAstV, even though IgA was required to prevent chronic colonization by both viruses), and in the context of IL-10 deficiency

or after exposure to DSS. These findings suggest that the development of immunopathology is dependent on the specific nature of the virus and the presence of additional pathogenic genetic and/or environmental trigger. This might also explain why only few IgA deficient patients develop complications.

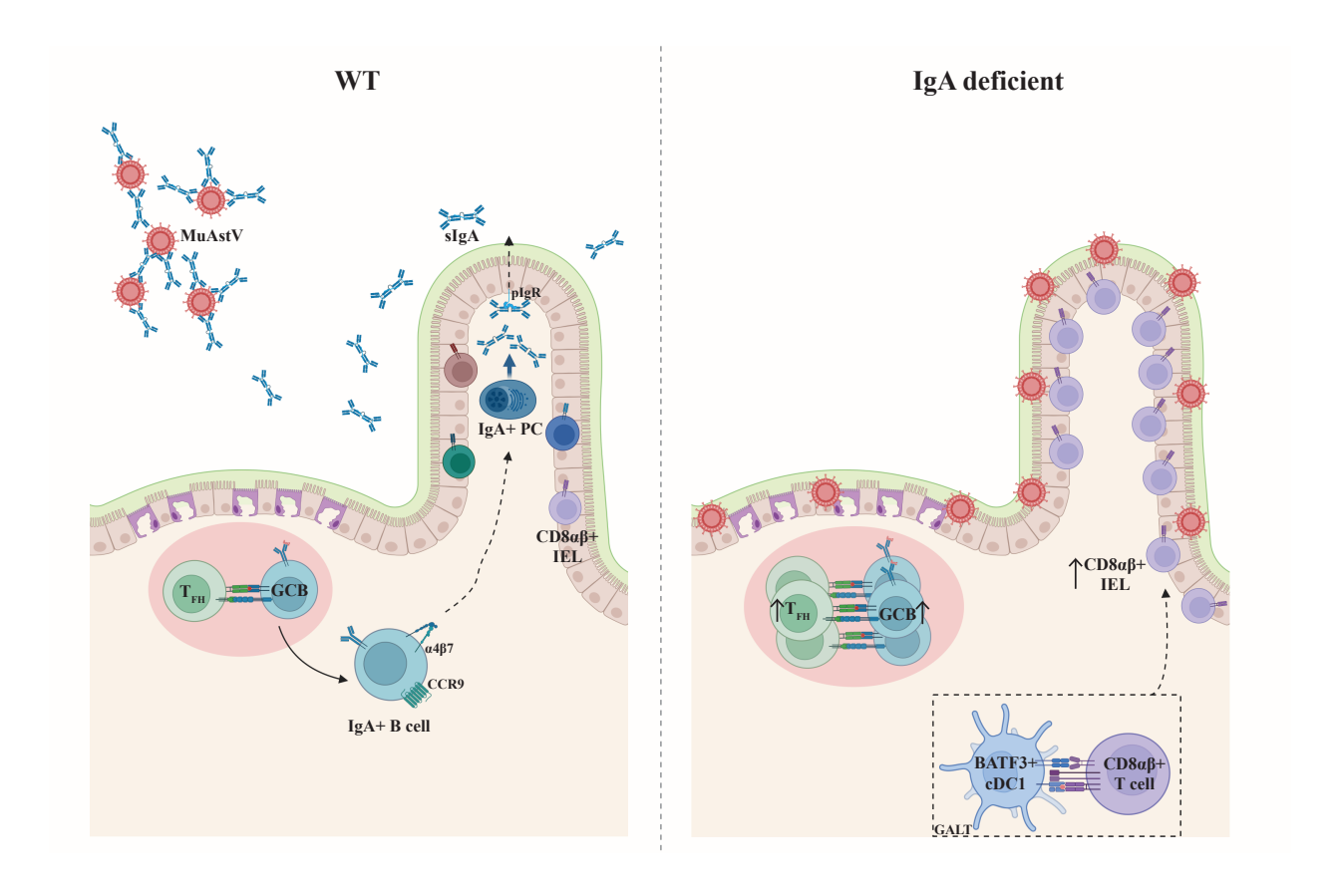


Figure 12 Model of sIgA mediated regulation of intestinal immune homeostasis.

T-dependent, GC-derived sIgA protect the WT hosts from MuAstV infection. In IgA deficient hosts, MuAstV colonizes the intestinal tissue chronically. To limit the viral load and type-I IFN responses, IgA deficient hosts mount compensatory CD8 $\alpha\beta$ + IEL response. These responses are primed by BATF3+ cDC1s, likely in the GALT. These CD8 $\alpha\beta$ + IELs are classically restricted, and their TCR repertoire show features of antigen-driven expansion. Functionally, the expanded IELs produce IFN γ and express cytotoxic molecules.

REFERENCES

- Abadie, V., Kim, S. M., Lejeune, T., Palanski, B. A., Ernest, J. D., Tastet, O., Voisine, J., Discepolo, V., Marietta, E. V., Hawash, M. B. F., Ciszewski, C., Bouziat, R., Panigrahi, K., Horwath, I., Zurenski, M. A., Lawrence, I., Dumaine, A., Yotova, V., Grenier, J.-C., . . . Jabri, B. (2020). IL-15, gluten and HLA-DQ8 drive tissue destruction in coeliac disease. *Nature*, *578*(7796), 600-604. https://doi.org/10.1038/s41586-020-2003-8
- Aghamohammadi, A., Cheraghi, T., Gharagozlou, M., Movahedi, M., Rezaei, N., Yeganeh, M., Parvaneh, N., Abolhassani, H., Pourpak, Z., & Moin, M. (2009). IgA deficiency: correlation between clinical and immunological phenotypes. *J Clin Immunol*, *29*(1), 130-136. https://doi.org/10.1007/s10875-008-9229-9
- Anderson, C. K., Reilly, E. C., Lee, A. Y., & Brossay, L. (2019). Qa-1-Restricted CD8(+) T Cells Can Compensate for the Absence of Conventional T Cells during Viral Infection. *Cell Rep*, 27(2), 537-548 e535. https://doi.org/10.1016/j.celrep.2019.03.059
- Apter, F. M., Michetti, P., Winner, L. S., Mack, J. A., Mekalanos, J. J., & Neutra, M. R. (1993). Analysis of the roles of antilipopolysaccharide and anti-cholera toxin immunoglobulin A (IgA) antibodies in protection against Vibrio cholerae and cholera toxin by use of monoclonal IgA antibodies in vivo. *Infection and Immunity*, 61(12), 5279-5285. https://doi.org/doi:10.1128/iai.61.12.5279-5285.1993
- Ashburner, M., Ball, C. A., Blake, J. A., Botstein, D., Butler, H., Cherry, J. M., Davis, A. P., Dolinski, K., Dwight, S. S., Eppig, J. T., Harris, M. A., Hill, D. P., Issel-Tarver, L., Kasarskis, A., Lewis, S., Matese, J. C., Richardson, J. E., Ringwald, M., Rubin, G. M., & Sherlock, G. (2000). Gene ontology: tool for the unification of biology. The Gene Ontology Consortium. *Nat Genet*, *25*(1), 25-29. https://doi.org/10.1038/75556
- Ballow, M. (2002). Primary immunodeficiency disorders: antibody deficiency. *J Allergy Clin Immunol*, 109(4), 581-591. https://doi.org/10.1067/mai.2002.122466
- Bankhead, P., Loughrey, M. B., Fernandez, J. A., Dombrowski, Y., McArt, D. G., Dunne, P. D., McQuaid, S., Gray, R. T., Murray, L. J., Coleman, H. G., James, J. A., Salto-Tellez, M., & Hamilton, P. W. (2017). QuPath: Open source software for digital pathology image analysis. *Sci Rep*, 7(1), 16878. https://doi.org/10.1038/s41598-017-17204-5
- Barber, C. L., Montecino-Rodriguez, E., & Dorshkind, K. (2011). Reduced production of B-1–specified common lymphoid progenitors results in diminished potential of adult marrow to generate B-1 cells. *Proceedings of the National Academy of Sciences*, *108*(33), 13700-13704. https://doi.org/doi:10.1073/pnas.1107172108
- Barlow, J. T., Bogatyrev, S. R., & Ismagilov, R. F. (2020). A quantitative sequencing framework for absolute abundance measurements of mucosal and lumenal microbial communities. *Nat Commun*, 11(1), 2590. https://doi.org/10.1038/s41467-020-16224-6

- Barros, M. D., Porto, M. H., Leser, P. G., Grumach, A. S., & Carneiro-Sampaio, M. M. (1985). Study of colostrum of a patient with selective IgA deficiency. *Allergol Immunopathol (Madr)*, *13*(4), 331-334. https://www.ncbi.nlm.nih.gov/pubmed/4083232
- Basic, M., Keubler, L. M., Buettner, M., Achard, M., Breves, G., Schroder, B., Smoczek, A., Jorns, A., Wedekind, D., Zschemisch, N. H., Gunther, C., Neumann, D., Lienenklaus, S., Weiss, S., Hornef, M. W., Mahler, M., & Bleich, A. (2014). Norovirus triggered microbiota-driven mucosal inflammation in interleukin 10-deficient mice. *Inflamm Bowel Dis*, 20(3), 431-443. https://doi.org/10.1097/01.MIB.0000441346.86827.ed
- Bergqvist, P., Gärdby, E., Stensson, A., Bemark, M., & Lycke, N. Y. (2006). Gut IgA Class Switch Recombination in the Absence of CD40 Does Not Occur in the Lamina Propria and Is Independent of Germinal Centers1. *The Journal of Immunology*, 177(11), 7772-7783. https://doi.org/10.4049/jimmunol.177.11.7772
- Bergstrom, K. S., Kissoon-Singh, V., Gibson, D. L., Ma, C., Montero, M., Sham, H. P., Ryz, N., Huang, T., Velcich, A., Finlay, B. B., Chadee, K., & Vallance, B. A. (2010). Muc2 protects against lethal infectious colitis by disassociating pathogenic and commensal bacteria from the colonic mucosa. *PLoS Pathog*, *6*(5), e1000902. https://doi.org/10.1371/journal.ppat.1000902
- Bevins, C. L., & Salzman, N. H. (2011). Paneth cells, antimicrobial peptides and maintenance of intestinal homeostasis. *Nat Rev Microbiol*, 9(5), 356-368. https://doi.org/10.1038/nrmicro2546
- Blanchet, E., Van de Velde, S., Matsumura, S., Hao, E., LeLay, J., Kaestner, K., & Montminy, M. (2015). Feedback inhibition of CREB signaling promotes beta cell dysfunction in insulin resistance. *Cell Rep*, *10*(7), 1149-1157. https://doi.org/10.1016/j.celrep.2015.01.046
- Blomström, A.-L., Widén, F., Hammer, A.-S., Belák, S., & Berg, M. (2010). Detection of a Novel Astrovirus in Brain Tissue of Mink Suffering from Shaking Mink Syndrome by Use of Viral Metagenomics. *Journal of Clinical Microbiology*, 48(12), 4392-4396. https://doi.org/doi:10.1128/jcm.01040-10
- Blutt, S. E., Miller, A. D., Salmon, S. L., Metzger, D. W., & Conner, M. E. (2012). IgA is important for clearance and critical for protection from rotavirus infection. *Mucosal Immunol*, *5*(6), 712-719. https://doi.org/10.1038/mi.2012.51
- Bogatyrev, S. R., Rolando, J. C., & Ismagilov, R. F. (2020). Self-reinoculation with fecal flora changes microbiota density and composition leading to an altered bile-acid profile in the mouse small intestine. *Microbiome*, 8(1), 19. https://doi.org/10.1186/s40168-020-0785-4
- Bolyen, E., Rideout, J. R., Dillon, M. R., Bokulich, N. A., Abnet, C. C., Al-Ghalith, G. A., Alexander, H., Alm, E. J., Arumugam, M., Asnicar, F., Bai, Y., Bisanz, J. E., Bittinger, K., Brejnrod, A., Brislawn, C. J., Brown, C. T., Callahan, B. J., Caraballo-Rodríguez, A. M., Chase, J., . . . Caporaso, J. G. (2019). Reproducible, interactive, scalable and extensible microbiome data

- science using QIIME 2. Nat Biotechnol, 37(8), 852-857. https://doi.org/10.1038/s41587-019-0209-9
- Bousbaine, D., Fisch, L. I., London, M., Bhagchandani, P., Rezende de Castro, T. B., Mimee, M., Olesen, S., Reis, B. S., VanInsberghe, D., Bortolatto, J., Poyet, M., Cheloha, R. W., Sidney, J., Ling, J., Gupta, A., Lu, T. K., Sette, A., Alm, E. J., Moon, J. J., . . . Bilate, A. M. (2022). A conserved Bacteroidetes antigen induces anti-inflammatory intestinal T lymphocytes. *Science*, *377*(6606), 660-666. https://doi.org/doi:10.1126/science.abg5645
- Bouziat, R., Biering, S. B., Kouame, E., Sangani, K. A., Kang, S., Ernest, J. D., Varma, M., Brown, J. J., Urbanek, K., Dermody, T. S., Ng, A., Hinterleitner, R., Hwang, S., & Jabri, B. (2018). Murine Norovirus Infection Induces T(H)1 Inflammatory Responses to Dietary Antigens. *Cell Host Microbe*, 24(5), 677-688 e675. https://doi.org/10.1016/j.chom.2018.10.004
- Bouziat, R., Hinterleitner, R., Brown, J. J., Stencel-Baerenwald, J. E., Ikizler, M., Mayassi, T., Meisel, M., Kim, S. M., Discepolo, V., Pruijssers, A. J., Ernest, J. D., Iskarpatyoti, J. A., Costes, L. M., Lawrence, I., Palanski, B. A., Varma, M., Zurenski, M. A., Khomandiak, S., McAllister, N., . . . Jabri, B. (2017). Reovirus infection triggers inflammatory responses to dietary antigens and development of celiac disease. *Science*, *356*(6333), 44-50. https://doi.org/10.1126/science.aah5298
- Brandl, K., Plitas, G., Schnabl, B., DeMatteo, R. P., & Pamer, E. G. (2007). MyD88-mediated signals induce the bactericidal lectin RegIII gamma and protect mice against intestinal Listeria monocytogenes infection. *J Exp Med*, 204(8), 1891-1900. https://doi.org/10.1084/jem.20070563
- Brown, J. R., Morfopoulou, S., Hubb, J., Emmett, W. A., Ip, W., Shah, D., Brooks, T., Paine, S. M. L., Anderson, G., Virasami, A., Tong, C. Y. W., Clark, D. A., Plagnol, V., Jacques, T. S., Qasim, W., Hubank, M., & Breuer, J. (2015). Astrovirus VA1/HMO-C: An Increasingly Recognized Neurotropic Pathogen in Immunocompromised Patients. *Clinical Infectious Diseases*, 60(6), 881-888. https://doi.org/10.1093/cid/ciu940
- Buchfink, B., Xie, C., & Huson, D. H. (2015). Fast and sensitive protein alignment using DIAMOND. *Nat Methods*, *12*(1), 59-60. https://doi.org/10.1038/nmeth.3176
- Bunker, J. J., & Bendelac, A. (2018). IgA Responses to Microbiota. *Immunity*, 49(2), 211-224. https://doi.org/10.1016/j.immuni.2018.08.011
- Bunker, J. J., Erickson, S. A., Flynn, T. M., Henry, C., Koval, J. C., Meisel, M., Jabri, B., Antonopoulos, D. A., Wilson, P. C., & Bendelac, A. (2017). Natural polyreactive IgA antibodies coat the intestinal microbiota. *Science*, *358*(6361). https://doi.org/10.1126/science.aan6619
- Bunker, J. J., Flynn, T. M., Koval, J. C., Shaw, D. G., Meisel, M., McDonald, B. D., Ishizuka, I. E., Dent, A. L., Wilson, P. C., Jabri, B., Antonopoulos, D. A., & Bendelac, A. (2015). Innate and Adaptive Humoral Responses Coat Distinct Commensal Bacteria with Immunoglobulin A. *Immunity*, 43(3), 541-553. https://doi.org/10.1016/j.immuni.2015.08.007

- Burger-van Paassen, N., van der Sluis, M., Bouma, J., Korteland-van Male, A. M., Lu, P., Van Seuningen, I., Boehm, G., van Goudoever, J. B., & Renes, I. B. (2011). Colitis development during the suckling-weaning transition in mucin Muc2-deficient mice. *Am J Physiol Gastrointest Liver Physiol*, 301(4), G667-678. https://doi.org/10.1152/ajpgi.00199.2010
- Burggraf, S., Huber, H., & Stetter, K. O. (1997). Reclassification of the crenarchael orders and families in accordance with 16S rRNA sequence data. *Int J Syst Bacteriol*, 47(3), 657-660. https://doi.org/10.1099/00207713-47-3-657
- Burns, J. W., Siadat-Pajouh, M., Krishnaney, A. A., & Greenberg, H. B. (1996). Protective effect of rotavirus VP6-specific IgA monoclonal antibodies that lack neutralizing activity. *Science*, 272(5258), 104-107. https://doi.org/10.1126/science.272.5258.104
- Caballero, S., Guix, S., El-Senousy, W. M., Calicó, I., Pintó, R. M., & Bosch, A. (2003). Persistent gastroenteritis in children infected with astrovirus: Association with serotype-3 strains. *Journal of Medical Virology*, 71(2), 245-250. https://doi.org/https://doi.org/10.1002/jmv.10476
- Cadwell, K., Patel, K. K., Maloney, N. S., Liu, T. C., Ng, A. C., Storer, C. E., Head, R. D., Xavier, R., Stappenbeck, T. S., & Virgin, H. W. (2010). Virus-plus-susceptibility gene interaction determines Crohn's disease gene Atg16L1 phenotypes in intestine. *Cell*, *141*(7), 1135-1145. https://doi.org/10.1016/j.cell.2010.05.009
- Caporaso, J. G., Lauber, C. L., Walters, W. A., Berg-Lyons, D., Lozupone, C. A., Turnbaugh, P. J., Fierer, N., & Knight, R. (2011). Global patterns of 16S rRNA diversity at a depth of millions of sequences per sample. *Proc Natl Acad Sci U S A*, *108 Suppl 1*(Suppl 1), 4516-4522. https://doi.org/10.1073/pnas.1000080107
- Castigli, E., Wilson, S. A., Scott, S., Dedeoglu, F., Xu, S., Lam, K. P., Bram, R. J., Jabara, H., & Geha, R. S. (2005). TACI and BAFF-R mediate isotype switching in B cells. *J Exp Med*, 201(1), 35-39. https://doi.org/10.1084/jem.20032000
- Catanzaro, J. R., Strauss, J. D., Bielecka, A., Porto, A. F., Lobo, F. M., Urban, A., Schofield, W. B., & Palm, N. W. (2019). IgA-deficient humans exhibit gut microbiota dysbiosis despite secretion of compensatory IgM. *Sci Rep*, *9*(1), 13574. https://doi.org/10.1038/s41598-019-49923-2
- Cazac, B. B., & Roes, J. (2000). TGF-β Receptor Controls B Cell Responsiveness and Induction of IgA In Vivo. *Immunity*, *13*(4), 443-451. https://doi.org/10.1016/S1074-7613(00)00044-3
- Cepek, K. L., Shaw, S. K., Parker, C. M., Russell, G. J., Morrow, J. S., Rimm, D. L., & Brenner, M. B. (1994). Adhesion between epithelial cells and T lymphocytes mediated by E-cadherin and the αΕβ7 integrin. *Nature*, *372*(6502), 190-193. https://doi.org/10.1038/372190a0

- Cerutti, A. (2008). The regulation of IgA class switching. *Nat Rev Immunol*, 8(6), 421-434. https://doi.org/10.1038/nri2322
- Cerutti, A., Cols, M., & Puga, I. (2013). Marginal zone B cells: virtues of innate-like antibody-producing lymphocytes. *Nature Reviews Immunology*, *13*(2), 118-132. https://doi.org/10.1038/nri3383
- Cervantes-Barragan, L., Chai, J. N., Tianero, M. D., Di Luccia, B., Ahern, P. P., Merriman, J., Cortez, V. S., Caparon, M. G., Donia, M. S., Gilfillan, S., Cella, M., Gordon, J. I., Hsieh, C.-S., & Colonna, M. (2017). *Lactobacillus reuteri* induces gut intraepithelial CD4+CD8αα+ T cells. *Science*, 357(6353), 806-810. https://doi.org/doi:10.1126/science.aah5825
- Cheroutre, H., Lambolez, F., & Mucida, D. (2011). The light and dark sides of intestinal intraepithelial lymphocytes. *Nature Reviews Immunology*, 11(7), 445-456. https://doi.org/10.1038/nri3007
- Chu, V. T., Beller, A., Rausch, S., Strandmark, J., Zanker, M., Arbach, O., Kruglov, A., & Berek, C. (2014). Eosinophils promote generation and maintenance of immunoglobulin-A-expressing plasma cells and contribute to gut immune homeostasis. *Immunity*, 40(4), 582-593. https://doi.org/10.1016/j.immuni.2014.02.014
- Chu, V. T., Fröhlich, A., Steinhauser, G., Scheel, T., Roch, T., Fillatreau, S., Lee, J. J., Löhning, M., & Berek, C. (2011). Eosinophils are required for the maintenance of plasma cells in the bone marrow. *Nature Immunology*, 12(2), 151-159. https://doi.org/10.1038/ni.1981
- Cinamon, G., Zachariah, M. A., Lam, O. M., Foss, F. W., & Cyster, J. G. (2008). Follicular shuttling of marginal zone B cells facilitates antigen transport. *Nature Immunology*, 9(1), 54-62. https://doi.org/10.1038/ni1542
- Collin, P., Maki, M., Keyrilainen, O., Hallstrom, O., Reunala, T., & Pasternack, A. (1992). Selective IgA deficiency and coeliac disease. *Scand J Gastroenterol*, *27*(5), 367-371. https://doi.org/10.3109/00365529209000089
- Cortez, V., Meliopoulos, V. A., Karlsson, E. A., Hargest, V., Johnson, C., & Schultz-Cherry, S. (2017). Astrovirus Biology and Pathogenesis. *Annu Rev Virol*, *4*(1), 327-348. https://doi.org/10.1146/annurev-virology-101416-041742
- Dallari, S., Heaney, T., Rosas-Villegas, A., Neil, J. A., Wong, S. Y., Brown, J. J., Urbanek, K., Herrmann, C., Depledge, D. P., Dermody, T. S., & Cadwell, K. (2021). Enteric viruses evoke broad host immune responses resembling those elicited by the bacterial microbiome. *Cell Host Microbe*, *29*(6), 1014-1029 e1018. https://doi.org/10.1016/j.chom.2021.03.015
- De Giovanni, M., Vykunta, V. S., Biram, A., Chen, K. Y., Taglinao, H., An, J., Sheppard, D., Paidassi, H., & Cyster, J. G. (2024). Mast cells help organize the Peyer's patch niche for induction of IgA responses. *Science Immunology*, *9*(93), eadj7363. https://doi.org/doi:10.1126/sciimmunol.adj7363

- Di Marco Barros, R., Roberts, N. A., Dart, R. J., Vantourout, P., Jandke, A., Nussbaumer, O., Deban, L., Cipolat, S., Hart, R., Iannitto, M. L., Laing, A., Spencer-Dene, B., East, P., Gibbons, D., Irving, P. M., Pereira, P., Steinhoff, U., & Hayday, A. (2016). Epithelia Use Butyrophilin-like Molecules to Shape Organ-Specific γδ T Cell Compartments. *Cell*, *167*(1), 203-218.e217. https://doi.org/https://doi.org/10.1016/j.cell.2016.08.030
- Dobin, A., Davis, C. A., Schlesinger, F., Drenkow, J., Zaleski, C., Jha, S., Batut, P., Chaisson, M., & Gingeras, T. R. (2013). STAR: ultrafast universal RNA-seq aligner. *Bioinformatics*, 29(1), 15-21. https://doi.org/10.1093/bioinformatics/bts635
- Donaldson, G. P., Ladinsky, M. S., Yu, K. B., Sanders, J. G., Yoo, B. B., Chou, W. C., Conner, M. E., Earl, A. M., Knight, R., Bjorkman, P. J., & Mazmanian, S. K. (2018). Gut microbiota utilize immunoglobulin A for mucosal colonization. *Science*, *360*(6390), 795-800. https://doi.org/10.1126/science.aaq0926
- Earley, Z. M. (2021). Epithelial GATA4 Regulates Bacterial Colonization and Regionalization of Intestinal Immunity in Homeostasis and Disease ProQuest Dissertations & Theses, University of Chicago]. Ann Arbor. http://gateway.proquest.com/openurl?url_ver=Z39.88-2004&rft_val_fmt=info:ofi/fmt:kev:mtx:dissertation&res_dat=xri:pqm&rft_dat=xri:pqdiss:28648 163
- https://dx.doi.org/10.6082/uchicago.3389
- Earley, Z. M., Lisicka, W., Sifakis, J. J., Aguirre-Gamboa, R., Kowalczyk, A., Barlow, J. T., Shaw, D. G., Discepolo, V., Tan, I. L., Gona, S., Ernest, J. D., Matzinger, P., Barreiro, L. B., Morgun, A., Bendelac, A., Ismagilov, R. F., Shulzhenko, N., Riesenfeld, S. J., & Jabri, B. (2023). GATA4 controls regionalization of tissue immunity and commensal-driven immunopathology. *Immunity*, 56(1), 43-57 e10. https://doi.org/10.1016/j.immuni.2022.12.009
- Eberl, G., Marmon, S., Sunshine, M.-J., Rennert, P. D., Choi, Y., & Littman, D. R. (2004). An essential function for the nuclear receptor RORγt in the generation of fetal lymphoid tissue inducer cells. *Nature Immunology*, *5*(1), 64-73. https://doi.org/10.1038/ni1022
- El Kaissouni, J., Bene, M. C., Thionnois, S., Monin, P., Vidailhet, M., & Faure, G. C. (1998). Maturation of B Cells in the Lamina Propria of Human Gut and Bronchi in the First Months of Human Life. Developmental Immunology, 5, 042138. https://doi.org/10.1155/1998/42138
- El-Asady, R., Yuan, R., Liu, K., Wang, D., Gress, R. E., Lucas, P. J., Drachenberg, C. B., & Hadley, G. A. (2005). TGF-β-dependent CD103 expression by CD8+ T cells promotes selective destruction of the host intestinal epithelium during graft-versus-host disease. *Journal of Experimental Medicine*, 201(10), 1647-1657. https://doi.org/10.1084/jem.20041044
- Espinosa, R., López, T., Bogdanoff, W. A., Espinoza, M. A., López, S., DuBois, R. M., & Arias, C. F. (2019). Isolation of Neutralizing Monoclonal Antibodies to Human Astrovirus and Characterization of Virus Variants That Escape Neutralization. *Journal of Virology*, *93*(2), 10.1128/jvi.01465-01418. https://doi.org/doi:10.1128/jvi.01465-18

- Fadlallah, J., El Kafsi, H., Sterlin, D., Juste, C., Parizot, C., Dorgham, K., Autaa, G., Gouas, D., Almeida, M., Lepage, P., Pons, N., Le Chatelier, E., Levenez, F., Kennedy, S., Galleron, N., de Barros, J. P., Malphettes, M., Galicier, L., Boutboul, D., . . . Gorochov, G. (2018). Microbial ecology perturbation in human IgA deficiency. *Sci Transl Med*, 10(439). https://doi.org/10.1126/scitranslmed.aan1217
- Fagarasan, S., Kawamoto, S., Kanagawa, O., & Suzuki, K. (2010). Adaptive immune regulation in the gut: T cell-dependent and T cell-independent IgA synthesis. *Annu Rev Immunol*, *28*, 243-273. https://doi.org/10.1146/annurev-immunol-030409-101314
- Fagarasan, S., Muramatsu, M., Suzuki, K., Nagaoka, H., Hiai, H., & Honjo, T. (2002). Critical Roles of Activation-Induced Cytidine Deaminase in the Homeostasis of Gut Flora. *Science*, 298(5597), 1424-1427. https://doi.org/doi:10.1126/science.1077336
- Fernandez, M. I., Pedron, T., Tournebize, R., Olivo-Marin, J. C., Sansonetti, P. J., & Phalipon, A. (2003). Anti-inflammatory role for intracellular dimeric immunoglobulin a by neutralization of lipopolysaccharide in epithelial cells. *Immunity*, 18(6), 739-749. https://doi.org/10.1016/s1074-7613(03)00122-5
- Finkbeiner, S. R., Li, Y., Ruone, S., Conrardy, C., Gregoricus, N., Toney, D., Virgin, H. W., Anderson, L. J., Vinjé, J., Wang, D., & Tong, S. (2009). Identification of a Novel Astrovirus (Astrovirus VA1) Associated with an Outbreak of Acute Gastroenteritis. *Journal of Virology*, 83(20), 10836-10839. https://doi.org/doi:10.1128/jvi.00998-09
- Frémond, M.-L., Pérot, P., Muth, E., Cros, G., Dumarest, M., Mahlaoui, N., Seilhean, D., Desguerre, I., Hébert, C., Corre-Catelin, N., Neven, B., Lecuit, M., Blanche, S., Picard, C., & Eloit, M. (2015). Next-Generation Sequencing for Diagnosis and Tailored Therapy: A Case Report of Astrovirus-Associated Progressive Encephalitis. *Journal of the Pediatric Infectious Diseases Society*, 4(3), e53-e57. https://doi.org/10.1093/jpids/piv040
- French, M. A., Denis, K. A., Dawkins, R., & Peter, J. B. (1995). Severity of infections in IgA deficiency: correlation with decreased serum antibodies to pneumococcal polysaccharides and decreased serum IgG2 and/or IgG4. *Clin Exp Immunol*, 100(1), 47-53. https://doi.org/10.1111/j.1365-2249.1995.tb03602.x
- Gene Ontology, C. (2021). The Gene Ontology resource: enriching a GOld mine. *Nucleic Acids Res*, 49(D1), D325-D334. https://doi.org/10.1093/nar/gkaa1113
- Gerbe, F., Sidot, E., Smyth, D. J., Ohmoto, M., Matsumoto, I., Dardalhon, V., Cesses, P., Garnier, L., Pouzolles, M., Brulin, B., Bruschi, M., Harcus, Y., Zimmermann, V. S., Taylor, N., Maizels, R. M., & Jay, P. (2016). Intestinal epithelial tuft cells initiate type 2 mucosal immunity to helminth parasites. *Nature*, *529*(7585), 226-230. https://doi.org/10.1038/nature16527

- Ghosh, S., Kumar, M., Santiana, M., Mishra, A., Zhang, M., Labayo, H., Chibly, A. M., Nakamura, H., Tanaka, T., Henderson, W., Lewis, E., Voss, O., Su, Y., Belkaid, Y., Chiorini, J. A., Hoffman, M. P., & Altan-Bonnet, N. (2022). Enteric viruses replicate in salivary glands and infect through saliva. *Nature*, 607(7918), 345-350. https://doi.org/10.1038/s41586-022-04895-8
- Gomes-Santos, A. C., Moreira, T. G., Castro-Junior, A. B., Horta, B. C., Lemos, L., Cruz, D. N., Guimaraes, M. A., Cara, D. C., McCafferty, D. M., & Faria, A. M. (2012). New insights into the immunological changes in IL-10-deficient mice during the course of spontaneous inflammation in the gut mucosa. *Clin Dev Immunol*, 2012, 560817. https://doi.org/10.1155/2012/560817
- Grasset, E. K., Chorny, A., Casas-Recasens, S., Gutzeit, C., Bongers, G., Thomsen, I., Chen, L., He, Z., Matthews, D. B., Oropallo, M. A., Veeramreddy, P., Uzzan, M., Mortha, A., Carrillo, J., Reis, B. S., Ramanujam, M., Sintes, J., Magri, G., Maglione, P. J., . . . Cerutti, A. (2020). Gut T cell–independent IgA responses to commensal bacteria require engagement of the TACI receptor on B cells. *Science Immunology*, 5(49), eaat7117. https://doi.org/doi:10.1126/sciimmunol.aat7117
- Gribble, F. M., & Reimann, F. (2016). Enteroendocrine Cells: Chemosensors in the Intestinal Epithelium. *Annual Review of Physiology*, 78(Volume 78, 2016), 277-299. https://doi.org/https://doi.org/10.1146/annurev-physiol-021115-105439
- Gros, M. J., Naquet, P., & Guinamard, R. R. (2008). Cell Intrinsic TGF-β1 Regulation of B Cells1. *The Journal of Immunology*, 180(12), 8153-8158. https://doi.org/10.4049/jimmunol.180.12.8153
- Gu, Z., Eils, R., & Schlesner, M. (2016). Complex heatmaps reveal patterns and correlations in multidimensional genomic data. *Bioinformatics*, *32*(18), 2847-2849. https://doi.org/10.1093/bioinformatics/btw313
- Hadis, U., Wahl, B., Schulz, O., Hardtke-Wolenski, M., Schippers, A., Wagner, N., Müller, W., Sparwasser, T., Förster, R., & Pabst, O. (2011). Intestinal Tolerance Requires Gut Homing and Expansion of FoxP3+ Regulatory T Cells in the Lamina Propria. *Immunity*, *34*(2), 237-246. https://doi.org/https://doi.org/10.1016/j.immuni.2011.016
- Hafemeister, C., & Satija, R. (2019). Normalization and variance stabilization of single-cell RNA-seq data using regularized negative binomial regression. *Genome Biol*, 20(1), 296. https://doi.org/10.1186/s13059-019-1874-1
- Hall, J. A., Bouladoux, N., Sun, C. M., Wohlfert, E. A., Blank, R. B., Zhu, Q., Grigg, M. E., Berzofsky, J. A., & Belkaid, Y. (2008). Commensal DNA limits regulatory T cell conversion and is a natural adjuvant of intestinal immune responses. *Immunity*, *29*(4), 637-649. https://doi.org/10.1016/j.immuni.2008.08.009
- Hammarstrom, L., Vorechovsky, I., & Webster, D. (2000). Selective IgA deficiency (SIgAD) and common variable immunodeficiency (CVID). *Clin Exp Immunol*, 120(2), 225-231. https://doi.org/10.1046/j.1365-2249.2000.01131.x

- Hansson, G. C., & Johansson, M. E. (2010). The inner of the two Muc2 mucin-dependent mucus layers in colon is devoid of bacteria. *Gut Microbes*, *I*(1), 51-54. https://doi.org/10.4161/gmic.1.1.10470
- Hao, Y., Hao, S., Andersen-Nissen, E., Mauck, W. M., 3rd, Zheng, S., Butler, A., Lee, M. J., Wilk, A. J., Darby, C., Zager, M., Hoffman, P., Stoeckius, M., Papalexi, E., Mimitou, E. P., Jain, J., Srivastava, A., Stuart, T., Fleming, L. M., Yeung, B., . . . Satija, R. (2021). Integrated analysis of multimodal single-cell data. *Cell*, *184*(13), 3573-3587 e3529. https://doi.org/10.1016/j.cell.2021.04.048
- Hapfelmeier, S., Lawson, M. A., Slack, E., Kirundi, J. K., Stoel, M., Heikenwalder, M., Cahenzli, J., Velykoredko, Y., Balmer, M. L., Endt, K., Geuking, M. B., Curtiss, R., 3rd, McCoy, K. D., & Macpherson, A. J. (2010). Reversible microbial colonization of germ-free mice reveals the dynamics of IgA immune responses. *Science*, 328(5986), 1705-1709. https://doi.org/10.1126/science.1188454
- Harriman, G. R., Bogue, M., Rogers, P., Finegold, M., Pacheco, S., Bradley, A., Zhang, Y., & Mbawuike, I. N. (1999). Targeted deletion of the IgA constant region in mice leads to IgA deficiency with alterations in expression of other Ig isotypes. *J Immunol*, *162*(5), 2521-2529. https://www.ncbi.nlm.nih.gov/pubmed/10072491
- Hase, K., Kawano, K., Nochi, T., Pontes, G. S., Fukuda, S., Ebisawa, M., Kadokura, K., Tobe, T., Fujimura, Y., Kawano, S., Yabashi, A., Waguri, S., Nakato, G., Kimura, S., Murakami, T., Iimura, M., Hamura, K., Fukuoka, S.-I., Lowe, A. W., . . . Ohno, H. (2009). Uptake through glycoprotein 2 of FimH+ bacteria by M cells initiates mucosal immune response. *Nature*, 462(7270), 226-230. https://doi.org/10.1038/nature08529
- He, B., Xu, W., Santini, P. A., Polydorides, A. D., Chiu, A., Estrella, J., Shan, M., Chadburn, A., Villanacci, V., Plebani, A., Knowles, D. M., Rescigno, M., & Cerutti, A. (2007). Intestinal bacteria trigger T cell-independent immunoglobulin A(2) class switching by inducing epithelial-cell secretion of the cytokine APRIL. *Immunity*, 26(6), 812-826. https://doi.org/10.1016/j.immuni.2007.04.014
- Hieshima, K., Kawasaki, Y., Hanamoto, H., Nakayama, T., Nagakubo, D., Kanamaru, A., & Yoshie, O. (2004). CC Chemokine Ligands 25 and 28 Play Essential Roles in Intestinal Extravasation of IgA Antibody-Secreting Cells 1. *The Journal of Immunology*, 173(6), 3668-3675. https://doi.org/10.4049/jimmunol.173.6.3668
- Hildner, K., Edelson, B. T., Purtha, W. E., Diamond, M., Matsushita, H., Kohyama, M., Calderon, B.,
 Schraml, B. U., Unanue, E. R., Diamond, M. S., Schreiber, R. D., Murphy, T. L., & Murphy, K.
 M. (2008). Batf3 deficiency reveals a critical role for CD8alpha+ dendritic cells in cytotoxic T cell immunity. *Science*, 322(5904), 1097-1100. https://doi.org/10.1126/science.1164206
- Ho, I. Y., Bunker, J. J., Erickson, S. A., Neu, K. E., Huang, M., Cortese, M., Pulendran, B., & Wilson, P. C. (2016). Refined protocol for generating monoclonal antibodies from single human and murine

- B cells. *Journal of Immunological Methods*, 438, 67-70. https://doi.org/https://doi.org/10.1016/j.jim.2016.09.001
- Hooper, L. V., Littman, D. R., & Macpherson, A. J. (2012). Interactions Between the Microbiota and the Immune System. *Science*, 336(6086), 1268-1273. https://doi.org/doi:10.1126/science.1223490
- Howitt, M. R., Lavoie, S., Michaud, M., Blum, A. M., Tran, S. V., Weinstock, J. V., Gallini, C. A., Redding, K., Margolskee, R. F., Osborne, L. C., Artis, D., & Garrett, W. S. (2016). Tuft cells, taste-chemosensory cells, orchestrate parasite type 2 immunity in the gut. *Science*, *351*(6279), 1329-1333. https://doi.org/10.1126/science.aaf1648
- Huang, Y. T., Wright, A., Gao, X., Kulick, L., Yan, H., & Lamm, M. E. (2005). Intraepithelial Cell Neutralization of HIV-1 Replication by IgA1. *The Journal of Immunology*, *174*(8), 4828-4835. https://doi.org/10.4049/jimmunol.174.8.4828
- Hüe, S., Mention, J.-J., Monteiro, R. C., Zhang, S., Cellier, C., Schmitz, J., Verkarre, V., Fodil, N., Bahram, S., Cerf-Bensussan, N., & Caillat-Zucman, S. (2004). A Direct Role for NKG2D/MICA Interaction in Villous Atrophy during Celiac Disease. *Immunity*, 21(3), 367-377. https://doi.org/https://doi.org/10.1016/j.immuni.2004.06.018
- Hutchings, A. B., Helander, A., Silvey, K. J., Chandran, K., Lucas, W. T., Nibert, M. L., & Neutra, M. R. (2004). Secretory immunoglobulin A antibodies against the sigmal outer capsid protein of reovirus type 1 Lang prevent infection of mouse Peyer's patches. *J Virol*, 78(2), 947-957. https://doi.org/10.1128/jvi.78.2.947-957.2004
- Ingle, H., Hassan, E., Gawron, J., Mihi, B., Li, Y., Kennedy, E. A., Kalugotla, G., Makimaa, H., Lee, S., Desai, P., McDonald, K. G., Diamond, M. S., Newberry, R. D., Good, M., & Baldridge, M. T. (2021). Murine astrovirus tropism for goblet cells and enterocytes facilitates an IFN-lambda response in vivo and in enteroid cultures. *Mucosal Immunol*, 14(3), 751-761. https://doi.org/10.1038/s41385-021-00387-6
- Ingle, H., Lee, S., Ai, T., Orvedahl, A., Rodgers, R., Zhao, G., Sullender, M., Peterson, S. T., Locke, M., Liu, T.-C., Yokoyama, C. C., Sharp, B., Schultz-Cherry, S., Miner, J. J., & Baldridge, M. T. (2019). Viral complementation of immunodeficiency confers protection against enteric pathogens via interferon-λ. *Nature Microbiology*, 4(7), 1120-1128. https://doi.org/10.1038/s41564-019-0416-7
- Ivanov, I. I., Atarashi, K., Manel, N., Brodie, E. L., Shima, T., Karaoz, U., Wei, D., Goldfarb, K. C., Santee, C. A., Lynch, S. V., Tanoue, T., Imaoka, A., Itoh, K., Takeda, K., Umesaki, Y., Honda, K., & Littman, D. R. (2009). Induction of Intestinal Th17 Cells by Segmented Filamentous Bacteria. *Cell*, 139(3), 485-498. https://doi.org/https://doi.org/10.1016/j.cell.2009.09.033
- Iwata, M., Hirakiyama, A., Eshima, Y., Kagechika, H., Kato, C., & Song, S.-Y. (2004). Retinoic Acid Imprints Gut-Homing Specificity on T Cells. *Immunity*, 21(4), 527-538. https://doi.org/https://doi.org/10.1016/j.immuni.2004.08.011

- Janowski, A. B., Bauer, I. K., Holtz, L. R., & Wang, D. (2017). Propagation of Astrovirus VA1, a Neurotropic Human Astrovirus, in Cell Culture. *J Virol*, 91(19). https://doi.org/10.1128/JVI.00740-17
- Johansen, F.-E., Pekna, M., Norderhaug, I. N., Haneberg, B., Hietala, M. A., Krajci, P., Betsholtz, C., & Brandtzaeg, P. (1999). Absence of Epithelial Immunoglobulin a Transport, with Increased Mucosal Leakiness, in Polymeric Immunoglobulin Receptor/Secretory Component–Deficient Mice. *Journal of Experimental Medicine*, 190(7), 915-922. https://doi.org/10.1084/jem.190.7.915
- Johansson, C., Wetzel, J. D., He, J., Mikacenic, C., Dermody, T. S., & Kelsall, B. L. (2007). Type I interferons produced by hematopoietic cells protect mice against lethal infection by mammalian reovirus. *J Exp Med*, 204(6), 1349-1358. https://doi.org/10.1084/jem.20061587
- Johansson, M. E., Gustafsson, J. K., Holmen-Larsson, J., Jabbar, K. S., Xia, L., Xu, H., Ghishan, F. K., Carvalho, F. A., Gewirtz, A. T., Sjovall, H., & Hansson, G. C. (2014). Bacteria penetrate the normally impenetrable inner colon mucus layer in both murine colitis models and patients with ulcerative colitis. *Gut*, 63(2), 281-291. https://doi.org/10.1136/gutjnl-2012-303207
- Johansson, M. E., Jakobsson, H. E., Holmen-Larsson, J., Schutte, A., Ermund, A., Rodriguez-Pineiro, A. M., Arike, L., Wising, C., Svensson, F., Backhed, F., & Hansson, G. C. (2015). Normalization of Host Intestinal Mucus Layers Requires Long-Term Microbial Colonization. *Cell Host Microbe*, 18(5), 582-592. https://doi.org/10.1016/j.chom.2015.10.007
- Jørgensen, S. F., Holm, K., Macpherson, M. E., Storm-Larsen, C., Kummen, M., Fevang, B., Aukrust, P., & Hov, J. R. (2019). Selective IgA deficiency in humans is associated with reduced gut microbial diversity. *Journal of Allergy and Clinical Immunology*, 143(5), 1969-1971.e1911. https://doi.org/10.1016/j.jaci.2019.01.019
- Kawabe, T., Naka, T., Yoshida, K., Tanaka, T., Fujiwara, H., Suematsu, S., Yoshida, N., Kishimoto, T., & Kikutani, H. (1994). The immune responses in CD40-deficient mice: Impaired immunoglobulin class switching and germinal center formation. *Immunity*, 1(3), 167-178. https://doi.org/https://doi.org/10.1016/1074-7613(94)90095-7
- Kawaguchi, M., Nanno, M., Umesaki, Y., Matsumoto, S., Okada, Y., Cai, Z., Shimamura, T., Matsuoka, Y., Ohwaki, M., & Ishikawa, H. (1993). Cytolytic activity of intestinal intraepithelial lymphocytes in germ-free mice is strain dependent and determined by T cells expressing gamma delta T-cell antigen receptors. *Proceedings of the National Academy of Sciences*, 90(18), 8591-8594. https://doi.org/doi:10.1073/pnas.90.18.8591
- Kim, K. S., Hong, S.-W., Han, D., Yi, J., Jung, J., Yang, B.-G., Lee, J. Y., Lee, M., & Surh, C. D. (2016). Dietary antigens limit mucosal immunity by inducing regulatory T cells in the small intestine. *Science*, *351*(6275), 858-863. https://doi.org/doi:10.1126/science.aac5560

- Koller, B. H., Marrack, P., Kappler, J. W., & Smithies, O. (2010). Normal development of mice deficient in beta 2M, MHC class I proteins, and CD8+ T cells. 1990. *J Immunol*, 184(9), 4592-4595. https://www.ncbi.nlm.nih.gov/pubmed/20410496
- Konkel, J. E., Maruyama, T., Carpenter, A. C., Xiong, Y., Zamarron, B. F., Hall, B. E., Kulkarni, A. B., Zhang, P., Bosselut, R., & Chen, W. (2011). Control of the development of CD8αα+ intestinal intraepithelial lymphocytes by TGF-β. *Nature Immunology*, *12*(4), 312-319. https://doi.org/10.1038/ni.1997
- Korotkevich, G., Sukhov, V., Budin, N., Shpak, B., Artyomov, M. N., & Sergushichev, A. (2021). Fast gene set enrichment analysis. *bioRxiv*, 060012. https://doi.org/10.1101/060012
- Koskinen, S. (1996). Long-term follow-up of health in blood donors with primary selective IgA deficiency. *J Clin Immunol*, *16*(3), 165-170. https://doi.org/10.1007/BF01540915
- Kuhn, R., Lohler, J., Rennick, D., Rajewsky, K., & Muller, W. (1993). Interleukin-10-deficient mice develop chronic enterocolitis. *Cell*, 75(2), 263-274. https://doi.org/10.1016/0092-8674(93)80068-p
- Kumar, V., Jarzabek-Chorzelska, M., Sulej, J., Karnewska, K., Farrell, T., & Jablonska, S. (2002). Celiac disease and immunoglobulin a deficiency: how effective are the serological methods of diagnosis? *Clin Diagn Lab Immunol*, *9*(6), 1295-1300. https://doi.org/10.1128/cdli.9.6.1295-1300.2002
- Lathrop, S. K., Bloom, S. M., Rao, S. M., Nutsch, K., Lio, C.-W., Santacruz, N., Peterson, D. A., Stappenbeck, T. S., & Hsieh, C.-S. (2011). Peripheral education of the immune system by colonic commensal microbiota. *Nature*, 478(7368), 250-254. https://doi.org/10.1038/nature10434
- Leishman, A. J., Gapin, L., Capone, M., Palmer, E., MacDonald, H. R., Kronenberg, M., & Cheroutre, H. (2002). Precursors of Functional MHC Class II- or Class II-Restricted CD8αα+ T Cells Are Positively Selected in the Thymus by Agonist Self-Peptides. *Immunity*, *16*(3), 355-364. https://doi.org/https://doi.org/10.1016/S1074-7613(02)00284-4
- Lemke, A., Kraft, M., Roth, K., Riedel, R., Lammerding, D., & Hauser, A. E. (2016). Long-lived plasma cells are generated in mucosal immune responses and contribute to the bone marrow plasma cell pool in mice. *Mucosal Immunology*, *9*(1), 83-97. https://doi.org/10.1038/mi.2015.38
- Lencioni, K. C., Seamons, A., Treuting, P. M., Maggio-Price, L., & Brabb, T. (2008). Murine norovirus: an intercurrent variable in a mouse model of bacteria-induced inflammatory bowel disease. *Comp Med*, 58(6), 522-533. https://www.ncbi.nlm.nih.gov/pubmed/19149409
- Levinson, K. J., Jesus, M. D., & Mantis, N. J. (2015). Rapid Effects of a Protective O-Polysaccharide-Specific Monoclonal IgA on Vibrio cholerae Agglutination, Motility, and Surface Morphology. *Infection and Immunity*, 83(4), 1674-1683. https://doi.org/doi:10.1128/iai.02856-14

- Li, D., Liu, C. M., Luo, R., Sadakane, K., & Lam, T. W. (2015). MEGAHIT: an ultra-fast single-node solution for large and complex metagenomics assembly via succinct de Bruijn graph. *Bioinformatics*, 31(10), 1674-1676. https://doi.org/10.1093/bioinformatics/btv033
- Li, L., Diab, S., McGraw, S., Barr, B., Traslavina, R., Higgins, R., Talbot, T., Blanchard, P., Rimoldi, G., Fahsbender, E., Page, B., Phan, T. G., Wang, C., Deng, X., Pesavento, P., & Delwart, E. (2013). Divergent astrovirus associated with neurologic disease in cattle. *Emerg Infect Dis*, *19*(9), 1385-1392. https://doi.org/10.3201/eid1909.130682
- Li, Y., Innocentin, S., Withers, David R., Roberts, Natalie A., Gallagher, Alec R., Grigorieva, Elena F., Wilhelm, C., & Veldhoen, M. (2011). Exogenous Stimuli Maintain Intraepithelial Lymphocytes via Aryl Hydrocarbon Receptor Activation. *Cell*, *147*(3), 629-640. https://doi.org/10.1016/j.cell.2011.09.025
- Lima-Junior, D. S., Krishnamurthy, S. R., Bouladoux, N., Collins, N., Han, S. J., Chen, E. Y., Constantinides, M. G., Link, V. M., Lim, A. I., Enamorado, M., Cataisson, C., Gil, L., Rao, I., Farley, T. K., Koroleva, G., Attig, J., Yuspa, S. H., Fischbach, M. A., Kassiotis, G., & Belkaid, Y. (2021). Endogenous retroviruses promote homeostatic and inflammatory responses to the microbiota. *Cell*, *184*(14), 3794-3811 e3719. https://doi.org/10.1016/j.cell.2021.05.020
- Lindner, C., Thomsen, I., Wahl, B., Ugur, M., Sethi, M. K., Friedrichsen, M., Smoczek, A., Ott, S., Baumann, U., Suerbaum, S., Schreiber, S., Bleich, A., Gaboriau-Routhiau, V., Cerf-Bensussan, N., Hazanov, H., Mehr, R., Boysen, P., Rosenstiel, P., & Pabst, O. (2015). Diversification of memory B cells drives the continuous adaptation of secretory antibodies to gut microbiota. *Nature Immunology*, 16(8), 880-888. https://doi.org/10.1038/ni.3213
- Linehan, J. L., Harrison, O. J., Han, S. J., Byrd, A. L., Vujkovic-Cvijin, I., Villarino, A. V., Sen, S. K., Shaik, J., Smelkinson, M., Tamoutounour, S., Collins, N., Bouladoux, N., Dzutsev, A., Rosshart, S. P., Arbuckle, J. H., Wang, C. R., Kristie, T. M., Rehermann, B., Trinchieri, G., . . . Belkaid, Y. (2018). Non-classical Immunity Controls Microbiota Impact on Skin Immunity and Tissue Repair. *Cell*, 172(4), 784-796 e718. https://doi.org/10.1016/j.cell.2017.12.033
- Litinskiy, M. B., Nardelli, B., Hilbert, D. M., He, B., Schaffer, A., Casali, P., & Cerutti, A. (2002). DCs induce CD40-independent immunoglobulin class switching through BLyS and APRIL. *Nat Immunol*, *3*(9), 822-829. https://doi.org/10.1038/ni829
- Liu, L., Gong, T., Tao, W., Lin, B., Li, C., Zheng, X., Zhu, S., Jiang, W., & Zhou, R. (2019). Commensal viruses maintain intestinal intraepithelial lymphocytes via noncanonical RIG-I signaling. *Nat Immunol*, 20(12), 1681-1691. https://doi.org/10.1038/s41590-019-0513-z
- Lockhart, A., Reed, A., Rezende de Castro, T., Herman, C., Campos Canesso, M. C., & Mucida, D. (2023). Dietary protein shapes the profile and repertoire of intestinal CD4+ T cells. *Journal of Experimental Medicine*, 220(8). https://doi.org/10.1084/jem.20221816

- Love, M. I., Huber, W., & Anders, S. (2014). Moderated estimation of fold change and dispersion for RNA-seq data with DESeq2. *Genome Biol*, 15(12), 550. https://doi.org/10.1186/s13059-014-0550-8
- Lum, S. H., Turner, A., Guiver, M., Bonney, D., Martland, T., Davies, E., Newbould, M., Brown, J., Morfopoulou, S., Breuer, J., & Wynn, R. (2016). An emerging opportunistic infection: fatal astrovirus (VA1/HMO-C) encephalitis in a pediatric stem cell transplant recipient. *Transplant Infectious Disease*, 18(6), 960-964. https://doi.org/https://doi.org/10.1111/tid.12607
- Lycke, N., Erlandsson, L., Ekman, L., Schon, K., & Leanderson, T. (1999). Lack of J chain inhibits the transport of gut IgA and abrogates the development of intestinal antitoxic protection. *J Immunol*, 163(2), 913-919. https://www.ncbi.nlm.nih.gov/pubmed/10395687
- Lycke, N. Y., & Bemark, M. (2017). The regulation of gut mucosal IgA B-cell responses: recent developments. *Mucosal Immunol*, 10(6), 1361-1374. https://doi.org/10.1038/mi.2017.62
- Macpherson, A. J., Gatto, D., Sainsbury, E., Harriman, G. R., Hengartner, H., & Zinkernagel, R. M. (2000). A primitive T cell-independent mechanism of intestinal mucosal IgA responses to commensal bacteria. *Science*, 288(5474), 2222-2226. https://doi.org/10.1126/science.288.5474.2222
- Malik, A., Sharma, D., Aguirre-Gamboa, R., McGrath, S., Zabala, S., Weber, C., & Jabri, B. (2023). Epithelial IFNγ signalling and compartmentalized antigen presentation orchestrate gut immunity. *Nature*, *623*(7989), 1044-1052. https://doi.org/10.1038/s41586-023-06721-1
- Mattioli, C. A., & Tomasi, T. B., Jr. (1973). The life span of IgA plasma cells from the mouse intestine. *J Exp Med*, 138(2), 452-460. https://doi.org/10.1084/jem.138.2.452
- Mazanec, M. B., Coudret, C. L., & Fletcher, D. R. (1995). Intracellular neutralization of influenza virus by immunoglobulin A anti-hemagglutinin monoclonal antibodies. *J Virol*, 69(2), 1339-1343. https://doi.org/10.1128/JVI.69.2.1339-1343.1995
- Mazzarino, P., Pietra, G., Vacca, P., Falco, M., Colau, D., Coulie, P., Moretta, L., & Mingari, M. C. (2005). Identification of effector-memory CMV-specific T lymphocytes that kill CMV-infected target cells in an HLA-E-restricted fashion. *European Journal of Immunology*, *35*(11), 3240-3247. https://doi.org/https://doi.org/10.1002/eji.200535343
- McDonald, Benjamin D., Bunker, Jeffrey J., Ishizuka, Isabel E., Jabri, B., & Bendelac, A. (2014). Elevated T Cell Receptor Signaling Identifies a Thymic Precursor to the TCRαβ+CD4–CD8β–Intraepithelial Lymphocyte Lineage. *Immunity*, 41(2), 219-229. https://doi.org/https://doi.org/10.1016/j.immuni.2014.07.008

- McNeal, M. M., & Ward, R. L. (1995). Long-term production of rotavirus antibody and protection against reinfection following a single infection of neonatal mice with murine rotavirus. *Virology*, 211(2), 474-480. https://doi.org/10.1006/viro.1995.1429
- Mesin, L., Ersching, J., & Victora, G. D. (2016). Germinal Center B Cell Dynamics. *Immunity*, 45(3), 471-482. https://doi.org/10.1016/j.immuni.2016.09.001
- Moor, K., Diard, M., Sellin, M. E., Felmy, B., Wotzka, S. Y., Toska, A., Bakkeren, E., Arnoldini, M., Bansept, F., Co, A. D., Voller, T., Minola, A., Fernandez-Rodriguez, B., Agatic, G., Barbieri, S., Piccoli, L., Casiraghi, C., Corti, D., Lanzavecchia, A., . . . Slack, E. (2017). High-avidity IgA protects the intestine by enchaining growing bacteria. *Nature*, *544*(7651), 498-502. https://doi.org/10.1038/nature22058
- Mora, J. R., Bono, M. R., Manjunath, N., Weninger, W., Cavanagh, L. L., Rosemblatt, M., & von Andrian, U. H. (2003). Selective imprinting of gut-homing T cells by Peyer's patch dendritic cells. *Nature*, 424(6944), 88-93. https://doi.org/10.1038/nature01726
- Moreau, M. C., Ducluzeau, R., Guy-Grand, D., & Muller, M. C. (1978). Increase in the Population of Duodenal Immunoglobulin A Plasmocytes in Axenic Mice Associated with Different Living or Dead Bacterial Strains of Intestinal Origin. *Infection and Immunity*, 21(2), 532-539. https://doi.org/doi:10.1128/iai.21.2.532-539.1978
- Morita, H., Yasuda, M., Yamamoto, M., Tomiyama, Y., Uchida, R., Ka, Y., Ogura, T., Kawai, K., Suemizu, H., & Hayashimoto, N. (2021). Pathogenesis of murine astrovirus in experimentally infected mice. *Exp Anim*, 70(3), 355-363. https://doi.org/10.1538/expanim.20-0162
- Mukherjee, S., & Hooper, L. V. (2015). Antimicrobial defense of the intestine. *Immunity*, 42(1), 28-39. https://doi.org/10.1016/j.immuni.2014.12.028
- Müller, S., Bühler-Jungo, M., & Mueller, C. (2000). Intestinal Intraepithelial Lymphocytes Exert Potent Protective Cytotoxic Activity During an Acute Virus Infection1. *The Journal of Immunology*, 164(4), 1986-1994. https://doi.org/10.4049/jimmunol.164.4.1986
- Murthy, A. K., Dubose, C. N., Banas, J. A., Coalson, J. J., & Arulanandam, B. P. (2006). Contribution of polymeric immunoglobulin receptor to regulation of intestinal inflammation in dextran sulfate sodium-induced colitis. *J Gastroenterol Hepatol*, *21*(9), 1372-1380. https://doi.org/10.1111/j.1440-1746.2006.04312.x
- Naccache, S. N., Peggs, K. S., Mattes, F. M., Phadke, R., Garson, J. A., Grant, P., Samayoa, E., Federman, S., Miller, S., Lunn, M. P., Gant, V., & Chiu, C. Y. (2015). Diagnosis of Neuroinvasive Astrovirus Infection in an Immunocompromised Adult With Encephalitis by Unbiased Next-Generation Sequencing. *Clinical Infectious Diseases*, 60(6), 919-923. https://doi.org/10.1093/cid/ciu912

- Nadjsombati, M. S., McGinty, J. W., Lyons-Cohen, M. R., Jaffe, J. B., DiPeso, L., Schneider, C., Miller, C. N., Pollack, J. L., Nagana Gowda, G. A., Fontana, M. F., Erle, D. J., Anderson, M. S., Locksley, R. M., Raftery, D., & von Moltke, J. (2018). Detection of Succinate by Intestinal Tuft Cells Triggers a Type 2 Innate Immune Circuit. *Immunity*, 49(1), 33-41 e37. https://doi.org/10.1016/j.immuni.2018.06.016
- Naik, S., Bouladoux, N., Linehan, J. L., Han, S. J., Harrison, O. J., Wilhelm, C., Conlan, S., Himmelfarb, S., Byrd, A. L., Deming, C., Quinones, M., Brenchley, J. M., Kong, H. H., Tussiwand, R., Murphy, K. M., Merad, M., Segre, J. A., & Belkaid, Y. (2015). Commensal-dendritic-cell interaction specifies a unique protective skin immune signature. *Nature*, 520(7545), 104-108. https://doi.org/10.1038/nature14052
- Navabi, N., Whitt, J., Wu, S. E., Woo, V., Moncivaiz, J., Jordan, M. B., Vallance, B. A., Way, S. S., & Alenghat, T. (2017). Epithelial Histone Deacetylase 3 Instructs Intestinal Immunity by Coordinating Local Lymphocyte Activation. *Cell Rep*, 19(6), 1165-1175. https://doi.org/10.1016/j.celrep.2017.04.046
- Ng, T. F., Kondov, N. O., Hayashimoto, N., Uchida, R., Cha, Y., Beyer, A. I., Wong, W., Pesavento, P. A., Suemizu, H., Muench, M. O., & Delwart, E. (2013). Identification of an astrovirus commonly infecting laboratory mice in the US and Japan. *PLoS One*, 8(6), e66937. https://doi.org/10.1371/journal.pone.0066937
- Nice, T. J., Strong, D. W., McCune, B. T., Pohl, C. S., & Virgin, H. W. (2013). A single-amino-acid change in murine norovirus NS1/2 is sufficient for colonic tropism and persistence. *J Virol*, 87(1), 327-334. https://doi.org/10.1128/JVI.01864-12
- Palm, Noah W., de Zoete, Marcel R., Cullen, Thomas W., Barry, Natasha A., Stefanowski, J., Hao, L., Degnan, Patrick H., Hu, J., Peter, I., Zhang, W., Ruggiero, E., Cho, Judy H., Goodman, Andrew L., & Flavell, Richard A. (2014). Immunoglobulin A Coating Identifies Colitogenic Bacteria in Inflammatory Bowel Disease. *Cell*, 158(5), 1000-1010. https://doi.org/https://doi.org/10.1016/j.cell.2014.08.006
- Pamer, E. G., Wang, C. R., Flaherty, L., Lindahl, K. F., & Bevan, M. J. (1992). H-2M3 presents a Listeria monocytogenes peptide to cytotoxic T lymphocytes. *Cell*, 70(2), 215-223. https://doi.org/10.1016/0092-8674(92)90097-v
- Pan, J., Kunkel, E. J., Gosslar, U., Lazarus, N., Langdon, P., Broadwell, K., Vierra, M. A., Genovese, M. C., Butcher, E. C., & Soler, D. (2000). Cutting Edge: A Novel Chemokine Ligand for CCR10 And CCR3 Expressed by Epithelial Cells in Mucosal Tissues1 2. *The Journal of Immunology*, 165(6), 2943-2949. https://doi.org/10.4049/jimmunol.165.6.2943
- Panda, S. K., Peng, V., Sudan, R., Ulezko Antonova, A., Di Luccia, B., Ohara, T. E., Fachi, J. L., Grajales-Reyes, G. E., Jaeger, N., Trsan, T., Gilfillan, S., Cella, M., & Colonna, M. (2023). Repression of the aryl-hydrocarbon receptor prevents oxidative stress and ferroptosis of intestinal intraepithelial lymphocytes. *Immunity*, *56*(4), 797-812.e794. https://doi.org/10.1016/j.immuni.2023.01.023

- Parsa, R., London, M., Rezende de Castro, T. B., Reis, B., Buissant des Amorie, J., Smith, J. G., & Mucida, D. (2022). Newly recruited intraepithelial Ly6A+CCR9+CD4+ T cells protect against enteric viral infection. *Immunity*, 55(7), 1234-1249.e1236. https://doi.org/https://doi.org/10.1016/j.immuni.2022.05.001
- Perkkiö, M., & Savilahti, E. (1980). Time of Appearance of Immunoglobulin-Containing Cells in the Mucosa of the Neonatal Intestine. *Pediatric Research*, *14*(8), 953-955. https://doi.org/10.1203/00006450-198008000-00012
- Peterson, D. A., McNulty, N. P., Guruge, J. L., & Gordon, J. I. (2007). IgA response to symbiotic bacteria as a mediator of gut homeostasis. *Cell Host Microbe*, *2*(5), 328-339. https://doi.org/10.1016/j.chom.2007.09.013
- Peterson, D. A., Planer, J. D., Guruge, J. L., Xue, L., Downey-Virgin, W., Goodman, A. L., Seedorf, H., & Gordon, J. I. (2015). Characterizing the interactions between a naturally primed immunoglobulin A and its conserved Bacteroides thetaiotaomicron species-specific epitope in gnotobiotic mice. *J Biol Chem*, 290(20), 12630-12649. https://doi.org/10.1074/jbc.M114.633800
- Phalipon, A., Cardona, A., Kraehenbuhl, J.-P., Edelman, L., Sansonetti, P. J., & Corthésy, B. (2002). Secretory Component: A New Role in Secretory IgA-Mediated Immune Exclusion In Vivo. *Immunity*, 17(1), 107-115. https://doi.org/10.1016/S1074-7613(02)00341-2
- Phalipon, A., Kaufmann, M., Michetti, P., Cavaillon, J. M., Huerre, M., Sansonetti, P., & Kraehenbuhl, J. P. (1995). Monoclonal immunoglobulin A antibody directed against serotype-specific epitope of Shigella flexneri lipopolysaccharide protects against murine experimental shigellosis. *J Exp Med*, 182(3), 769-778. https://doi.org/10.1084/jem.182.3.769
- Porter, N. T., Canales, P., Peterson, D. A., & Martens, E. C. (2017). A Subset of Polysaccharide Capsules in the Human Symbiont Bacteroides thetaiotaomicron Promote Increased Competitive Fitness in the Mouse Gut. *Cell Host & Microbe*, *22*(4), 494-506.e498. https://doi.org/https://doi.org/10.1016/j.chom.2017.08.020
- Price, A. E., Shamardani, K., Lugo, K. A., Deguine, J., Roberts, A. W., Lee, B. L., & Barton, G. M. (2018). A Map of Toll-like Receptor Expression in the Intestinal Epithelium Reveals Distinct Spatial, Cell Type-Specific, and Temporal Patterns. *Immunity*, 49(3), 560-575 e566. https://doi.org/10.1016/j.immuni.2018.07.016
- Quan, P. L., Wagner, T. A., Briese, T., Torgerson, T. R., Hornig, M., Tashmukhamedova, A., Firth, C., Palacios, G., Baisre-De-Leon, A., Paddock, C. D., Hutchison, S. K., Egholm, M., Zaki, S. R., Goldman, J. E., Ochs, H. D., & Lipkin, W. I. (2010). Astrovirus encephalitis in boy with X-linked agammaglobulinemia. *Emerg Infect Dis*, 16(6), 918-925. https://doi.org/10.3201/eid1606.091536
- Quast, C., Pruesse, E., Yilmaz, P., Gerken, J., Schweer, T., Yarza, P., Peplies, J., & Glöckner, F. O. (2013). The SILVA ribosomal RNA gene database project: improved data processing and web-

- based tools. *Nucleic Acids Res*, 41(Database issue), D590-596. https://doi.org/10.1093/nar/gks1219
- Raso, F., Liu, S., Simpson, M. J., Barton, G. M., Mayer, C. T., Acharya, M., Muppidi, J. R., Marshak-Rothstein, A., & Reboldi, A. (2023). Antigen receptor signaling and cell death resistance controls intestinal humoral response zonation. *Immunity*, *56*(10), 2373-2387 e2378. https://doi.org/10.1016/j.immuni.2023.08.018
- Rawla, P., Killeen, R. B., & Joseph, N. I. (2024). Selective IgA Deficiency. In *StatPearls*. https://www.ncbi.nlm.nih.gov/pubmed/30855793
- Reboldi, A., Arnon, T. I., Rodda, L. B., Atakilit, A., Sheppard, D., & Cyster, J. G. (2016). IgA production requires B cell interaction with subepithelial dendritic cells in Peyer's patches. *Science*, 352(6287), aaf4822. https://doi.org/10.1126/science.aaf4822
- Reikvam, D. H., Derrien, M., Islam, R., Erofeev, A., Grcic, V., Sandvik, A., Gaustad, P., Meza-Zepeda, L. A., Jahnsen, F. L., Smidt, H., & Johansen, F. E. (2012). Epithelial-microbial crosstalk in polymeric Ig receptor deficient mice. *Eur J Immunol*, 42(11), 2959-2970. https://doi.org/10.1002/eji.201242543
- Ricemeyer, L., Aguilar-Hernández, N., López, T., Espinosa, R., Lanning, S., Mukherjee, S., Cuellar, C., López, S., Arias, C. F., & DuBois, R. M. (2022). Structures of Two Human Astrovirus Capsid/Neutralizing Antibody Complexes Reveal Distinct Epitopes and Inhibition of Virus Attachment to Cells. *Journal of Virology*, *96*(1), e01415-01421. https://doi.org/doi:10.1128/JVI.01415-21
- Rios, D., Wood, M. B., Li, J., Chassaing, B., Gewirtz, A. T., & Williams, I. R. (2016). Antigen sampling by intestinal M cells is the principal pathway initiating mucosal IgA production to commensal enteric bacteria. *Mucosal Immunology*, *9*(4), 907-916. https://doi.org/https://doi.org/10.1038/mi.2015.121
- Ritchie, M. E., Phipson, B., Wu, D., Hu, Y., Law, C. W., Shi, W., & Smyth, G. K. (2015). limma powers differential expression analyses for RNA-sequencing and microarray studies. *Nucleic Acids Res*, 43(7), e47. https://doi.org/10.1093/nar/gkv007
- Rodgers, J. R., & Cook, R. G. (2005). MHC class Ib molecules bridge innate and acquired immunity. *Nat Rev Immunol*, 5(6), 459-471. https://doi.org/10.1038/nri1635
- Rogier, E. W., Frantz, A. L., Bruno, M. E., & Kaetzel, C. S. (2014). Secretory IgA is Concentrated in the Outer Layer of Colonic Mucus along with Gut Bacteria. *Pathogens*, *3*(2), 390-403. https://doi.org/10.3390/pathogens3020390

- Rollenske, T., Burkhalter, S., Muerner, L., von Gunten, S., Lukasiewicz, J., Wardemann, H., & Macpherson, A. J. (2021). Parallelism of intestinal secretory IgA shapes functional microbial fitness. *Nature*, *598*(7882), 657-661. https://doi.org/10.1038/s41586-021-03973-7
- Schneider, C., O'Leary, C. E., von Moltke, J., Liang, H. E., Ang, Q. Y., Turnbaugh, P. J., Radhakrishnan, S., Pellizzon, M., Ma, A., & Locksley, R. M. (2018). A Metabolite-Triggered Tuft Cell-ILC2 Circuit Drives Small Intestinal Remodeling. *Cell*, *174*(2), 271-284 e214. https://doi.org/10.1016/j.cell.2018.05.014
- Schön, M. P., Arya, A., Murphy, E. A., Adams, C. M., Strauch, U. G., Agace, W. W., Marsal, J., Donohue, J. P., Her, H., Beier, D. R., Olson, S., Lefrancois, L., Brenner, M. B., Grusby, M. J., & Parker, C. M. (1999). Mucosal T Lymphocyte Numbers Are Selectively Reduced in Integrin αE (CD103)-Deficient Mice. *The Journal of Immunology*, *162*(11), 6641-6649. https://doi.org/10.4049/jimmunol.162.11.6641
- Sheridan, Brian S., Pham, Q.-M., Lee, Y.-T., Cauley, Linda S., Puddington, L., & Lefrançois, L. (2014). Oral Infection Drives a Distinct Population of Intestinal Resident Memory CD8+ T Cells with Enhanced Protective Function. *Immunity*, 40(5), 747-757. https://doi.org/10.1016/j.immuni.2014.03.007
- Shouval, Dror S., Biswas, A., Goettel, Jeremy A., McCann, K., Conaway, E., Redhu, Naresh S., Mascanfroni, Ivan D., Al Adham, Z., Lavoie, S., Ibourk, M., Nguyen, Deanna D., Samsom, Janneke N., Escher, Johanna C., Somech, R., Weiss, B., Beier, R., Conklin, Laurie S., Ebens, Christen L., Santos, Fernanda G. M. S., Snapper, Scott B. (2014). Interleukin-10 Receptor Signaling in Innate Immune Cells Regulates Mucosal Immune Tolerance and Anti-Inflammatory Macrophage Function. *Immunity*, 40(5), 706-719. https://doi.org/https://doi.org/10.1016/j.immuni.2014.03.011
- Shulzhenko, N., Dong, X., Vyshenska, D., Greer, R. L., Gurung, M., Vasquez-Perez, S., Peremyslova, E., Sosnovtsev, S., Quezado, M., Yao, M., Montgomery-Recht, K., Strober, W., Fuss, I. J., & Morgun, A. (2018). CVID enteropathy is characterized by exceeding low mucosal IgA levels and interferon-driven inflammation possibly related to the presence of a pathobiont. *Clin Immunol*, 197, 139-153. https://doi.org/10.1016/j.clim.2018.09.008
- Silvey, K. J., Hutchings, A. B., Vajdy, M., Petzke, M. M., & Neutra, M. R. (2001). Role of immunoglobulin A in protection against reovirus entry into Murine Peyer's patches. *J Virol*, 75(22), 10870-10879. https://doi.org/10.1128/JVI.75.22.10870-10879.2001
- Singh, K., Chang, C., & Gershwin, M. E. (2014). IgA deficiency and autoimmunity. *Autoimmun Rev*, *13*(2), 163-177. https://doi.org/10.1016/j.autrev.2013.10.005
- Smits, S. L., Leeuwen, M. v., Eijk, A. A. v. d., Fraaij, P. L. A., Escher, J. C., Simon, J. H., & Osterhaus, A. D. M. E. (2010). Human Astrovirus Infection in a Patient with New-Onset Celiac Disease. *Journal of Clinical Microbiology*, 48(9), 3416-3418. https://doi.org/doi:10.1128/jcm.01164-10

- Strohmeier, V., Andrieux, G., Unger, S., Pascual-Reguant, A., Klocperk, A., Seidl, M., Marques, O. C., Eckert, M., Grawe, K., Shabani, M., von Spee-Mayer, C., Friedmann, D., Harder, I., Gutenberger, S., Keller, B., Proietti, M., Bulashevska, A., Grimbacher, B., Provaznik, J., . . . Warnatz, K. (2023). Interferon-Driven Immune Dysregulation in Common Variable Immunodeficiency-Associated Villous Atrophy and Norovirus Infection. *J Clin Immunol*, 43(2), 371-390. https://doi.org/10.1007/s10875-022-01379-2
- Suzuki, H., Jeong, K. I., Itoh, K., & Doi, K. (2002). Regional Variations in the Distributions of Small Intestinal Intraepithelial Lymphocytes in Germ-Free and Specific Pathogen-Free Mice. *Experimental and Molecular Pathology*, 72(3), 230-235. https://doi.org/https://doi.org/10.1006/exmp.2002.2433
- Suzuki, K., Meek, B., Doi, Y., Muramatsu, M., Chiba, T., Honjo, T., & Fagarasan, S. (2004). Aberrant expansion of segmented filamentous bacteria in IgA-deficient gut. *Proceedings of the National Academy of Sciences*, 101(7), 1981-1986. https://doi.org/doi:10.1073/pnas.0307317101
- Suzuki, K., Meek, B., Doi, Y., Muramatsu, M., Chiba, T., Honjo, T., & Fagarasan, S. (2004). Aberrant expansion of segmented filamentous bacteria in IgA-deficient gut. *Proc Natl Acad Sci U S A*, 101(7), 1981-1986. https://doi.org/10.1073/pnas.0307317101
- Swanson, P. A., II, Pack, C. D., Hadley, A., Wang, C.-R., Stroynowski, I., Jensen, P. E., & Lukacher, A. E. (2008). An MHC class Ib–restricted CD8 T cell response confers antiviral immunity. *Journal of Experimental Medicine*, 205(7), 1647-1657. https://doi.org/10.1084/jem.20080570
- Tomasec, P., Braud, V. M., Rickards, C., Powell, M. B., McSharry, B. P., Gadola, S., Cerundolo, V., Borysiewicz, L. K., McMichael, A. J., & Wilkinson, G. W. G. (2000). Surface Expression of HLA-E, an Inhibitor of Natural Killer Cells, Enhanced by Human Cytomegalovirus gpUL40. Science, 287(5455), 1031-1033. https://doi.org/doi:10.1126/science.287.5455.1031
- Vaishnava, S., Behrendt, C. L., Ismail, A. S., Eckmann, L., & Hooper, L. V. (2008). Paneth cells directly sense gut commensals and maintain homeostasis at the intestinal host-microbial interface. *Proc Natl Acad Sci U S A*, 105(52), 20858-20863. https://doi.org/10.1073/pnas.0808723105
- Vaishnava, S., Yamamoto, M., Severson, K. M., Ruhn, K. A., Yu, X., Koren, O., Ley, R., Wakeland, E. K., & Hooper, L. V. (2011). The antibacterial lectin RegIIIgamma promotes the spatial segregation of microbiota and host in the intestine. *Science*, *334*(6053), 255-258. https://doi.org/10.1126/science.1209791
- van de Ven, A. A., Janssen, W. J., Schulz, L. S., van Loon, A. M., Voorkamp, K., Sanders, E. A., Kusters, J. G., Nierkens, S., Boes, M., Wensing, A. M., & van Montfrans, J. M. (2014). Increased prevalence of gastrointestinal viruses and diminished secretory immunoglobulin a levels in antibody deficiencies. *J Clin Immunol*, *34*(8), 962-970. https://doi.org/10.1007/s10875-014-0087-3

- van der Heijden, P. J., Stok, W., & Bianchi, A. T. (1987). Contribution of immunoglobulin-secreting cells in the murine small intestine to the total 'background' immunoglobulin production. *Immunology*, 62(4), 551-555. https://www.ncbi.nlm.nih.gov/pubmed/3323031
- Van der Sluis, M., De Koning, B. A., De Bruijn, A. C., Velcich, A., Meijerink, J. P., Van Goudoever, J. B., Buller, H. A., Dekker, J., Van Seuningen, I., Renes, I. B., & Einerhand, A. W. (2006). Muc2-deficient mice spontaneously develop colitis, indicating that MUC2 is critical for colonic protection. *Gastroenterology*, 131(1), 117-129. https://doi.org/10.1053/j.gastro.2006.04.020
- van Ginkel, F. W., Wahl, S. M., Kearney, J. F., Kweon, M. N., Fujihashi, K., Burrows, P. D., Kiyono, H., & McGhee, J. R. (1999). Partial IgA-deficiency with increased Th2-type cytokines in TGF-beta 1 knockout mice. *J Immunol*, *163*(4), 1951-1957.
- Vandereyken, M., James, O. J., & Swamy, M. (2020). Mechanisms of activation of innate-like intraepithelial T lymphocytes. *Mucosal Immunology*, *13*(5), 721-731. https://doi.org/10.1038/s41385-020-0294-6
- Victora, G. D., & Nussenzweig, M. C. (2022). Germinal Centers. *Annu Rev Immunol*, 40, 413-442. https://doi.org/10.1146/annurev-immunol-120419-022408
- von Moltke, J., Ji, M., Liang, H. E., & Locksley, R. M. (2016). Tuft-cell-derived IL-25 regulates an intestinal ILC2-epithelial response circuit. *Nature*, *529*(7585), 221-225. https://doi.org/10.1038/nature16161
- Vugmeyster, Y., Glas, R., Perarnau, B., Lemonnier, F. A., Eisen, H., & Ploegh, H. (1998). Major histocompatibility complex (MHC) class I KbDb -/- deficient mice possess functional CD8+ T cells and natural killer cells. *Proc Natl Acad Sci U S A*, 95(21), 12492-12497. https://doi.org/10.1073/pnas.95.21.12492
- Wilson , E., & Butcher , E. C. (2004). CCL28 Controls Immunoglobulin (Ig)A Plasma Cell Accumulation in the Lactating Mammary Gland and IgA Antibody Transfer to the Neonate. *Journal of Experimental Medicine*, 200(6), 805-809. https://doi.org/10.1084/jem.20041069
- Woodrow, K. A., Bennett, K. M., & Lo, D. D. (2012). Mucosal vaccine design and delivery. *Annu Rev Biomed Eng*, 14, 17-46. https://doi.org/10.1146/annurev-bioeng-071811-150054
- Wright, A., Yan, H., Lamm, M. E., & Huang, Y. T. (2006). Immunoglobulin A antibodies against internal HIV-1 proteins neutralize HIV-1 replication inside epithelial cells. *Virology*, *356*(1), 165-170. https://doi.org/10.1016/j.virol.2006.08.006
- Xing, Q., Chang, D., Xie, S., Zhao, X., Zhang, H., Wang, X., Bai, X., & Dong, C. (2024). BCL6 is required for the thymic development of TCRαβ+CD8αα+ intraepithelial lymphocyte lineage. *Science Immunology*, *9*(92). https://doi.org/doi:10.1126/sciimmunol.adk4348

- Yang, Y., Torchinsky, M. B., Gobert, M., Xiong, H., Xu, M., Linehan, J. L., Alonzo, F., Ng, C., Chen, A., Lin, X., Sczesnak, A., Liao, J.-J., Torres, V. J., Jenkins, M. K., Lafaille, J. J., & Littman, D. R. (2014). Focused specificity of intestinal TH17 cells towards commensal bacterial antigens. *Nature*, 510(7503), 152-156. https://doi.org/10.1038/nature13279
- Yokoyama, C. C., Loh, J., Zhao, G., Stappenbeck, T. S., Wang, D., Huang, H. V., Virgin, H. W., & Thackray, L. B. (2012). Adaptive immunity restricts replication of novel murine astroviruses. *J Virol*, 86(22), 12262-12270. https://doi.org/10.1128/JVI.02018-12
- Zhang, N., & Bevan, Michael J. (2013). Transforming Growth Factor-β Signaling Controls the Formation and Maintenance of Gut-Resident Memory T Cells by Regulating Migration and Retention. *Immunity*, 39(4), 687-696. https://doi.org/10.1016/j.immuni.2013.08.019
- Zheng, Y., Valdez, P. A., Danilenko, D. M., Hu, Y., Sa, S. M., Gong, Q., Abbas, A. R., Modrusan, Z., Ghilardi, N., de Sauvage, F. J., & Ouyang, W. (2008). Interleukin-22 mediates early host defense against attaching and effacing bacterial pathogens. *Nat Med*, *14*(3), 282-289. https://doi.org/10.1038/nm1720
- Zhou, D., Zhang, Y., Li, Q., Chen, Y., He, B., Yang, J., Tu, H., Lei, L., & Yan, H. (2011). Matrix Protein-Specific IgA Antibody Inhibits Measles Virus Replication by Intracellular Neutralization. *Journal of Virology*, 85(21), 11090-11097. https://doi.org/doi:10.1128/jvi.00768-11
- Zhou, R., Wei, H., Sun, R., Zhang, J., & Tian, Z. (2007). NKG2D recognition mediates Toll-like receptor 3 signaling-induced breakdown of epithelial homeostasis in the small intestines of mice. *Proceedings of the National Academy of Sciences*, 104(18), 7512-7515. https://doi.org/doi:10.1073/pnas.0700822104